DOCTOR OF PHILOSOPHY

Novel bioactive peptides from the defensive skin secretion of Phyllomedusinae frogs

Tan, Yining

Award date:
2018

Awarding institution:
Queen's University Belfast

Novel Bioactive Peptides from the Defensive Skin Secretions of Phyllomedusinae Frogs

Yining Tan

School of Pharmacy,
Faculty of Medicine, Health and Life Sciences,
Queen's University Belfast

A THESIS SUBMITTED TO THE QUEEN'S UNIVERSITY BELFAST FOR THE DEGREE OF DOCTOR OF PHILOSOPHY (PhD)

July 2018

Contents

ACKNOWLEDGEMENTS VIII

DECLARATION IX

Abstract X

Chapter 1 General Introduction 1

1.1 Amphibians 2

1.1.1 Characteristics of amphibians 2

1.1.2 Skin structure of amphibians 3

1.1.3 Skin secretions of amphibians 4

1.2 Antimicrobial peptides (AMPs) 7

1.2.1 Mechanisms of action of AMPs 8

1.2.2 Nomenclature of AMPs 11

1.2.3 Diversity of structures of AMPs 12

1.2.4 Structure-activity relationship studies on AMPs 14

1.3 Anti-cancer activity of AMPs 18

1.3.1 Mechanisms of action 18

1.3.2 Peptides with anticancer activity 19

1.4 Aims and objectives of this thesis 22

Chapter 2 Materials and Methods 23

2.1 Specimen Biodata and Secretion Harvesting 24

2.2 Molecular Cloning 24

2.2.1 mRNA Isolation 24

2.2.2 cDNA library construction 25

2.2.3 Rapid amplification of cDNA ends (RACE) PCR..... 27
2.2.4 Gel analysis 29
2.2.5 PCR products purification 29
2.2.6 Ligation 30
2.2.7 Transformation 31
2.2.7 Blue-White colony screening 32
2.2.8 Isolation of recombinant plasmid DNA..... 32
2.2.9 Cloning PCR..... 33
2.2.10 Gel electrophoresis & selected cloning PCR products purification 34
2.2.11 DNA cycle sequencing reaction..... 34
2.2.12 Ethanol purification 35
2.2.13 Sequencing 36
2.3 Solid Phase Peptide Synthesis (SPPS) 36
2.3.1 Peptide synthesis 36
2.3.2 Cleavage and deprotection of peptides..... 37
2.3.3 Washing and drying 38
2.4 Reverse Phase High Performance Liquid Chromatography HPLC (RP-HPLC) 39
2.4.1 Preparation of RP-HPLC mobile phase..... 39
2.4.2 RP-HPLC analysis of amphibian skin secretion..... 39
2.4.3 RP-HPLC purification of synthetic peptides 40
2.5 Mass Spectrometry..... 40
2.5.1 Matrix-assisted laser desorption, ionization, time-of-flight (MALDI-TOF) mass spectrometry 40
2.5.2 LCQ Fleet™ Ion Trap Mass Spectrometer Sequencing 41
2.6 Determination of Peptide Secondary Structures 41
2.6.1 Circular Dichroism (CD) analysis of synthetic peptides 41
2.6.2 Computational analysis of synthetic peptides 42
2.7 Antimicrobial Assays 42

2.7.1 Viable cell counting 42
2.7.2 Minimum inhibitory concentration (MIC) assays 43
2.7.3 Minimum bactericidal concentration (MBC) assays 44
2.7.4 Biofilm assays 44
2.7.5 Cytoplasmic material leakage assays 46
2.8 Haemolysis assays 46
2.9 Anti-cancer cell proliferation assays 48
2.9.1 Thawing frozen samples of cells 48
2.9.2 Sub-culturing of adherent cells 48
2.9.3 Seeding of cell culture 49
2.9.4 MTT assay 49
2.10 Statistical Analyses 50

Chapter 3 Biological activities of cationicity-enhanced and hydrophobicity-optimized analogues of an antimicrobial peptide, dermaseptin-PS3, from the skin secretion of *Phyllomedusa sauvagii* 51

Abstract 52
3.1 Introduction 53
3.2 Materials and Methods 54
3.2.1 Acquisition of *Phyllomedusa sauvagii* Dermal Secretions 54
3.2.2 "Shotgun" cloning of a cDNA Encoding DPS3 Peptide Biosynthetic Precursor 54
3.2.3 Identification and Analysis of Amino-acid Sequence 55
3.2.4 Design and Synthesis of DPS3 and its Two Analogues 55
3.2.5 CD Analysis of Synthetic Peptides 56
3.2.6 Antimicrobial Assays 56
3.2.7 Assessment of Cytotoxic Effects of Peptides on Human Cancer Cells Using MTT Assay 56
3.2.8 Haemolysis Assay 56

3.2.9 Statistical Analyses 57

3.3 Results 57

3.3.1 Molecular Cloning of a DPS3 Precursor cDNA from a Skin Secretion-Derived cDNA Library 57

3.3.2 Isolation and Structural Characterisation of DPS3 58

3.3.3 Physicochemical Properties and Secondary Structures of DPS3 and its Analogues 61

3.3.4 Antimicrobial Activity 63

3.3.5 Cytotoxicity of Peptides on Human Cancer Cells 63

3.3.6 Haemolysis Activity 66

3.4 Discussion 67

Chapter 4 Isolation and Identification of a novel dermaseptin, Dermaseptin-PC1, from skin secretion of *Phyllomedusa camba.* 71

Abstract 72

4.1 Introduction 73

4.2 Materials and Methods 75

4.2.1 "Shotgun" cloning of cDNAs encoding novel peptide biosynthetic precursors. 75

4.2.2 Identification and structural analysis of the novel peptide 75

4.2.3 Solid-phase peptide synthesis 75

4.2.4 Assays of antimicrobial activity 76

4.2.5 Haemolysis assay 76

4.2.6 MTT cell viability assay 76

4.2.7 Statistical Analyses 77

4.3 Results 77

4.3.1 Molecular cloning of the peptide precursor and analysis of the primary and secondary structure 77

4.3.2 Identification and structural analysis of DPC1 79

4.3.3 Purification of synthetic DPC1 81

4.3.4 Prediction of Secondary Structure and Physiochemical Properties 82

4.3.5 Antimicrobial Assay 84

4.3.6 Haemolytic activity of DPC1 85

4.3.7 Cancer cell viability following treatment with DPC1 86

4.4 Discussion 87

Chapter 5 Discovery of Distinctin-Like-Peptide-PH (DLP-PH) from the Skin Secretion of *Phyllomedusa hypochondrialis*, a Prototype of a Novel Family of Antimicrobial Peptides.....92

Abstract 93

5.1 Introduction 94

5.2 Materials and Methods 95

5.2.1 Secretion Acquisition and Maintenance of Experimental Specimens 95

5.2.2 Construction of A Skin Secretion-derived cDNA Library and "Shotgun" Cloning 96

5.2.3 Identification and Primary Structure Analysis of Mature Peptide in Crude Skin Secretion 96

5.2.4 Solid-Phase Peptide Synthesis 96

5.2.5 Determination and Visualization of Peptide Secondary Structures 97

5.2.6 Antimicrobial Susceptibility Assays 98

5.2.7 Cytoplasmic Materials Leakage Assay 99

5.2.8 Haemolysis Assay 100

5.2.9 Assessment of Anti-proliferation Effect and Cytotoxicity on Human Cancer and Normal Cell Lines 100

5.2.10 Statistical Analyses 101

5.3 Result 101

5.3.1 Identification and Characterization of a DLP-PH Precursor cDNA from a Skin Secretion-derived cDNA Library 101

5.3.2 Prediction of Secondary Structure and Physiochemical Properties 105

5.3.3 Antimicrobial Activities 108

5.3.4 Bioactivity of DLP-PH on Mammalian Cells 111

5.4 Discussion 112

Chapter 6 General discussion 117

6.1 The Significance of AMPs 118

6.2 The Findings in This Thesis 120

6.3 Things Which Need To Be Considered 123

References 125

ACKNOWLEDGEMENTS

I would like to express my gratitude to Prof. Chris Shaw and Dr. Tianbao Chen for giving me the chance to study in the School of Pharmacy, Queen's University Belfast. Especially, I would like to thank Dr. Tianbao Chen, who helped me a lot in both study and daily life in Northern Ireland. I also want to thank my supervisors, Dr. Lei Wang, Dr. Mei Zhou, Dr. Xinping Xi and Dr. Chengbang Ma for their expertise and professional guidance in my research.

In the meantime, I really appreciate the help from my colleagues, especially Dr. Yitian Gao, Dr. Di Wu and Dr. Xiaoling Chen, who demonstrated all the experiments to me and trained me to do these in the right way. I could not have made this thesis without their valuable help and suggestions. I also want to say thank you to our technician, Mr. David Vance, who helped me to prepare many experimental materials. His hard-work is a treasure in this lab.

Last but not least, a big thanks to my parents and family, my constant source of love, support, and encouragement. Thank you so much for your trust.

DECLARATION

I declare that the research reported in this thesis is my own work except where acknowledgement has been made. All work was carried out in the Molecular Therapeutics Research Group, School of Pharmacy, Faculty of Medicine, Life and Health Sciences, Queen's University, Belfast.

I hereby declare that for 5 years following the date on which the thesis is deposited in the Library of Queen's University, Belfast, the thesis shall remain confidential with access or copying prohibited. Following expiry of the period I permit the librarian of the University to allow the thesis to be copied in whole or in part without reference to me on the understanding that such authority applies to the provision of single copies made for study purposes or for inclusion within the stock of another library. This restriction does not apply to the British Library Thesis Service.

IT IS A CONDITION OF USE OF THIS THESIS THAT ANYONE WHO CONSULTS IT MUST RECOGNISE THAT THE COPYRIGHT RESTS WITH THE AUTHOR AND THAT NO QUOTATION FROM THE THESIS AND NO INFORMATION DERIVED FROM IT MAY BE PUBLISHED UNLESS THE SOURCE IS PROPERLY ACKNOWLEDGED.

Abstract

Amphibian skin secretion contains a variety of bio-components, of which bioactive peptides are predominant. They produce such peptides to protect themselves from the threats in their environment like predatory attack and microorganism invasion. Antimicrobial peptides (AMPs) act as the first line of self-defence and plays an important role in preventing microbe infections via the skin contact. The skin secretion of phyllomedusinae tree frog contains massive quantities of AMPs, belonging to the dermaseptin superfamily, which exhibit remarkable antimicrobial activity against Gram-positive bacteria, Gram-negative bacteria and fungi.

In this thesis, we employed "shot-gun" molecular cloning and MS/MS sequencing techniques to identify novel AMPs from the skin secretion of selected *Phyllomedusa* species. Afterwards, we chemically synthesised these peptides to evaluate their biological activity as well as their cytotoxicity.

In Chapter 3, a novel dermaspetin peptide was identified from the skin secretion of *Phyllomedusa sauvagii*, namely dermaseptin-PS3 (DPS3). This peptide exhibited moderate antimicrobial activity only against *S. aureus*, *E. coli*, and *C. albicans* (MICs are 512, 64, 128 mg/L, respectively). Additionally, DPS3 induced cell lysis on both cancer cells and red blood cells. Subsequently, one cationicity enhanced analogue and one hydrophobicity enhanced analogue were designed to determine the influence of both factors on the antimicrobial activity, anticancer activity and haemolytic activity.

In Chapter 4, another novel dermaseptin peptide was identified by means of the same strategy, from the skin secretion of *Phyllomedusa camba*, namely dermaseptin-PC1 (DPC1). It is the first time a dermaseptin from has been identified in this species. DPC1 exhibited more potent antimicrobial activity against *S. aureus*, *E. coli*, and *C. albicans* (MICs are 64, 16, 64 mg/L, respectively) with a low degree of haemolytic activity. Furthermore, DPC1 showed anti-biofilm activity against both *S. aureus* and *E. coli*.

In Chapter 5, we described the discovery of a prototype of a novel family of AMP from the skin secretion of *Phyllomedusa hypochondrialis* (now amended to *Pithecopus hypochondrialis* in RedList). This AMP showed a high degree of similarity to the chain B of distinctin, namely distinctin-like-peptide-PH (DLP-PH). DLP-PH showed antimicrobial activity against *S. aureus*, *E. coli*, and *C. albicans* at 256, 32, and 64 mg/L, and it also inhibited the growth of *P. aeruginosa* (MIC=64 mg/L). Subsequently, we investigated the biological function of both C- and N-terminal fragments of DLP-PH.

The results of these chapters revealed that the genes of the dermaseptin superfamily are highly conserved, indicating the one-gene generated skin peptide library via gene duplication, focal hypermutation, and diversifying selection. Although these peptides display important antimicrobial and anticancer activities, the cytotoxicity and haemolysis cannot be nullified. Further investigation on reducing the membrane-lytic activity as well as improving biocompatibility should be taken into consideration. In conclusion, this thesis offered the chance to study novel dermaseptins and the prototype of novel antimicrobial templates.

Chapter 1

General Introduction

1.1 Amphibians

1.1.1 Characteristics of amphibians

Amphibians are ectothermic, tetrapod vertebrates of the class Amphibia. Throughout the evolution of life, the animal community has experienced a long process from aquatic to terrestrial existence, and amphibians are the first vertebrates to ascend to the land from the water. During the life cycle of amphibians, its eggs have no protective device, and larvae are fish-shaped without limbs and breathe in the water with gills. The larvae undergo metamorphosis, and some of their larval organs become atrophied, and producing an adult that can live on land. Adult amphibians have five-toed appendages and are typically lung breathing (skin has an assisted breathing function and is characteristic of aquatic organisms). These structures created the necessary conditions for amphibians to be active on land, but they still cannot leave the water for long because the low degree of epidermal keratinisation, and the long time after leaving the water will be dehydrated. Although they use the lung as the primary respiratory organ, the structure of the lungs is simple, consisting of only a few air chambers thus requiring skin as an auxiliary respiratory organ. There are about 4,000 species of amphibians in the world, and they can be classified into three modern orders according to their morphology: Anura (the frogs and toads), Urodela (the salamanders), and Apoda (the caecilians). Apart from the oceans and some deserts, there are found in all other habitats. Although the amphibians mainly eat animal food, they have a weak ability to defend against enemies. Fish, snakes, birds and beasts are their natural enemies.

1.1.2 Skin structure of amphibians

Amphibian skin mainly consists of two layers, epidermis and dermis. There are two main types of adult skin glands: mucus glands and granular glands. The granular gland is also known as poison or venom gland, serous gland or serous granular gland. In addition, the third gland, the lipid gland, is observed in the skin of some species of *Phyllomedusa* only, in recent years.

Mucus gland: The shape is smaller than the granular gland, and the quantity is much more than that of the granular gland. It is about ten times more abundant than the granular gland. Mucus glands secrete clear mucus that covers the surface to form a moist, thin film with the functions of defense, reproduction, moisturising, skin respiration, temperature regulation, and pH adjustment. The main components of mucus are glycosaminoglycans and proteoglycan (Toledo & Jared, 1995). Microscopic observation of the mucus gland showed that the epithelial cells were cubic, filled with fine amorphous particles, and the connection between the cells were desmosomes. The secretory mechanism of the mucus gland is merocrine.

Lipid gland: These glands could not be distinguished in paraffin sections. They strongly stained for Sudan IV, suggesting a high lipid content and therefore they became known as the lipid gland. Its size is between the mucus gland and the granular gland. The gland cavity contains many particles of various sizes. Microscopic studies showed that there are many lateral thin sheets in these particles. It is generally believed that the secretory mechanism of the lipid gland is merocrine (Lacombe et al., 2000).

Granular gland: The body is large and unevenly distributed on the body surface, especially on the head, shoulders, back, and tail. Granular glands aggregate locally to

form particular glandular structures (Zug et al. 2001). There are no apparent boundaries between the granular gland and epithelial cells, and without connections between the cells such as desmosomes. Thus it is generally considered that the epithelial cells of the granular gland are syncytial. Microscopic observations showed that their particles have a variety of shapes. For example, the particles of *P. bicolor* are round, while the particles of *Xenopus laevis* are oval (Lacombe et al., 2000). Granular glands are divided into two types: Type I endoplasmic reticulum is underdeveloped, stimulation (injection of norepinephrine or electric shock) can cause much secretion; Type II endoplasmic reticulum is developed, and stimulation has no significant effect on secretion (Delfino et al., 2001). The active peptides secreted by the granular glands fall into two broad categories, namely antimicrobial peptides and pharmacologically active peptides. The secretory mechanism of granules is holocrine.

1.1.3 Skin secretions of amphibians

Amphibians have exposed skin, which in high humidity, has respiratory functions. This morphological and physiological specificity requires that they only survive in moist environments. This is also an excellent environment for the survival of some pathogenic microorganisms. To develop and adapt to a wide range of habitats and diverse ecological environments, some amphibian peptides eventually emerged as important effector molecules in innate immunity released by the skin glands in the defense system against pathogenic microorganisms - antimicrobial peptides, which have important effects in the immune defense mechanism of amphibians when they are stimulated by adrenaline, stress, trauma, etc. After long-term evolution, there have been multiple replications and mutations in antimicrobial peptide genes, resulting in many structures and a wide variety

of antimicrobial peptides.

In the tailless amphibians (Anura), it was early stablished that their skin contains many active substances. In 1970, Csordas et al. discovered the first hemolytic peptide Bombinin in the study of the cytotoxic substances in the skin secretion of *Bombina variegata* (Mor et al., 1994). Then in 1987, Zasloff obtained the Magainins from the skin secretions of *Xenopus laevis*, and people began to pay attention to the study of these peptides (Zasloff, 1987). According to incomplete statistics, antibacterial peptides have been extracted from the skins of eight genera of Anura and their sequences have been determined. The 8 genera are *Bombina*, *Kassina*, *Litoria*, *Phyllomedusa*, *Pseudis*, *Rana*, *Uperoleia* and *Xenopus*.

Table 1.1 The representative antimicrobial peptides from frog skin

Peptide	Species	Amino acid sequence	Accession No.
Bombinin H3	*Bombina variegata*	IIGPVLGMVGSALGGLLKKI.NH_2	P82282
Brevinin-1ARa	*Rana areolata*	FLPLVRVAAKILPSVFCAISKRC	P85056
Brevinin-2E	*Rana esculenta*	GIMDTLKNLAKTAGKGALQSLLNK ASCKLSGQC	P32413
Dermadistinctin K	*Phyllomedusa distincta*	GLWSKIKAAGKEAAKAAAKAAGKA ALNAVSEAV	P83638
Distinctin	*Phyllomedusa distincta*	Chain A ENREVPPGFTALIKTLRKCKII Chain B NLVSGLIEARKYLEQLHRKLKNCKV	Q17UZ0
Japonicin-2	*Rana japonica*	FGLPMLSILPKALCILLKRKC	P83306
Magainin-2 PGS	*Xenopus laevis*	GIGKFLHSAKKFGKAFVGEIMNS	P11006
Maximin H1	*Bombina maxima*	ILGPVISTIGGVLGGLLKNL.NH_2	P83080
Nigrocin 1	*Rana nigromaculata*	GLLDSIKGMAISAGKGALQNLLKVA SCKLDKTC	P0C008
Palustrin-3a	*Rana palustris*	IFPKIIGKGIKTGIVNGIKSLVKGVGM KVFKAGLNNIGNTGCNEDEC	P84281
Temporin A	*Rana*	FLPLIGRVLSGLL.NH_2	P56917

	temporaria		
Tigernin-1	*Rana tigerina*	FCTMIPIPRCY.NH_2	P82651
XT-1	*Xenopus tropicalis*	GFLGPLLKLAAKGVAKVIPHLIPSRQQ	P84387

1.2 Antimicrobial peptides (AMPs)

Although the structure of antimicrobial peptides varies, almost all antimicrobial peptides share some common features. Natural antibacterial peptides are usually small molecule cationic peptides consist of 12 to 60 amino acids, rich in lysine, arginine, histidine and other basic amino acids. The peptides usually have 2 to 7 positive charges and the isoelectric point is greater than 7 thus showing strong cationicity characteristics. Antibacterial peptides generally have an amphiphilic structure, with one hydrophobic region bound to the lipid and one positively charged hydrophilic region bound to water or a negatively charged residue. These properties allow antimicrobial peptides to bind well to cell membranes composed of amphiphilic molecules, especially electronegative cells, which is the structural basis for the interaction of antimicrobial peptides with bacterial cell membranes (Jeżowskabojczuk & Stokowasołtys, 2018). Most of the antimicrobial peptides have thermal stability and can maintain their activity when heated at 100°C for 10-15 min. Studies have shown that there is a negative correlation between the antibacterial activity of some antibacterial peptides and the concentration of Na^+ in the solution. When NaCl concentration reaches 150 mmol/L, peptides lose activity. Many factors can reduce the activity of antimicrobial peptides, such as high concentrations of monovalent and divalent cations, polyanions, serum, apolipoprotein A-I, and proteases

(Brogden, 2005). However, some antibacterial peptides are highly resistant to higher ionic strength and lower or higher pH. Some antibacterial peptides can resist trypsin or pepsin hydrolysis (Travkova et al., 2017). In addition, antimicrobial peptides also have the advantages of good water solubility and no drug-resistance.

So far, more than 2,600 antimicrobial peptides have been discovered (Wang et al., 2016), which are widely distributed in organisms such as viruses, bacteria, fungi, fish, birds, insects, amphibians, molluscs, and mammals.

1.2.1 Mechanisms of action of AMPs

The mechanisms of antimicrobial peptides process can be divided into 4 steps: attraction, adhesion, insertion and destruction. Antimicrobial peptides are attracted to the surface of bacteria, and the anionic or cationic antimicrobial peptides adhere by electrostatic interaction between peptides and bacterial surfaces. In the first instance, cationic antimicrobial peptides interact with the net negative charge on the surface of the Gram-negative bacteria, such as anionic phospholipids and lipopolysaccharide phosphate groups. When the peptide concentration is low on the lipid, it is in parallel to the lipid bilayer. With the increase of concentration, peptide starts to adopt a vertical orientation on the membrane. In high peptide-lipid concentrations, peptide molecules vertically translocate and insert into the lipid bilayer, forming the membrane pore space.

The processes of killing are generally accepted as the following three models:

1) Toroidal-pore model

The cell membrane can be inserted by antimicrobial peptides spatially, which leads to

the lipid monolayer continuously bending through the cell membrane, forming the hydrophilic core area. In order to form a ring hole, the peptide polar surface interacts with the lipid polar head, which connects the other side of the lipid layer. It forms holes from the top to the end of the lipid bilayer, consisting of peptide and lipid head. Comparing with Toroidal-pore model, the peptides always interact with the lipid head when it inserts vertically into the lipid bilayer.

2) Barrel-stave model

Peptides screw into the cell membrane and form an augmented pore as a barrel-stave on the cell membrane. The hydrophobic region paralleled to the core region of the lipid bilayer, the hydrophilic region is formed the inside surface of the pore. The efficient number and of the peptides could be changed by the lipid bilayer. Firstly, the peptide combined with the surface of the membrane. Next, the hydrophobic regions of peptide interact with cell membrane when the peptide inserted into the membrane. When the peptides arrive at the region of the hydrophobic regions of the cell membrane, they form a transmembrane pore with the hydrophilic region.

3) Carpet model

Antimicrobial peptides attach parallel to the surface of the cell membrane by electrostatic attraction of anionic lipid head groups. This model produces a peptide blanket to cover the membrane surface. When the concentration of antimicrobial peptides reaches the threshold, the lipid micelles can be formed. The hole is produced immediately at the concentration of the critical threshold, and it allows more antimicrobial peptides through the membrane, which leads to the membrane collapse.

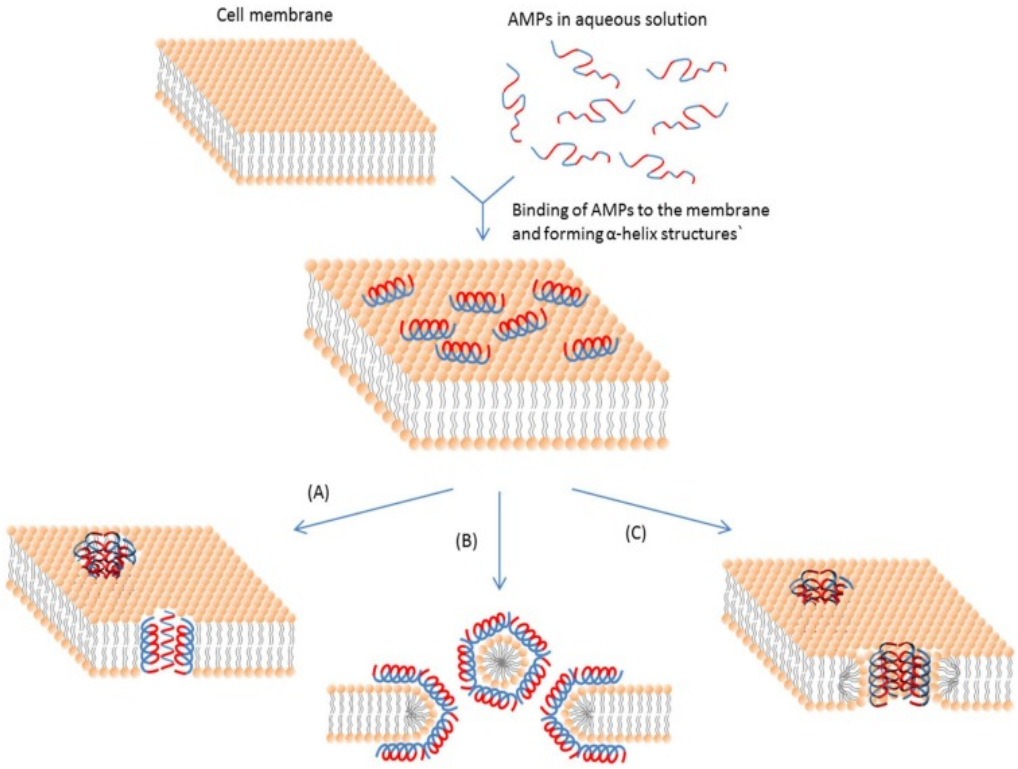

Figure 1.1 Brief schematic representation of membrane-active AMP action mechanisms. (A) Barrel-stave model. The AMP molecules aggregate and insert vertically into the membrane bilayer. In this model, the hydrophobic regions of peptide are responsible for connecting with the lipid core. The hydrophilic regions form the interior region of the channel. (B) Carpet model. Some parts of the membrane are covered with the hydrophobic sides of AMP molecules. Then, pores are formed in the membrane. (C) Toroidal model. This model looks like the Barrel-Stave model. AMP molecules insert into the membrane, but they usually contact the membrane at the phospholipid head groups. The hydrophobic regions of AMPs are shown as blue and the hydrophilic regions of AMPs are shown as red. (http://www.mdpi.com/1424-8247/6/12/1543)

The hydrophobic interactions and electrostatic interactions on the membrane surface can lead to the death of microorganisms, but it is not the only way that AMPs can inhibit bacteria. When antimicrobial peptides act on target sites in cells, some antibacterial peptides can kill the bacteria without destroying the cell membrane. Gel electrophoresis, Western blotting, and DNA footprinting are commonly used to study the action of antimicrobial peptides on target sites. The study found that antimicrobial peptides can act against or even kill microorganisms by interfering with metabolism. The mode of action of antimicrobial peptides and target sites can be summarized as follows: 1) binding to acidic substances in cells, blocking DNA replication and RNA synthesis; 2) inhibiting cell wall synthesis and impeding cell division; 3) affecting protein synthesis; 4) Inhibiting intracellular enzyme activity (Seefeldt et al., 2015). In summary, the ways in which the antimicrobial peptides exterminate microorganisms are more likely to be caused by extracellular and cell membrane interactions and synergy between intracellular and target sites.

1.2.2 Nomenclature of AMPs

Based on the basic structure of natural antibacterial peptides, scientists began to design, modify, or replace amino acid residues of polypeptide sequences, which significantly increased the number of antimicrobial peptides. Therefore, it became challenging to classify all antibacterial peptides according to one criterion. However, the classification structure of the secondary structure and amino acid composition of the root antimicrobial peptides has been widely used. The antimicrobial peptides are roughly classified as follows: (1) α-helix antimicrobial peptides, including α-defensins, Cecropins, Magainins, Melittin, and Piscidins, etc. (2) β-sheet antibacterial peptides, which have a circular β-

sheet, β-sheets consisting of two or more disulphide bonds, such as β-defensins, Gramicidins, Tachyplesins, Protegrins, Thionin, Polymycin B, etc.; (3) Cyclic antimicrobial peptides, etc.

The results of biophysics studies using the Circular Dichroism (CD) and Nuclear Magnetic Resonance (MNR) techniques confirmed that most of the antimicrobial peptides are in the α-helix or β-sheet structure. The α-helix antibacterial peptides are generally in the form of disordered structures in the hydrophilic environment, while in the hydrophobic environment they are helical structures; conversely, the β-sheet antibacterial peptide is stabilised by its disulphide bond resulting in a relatively conserved secondary structure. It is a folded state whether in hydrophilic and hydrophobic environments (Evan et al., 2009; Salgadoa et al., 2001).

1.2.3 Diversity of structures of AMPs

Primary structure

Primary structures of antimicrobial peptides are characterized as amino acid sequences. Antimicrobial peptides have an uneven distribution of amino acid residues. The N-terminus is rich in cationic hydrophilic amino acids such as lysine, arginine and histidine, and the C-terminus often contains non-polar hydrophobic amino acids such as alanine, glycine and leucine, etc., thereby forming amphipathic cationic antibacterial peptide molecules. This structure is conducive to the electrostatic interaction between antimicrobial peptides and cell membranes, resulting in antibacterial activity. The primary structure is usually unstable, easily deformed when the environment changes and converts into a higher structure in a hydrophobic environment such as a cell membrane.

Secondary structure

Although the secondary structure of antimicrobial peptides is complex and diverse, they can be divided into four major types: α-helix structure, β-sheet structure, β-hairpin structure (or loop structure), and extended structure. Typically, the structure of antimicrobial peptides is not uniform, but some secondary structures appear in hydrophobic solutions that act on lipid membranes (Evan et al., 2009; Brogden et al., 2005; Smith et al., 2010). In general, antimicrobial peptides carry different amounts of positively charged amino acids, making the antimicrobial peptides closer to the cell membrane. At the same time, the hydrophobic amino acid and hydrophilic amino acid distribution of antibacterial peptides are arranged in the process of interaction with hydrophobic membranes, forming amphiphilic structures. By changing the permeability of the membrane, cells are inhibited or cell leakage and demise ensues.

Tertiary and quaternary structure

Many antimicrobial peptides not only have a secondary structure but also show the multi-structure in different environments. Won's study showed that GGN4 does not have a fixed tertiary structure in aqueous solution, but both β-sheet and a-helix structures present in lipid solutions. A more detailed study of the tertiary structure of GGN4 using nuclear magnetic resonance showed that the tertiary structure of GGN4 also varied in different lipid solutions such as 50% TFE aqueous solution and 80% aqueous methanol solution (Won et al., 2009). Similar results were obtained for the tertiary structure of nisin. It showed a very flexible structure in aqueous solution, but the stable molecular structure can be formed in a solution of dimethyl sulphoxide or trifluoroethanol. Its amphiphilic helical structure consists of two trisulphide rings. The 1 to 2 positions of the N-terminus and the 29 to 34 amino acid residues of the C-terminus form two hinge regions between

two trisulphide ring structures (Oman & van der Donk, 2009).

1.2.4 Structure-activity relationship studies on AMPs

The activity of antimicrobial peptides depends on the physicochemical parameters of amino acids (Pane et al., 2017; Zhang et al., 2017) The results show that several parameters are closely related to the activity of antimicrobial peptides as follows: secondary structure, cationicity, amphiphilicity, hydrophobic moment, hydrophobicity and polar angle (Hollmann et al., 2016; Hädicke et al., 2016; Rice & Wereszczynski, 2017; Mahindra et al., 2014). Any of the parameters can be changed which leads to changes in the activity of these bioactive peptides (Manzor et al. 2017).

Those characteristics can influence the antimicrobial activity and the toxicity of antimicrobial peptides (Yeaman & Yount, 2003). There is a strong correlation between all the factors, however the antimicrobial activity and hemolysis activity predicted by the given amino acid sequence is not comprehensive enough. Therefore, the design of the antimicrobial peptide should be considered by various influencing factors as follows.

1) Charge

The lipopolysaccharide (LPS) of the Gram-negative bacteria, and the peptidoglycan and teichoic acid of the Gram-positive lead to the negatively charged bacterial envelope. The peptides can be attracted to the surface of the bacteria by the electrostatic force between the negatively-charged bacteria and the positively-charged antimicrobial peptides (Giuliani et al., 2007). The positively-charged antimicrobial peptides substitute Mg^{2+} or Ca^{2+} on the structure of the gram-negative bacteria, which makes the cell membrane structural disorder, leading to more uptake of the molecule. The composition of the

electrical negative phospholipids of pathogenic bacteria cell membrane is phosphatidylglycerol, phosphatidylserine and cardiolipin, resulting a significant amount of negative charge on the surface of bacteria. The antimicrobial peptides are rich in arginine and lysine, it guarantees that the peptides can accumulate on the surface of the microbial cell membrane (Hancock & Sahl, 2006). The activity of natural antimicrobial peptides is related to cationicity, the positively charged amino acid can be used to substitute the acidic amino acid for increasing the activity of peptide (Tencza et al., 1999). On the contrary, the activity could be reduced by removing the positively charged amino acid residue. However, the relationship is not clear so far, as some instances also show that there is a direct, indirect or inverse relationship. However, with the increase of net charge in a specific range, the activity of peptide can be increased correspondingly (Yeaman & Yount, 2003).

By studying analogues of magainin-2, it was found that under the situation of maintaining hydrophobic and helicity, the net charge increasing to +3 or +5 could enhance the antimicrobial activity on Gram-negative bacteria and Gram-positive bacteria. The antimicrobial activity does not enhance with further increases in the net charge to +6 or +7, while the hemolytic activity of peptide is significantly increased (Dathe et al., 2001). For example, the antimicrobial activity of pseudin-2 exhibited a 16-fold increase by adding 2 more positive charges, but then no significant increases showed when continuing to increase the net charge (Pál et al., 2005). Jiang pointed out that the number of positively charged residues on the polar surface and net charge make major impacts on the antimicrobial and hemolytic activity of antimicrobial peptides. Through studying the synthesised 26 amino acid residues amphipathic α helix antimicrobial peptide, V13K, it was shown when positively charged peptides increased from +4 to +8, the antimicrobial

activity increased, but hemolytic activity remained at a low level. However, further increasing the electrostatic charge to +8 and +9, the hemolytic activity naturally enhanced. On the contrary, when the electrostatic charge was reduced below +4, the antimicrobial and hemolytic activity disappeared (Jiang et al., 2008).

2) Hydrophobicity

The hydrophobic region of antimicrobial peptides plays an essential role in their distribution into the biological lipid bilayer membrane. Most natural antimicrobial peptides contain about 50% hydrophobicity when they form their secondary structure (Yeaman & Yount, 2003). As host defense peptides, the hydrophobicity usually needs to satisfy two requirements (Nicolas& El Amri, 2009): firstly, the peptides need to be sufficiently soluble in aqueous solution in order to reach a certain concentration and can be transported to the target microorganism quickly (requiring low hydrophobicity)(Wang et al., 2013); secondly, the peptides must be able to interact with hydrophobic regions of the bilayer, interfering with the structure of bilayer membrane and enhancement of permeability (requiring high hydrophobicity); finally, the very high degree of hydrophobicity of antimicrobial peptides can hinder the targeting to microorganisms and the extremely low hydrophobic antimicrobial peptides could have insufficient affinity to lipids of cell membranes (Dathe & Wieprecht, 1999). Hydrophobicity is a pivotal factor to affect the effectiveness of antimicrobial activity, and it is one of the decisive parameters for the interaction.

Studies on antimicrobial peptides also showed that the correlation between the hydrophobicity and antimicrobial activity is not very correlated, but a direct relationship between the hemolytic activity and hydrophobicity seems more outstanding. The stronger hydrophobicity can induce more hemolytic activity (Hof et al., 2001). However, with the

positively-charged residues introduced on the non-polar surface of the helix of the peptide, the hemolytic activity could be reduced by the decrease of hydrophobicity. Through the study of analogues of magainin, it was found that with the increase of hydrophobicity, the selectivity of activity on membrane disruption was reduced dramatically (Dathe et al., 1997). The hydrophobicity can be reduced through the introduction to the hydrophobic face of a positively charged amino acid, D-amino acids or peptide-like residue or peptide cyclization (Matsuzaki, 2009).

3) Other parameters that influence the activity

The antimicrobial activity of α-helix broad-spectrum antimicrobial peptides is closely related to amphiphilic of antimicrobial peptide. In structures of α-helix antimicrobial peptides, peptides align along the polar side of hydrophilic amino acid residues, hydrophobic amino acid residues along the opposite side of the spiral, the structure of antimicrobial peptides and amphiphilic biofilm provides an optimised interaction. The hydrophobic moment generally expresses the amphiphilicity of the α-helix antimicrobial peptide (Yeaman & Yount, 2003), and it is a hydrophobic index vector, as a regular screw axis vector. The hydrophobic moment can lead to an increase of the role of antimicrobial peptides through the membrane and the hemolytic activity increases. Increasing the hydrophobic moment can lead to a rise of the membrane penetration and hemolysis activity of the antimicrobial peptides. However, the membrane disintegration activity could be adjusted by hydrophobic moment in a limited range (Dathe& Wieprecht. 1999).

Polar residues in the α-helix antimicrobial peptide are distributed periodically and stabilised the spiral structure (Hernández-Carneado et al., 2004). We can use some amino acids which have an effect on promoting or destroying spirals to adjust the screw of the antimicrobial peptides. The study found that in LL-37, Buforn-II and its homologue,

antimicrobial activity was associated with the degree of the alpha helix. With the increase of the number of alpha helices, the antimicrobial activity of the peptides increased as well (Park et al., 2000). Pouny (1992) pointed out that the spiral degrees in neutral are more critical than negative of the double membrane.

In addition to the content in antimicrobial peptides of amphiphilicity, spirals, the length of the antimicrobial peptides on the surface of the polar angle factors may also affect the activity of antimicrobial peptides, and the modification of some parameter structure can also cause the change of the other structure parameters as the structure parameters affect each other.

1.3 Anti-cancer activity of AMPs

1.3.1 Mechanisms of action

Research shows that in addition to the antibacterial activity of antimicrobial peptides, many antimicrobial peptides also exhibit anticancer activity. Similarly, the anti-tumour mechanism of antimicrobial peptides is also not precisely known. Many current studies have shown that the anti-cancer mechanism of antimicrobial peptides is not as same as the antibacterial mechanism. It is more complicated than the antimicrobial mechanism and can be summarised as follows: On the one hand, antimicrobial peptides can resist the invasion of cancer cells by mobilising the body's immune function from humoral immunity. On the other hand, it has direct contact with tumour cells by the cell membrane, mitochondria, nuclear membrane and other aspects, thus show the effect of inhibiting or killing cancer cells (Hoskin & Ramamoorthy, 2007; Chen et al., 2001).

For the mechanism of cell membrane attack, the current tendency believes that the anticancer mechanism of the antibacterial peptide is similar to the antibacterial mechanism. AMPs interact with the cell membrane through electrostatic and hydrophobic properties and destroy the membrane (Lehmann et al., 2006; Shai, 1999). Compared with normal eukaryotic cell membranes, the cell membrane of cancer cells contains a higher proportion of phosphatidylserine and glycosylated components (including glycoproteins and glycolipids), resulting in the higher electronegativity, fluidity, and surface area, which is conducive to improving the selectivity and tropism of antimicrobial peptides on cancer cells. Cecropin antibacterial peptides are bound by the electrostatic attraction between the positive charge on the peptide and the negative charge on the membrane phospholipid molecule, and then the hydrophobic surface of the antibacterial peptide is inserted into the hydrophobic membrane centre. The α-helix is left on the surface of the plasma membrane, disturbing the original order of proteins and lipids on the plasma membrane and increasing the positive charge outside the membrane, leading to membrane depolarisation. Due to the amphipathic nature of the α-helix structure, the antibacterial peptide can aggregate to form ion channels in cells, leading to leakage of the contents and disruption of osmotic pressure (Papo & Shai, 2005; Shin et al., 2007).

1.3.2 Peptides with anticancer activity

α-helix structure peptides

α-helix antimicrobial peptides are widely found in Nature and are the most typical structural type of antimicrobial peptides (Dennisona et al., 2007). Moreover, some of

these have also been found to have antitumor activity. Cecropins isolated from *Hyalophora cecropia*, insects and mammals have been confirmed by many researchers as having potential antitumor activity. The most antimicrobial peptides isolated from amphibians have α-helix structures, such as Magainins, Aureins, Citropins, Dahleins, Maculatins, Uperins, and Caerins families (Dennison et al., 2007). Moreover, the first antimicrobial peptide shown to have anticancer activity was Magainin-2 derived from *Xenopus laevis*. Studies have shown that Magainin-2 can kill a variety of cancer cells *in vitro* and also significantly inhibits the growth of mouse ascites tumours *in vivo*, and improve the survival rate of tumour-bearing mice (Lehmann et al., 2006). A large proportion of amphibian antimicrobial peptides were isolated from frog epidermal secretions, and such α-helix antimicrobial peptides have significant killing effects on approximately 55 tumour cell lines (Apponyi et al., 2004).

β-sheet structure peptides

β-sheet antibacterial peptides are derived from many animals and plants. Compared with α-helix antibacterial peptides, their structures of many β-sheet antibacterial peptides contain α-helical units. Generally, the β-sheet antibacterial peptide contains a significant amount of cysteine and forms a disulphide bond structure. The disulphide bond structure plays a vital role in stabilising the structure of antibacterial peptides and preventing protease hydrolysis. β-sheet antibacterial peptides mainly include mammalian α and β defensins, plant defensins, insect defensins, proline-rich antibacterial peptides and lactoferrin, etc.

Linear structure peptides

The linear structure of anticancer peptides refers to a linear peptide having no secondary structure. This kind of anticancer peptide is typified by PR-39 and so on. PR-39 belongs

to the *Cathelicidin* family, generally isolated from the porcine intestine and neutrophils, containing 39 amino acid residues with the sequence: RRRPRPPYLPRPRPPPFFPPRLPPRIPPGFPPRFPPRFP. In addition to its biological activities of anti-microbial, angiogenesis and tissue repair, PR-39 can also significantly inhibit the invasive activity of HLF hepatoma cells, thereby achieving anti-cancer effects (Gao et al., 2014), but its mechanism is not yet clear.

Hybrid peptides

Through the design and modification of antimicrobial peptides, a variety of hybrid peptides were obtained. Typically, one antibacterial peptide is selected, some amino acid residues are replaced or deleted and then merged with another antibacterial peptide fragment. Studies have shown that some of the modified antimicrobial peptides have similar or higher activities than the natural forms, as well as a lower degree of toxicity (Masayuki et al., 2011).

1.4 Aims and objectives of this thesis

1. Isolation and identification of novel peptides from lyophilised skin secretion of Phyllomedusinae frogs by using reverse-phase HPLC, MALDI-TOF MS and ESI-tandem MS(ESI-MS/MS).

2. Screening of fractions derived from above for antimicrobial and pharmacological activity using antimicrobial assays.

3. Construction of a cDNA library from lyophilised skin secretion and from this, molecular cloning of biosynthetic precursor-encoding cDNAs of novel peptides.

4. Solid-phase chemical synthesis of novel peptides whose primary structures and bioactivities have been unequivocally established by the above procedures.

5. Quantitative bioassay of the synthetic replicate of the novel peptide in functional biological assays.

Chapter 2

Materials and Methods

2.1 Specimen Biodata and Secretion Harvesting

Adult specimens of frogs were captured and maintained in a purpose-designed amphibian facility at 20-25℃ under a 12h-light/12h-dark cycle in Animal Facility of Queen's University Belfast. The specimens were fed multivitamin-loaded crickets three times per week for at least 4 weeks prior to secretion harvesting.

The dorsal skin surface of all specimens was stimulated by gentle transdermal electrical stimulation (6V DC;4 ms pulse-width; 50 Hz) through platinum electrodes for two periods of 20s. The resultant viscous white secretions were washed from the skin with deionised water, snap-frozen in liquid nitrogen and finally lyophilised and stored a -20 ℃ before analysis. All procedures were subjected to ethical approval and carried out under appropriate UK animal research personal and project licenses.

2.2 Molecular Cloning

2.2.1 mRNA Isolation

Five milligrams of lyophilised skin secretion were added into an RNase-free micro centrifuge 1.5 ml tube (I), and 1 ml Lysis/Binding buffer was used to dissolve this. The mixture was vortexed for 2 min then transferred onto ice for 30s. The procedure was repeated for 20 min. Then, 250 µl of Dynabeads® Oligo $(dT)_{25}$ beads were transferred into an RNase-free 1.5 ml tube (II) after thorough resuspension and the tube was placed on a magnetic rack to separate the beads and storage buffer. After the beads attached to one side of the tube, the supernatant was discarded. 250 µl of Lysis/Binding Buffer were transferred into tube (II) to wash the beads. The supernatant was discarded and

resuspended with 250 µl of lysis/binding buffer.

The skin secretion was mixed with 500 µl of lysis/binding buffer which was provided in the kit, followed by a 20min vortexing in total with a 1-min ice cool in each 1min interval so as to obtain the undegraded mRNA. Then, mixture of skin secretion was centrifuged for 5 min at 13,000 ×g. Then, the supernatant was transferred to the prepared Dynabeads. The tube was gently shaken at room temperature for 1 min with a subsequent 10s ice cool. This cycle took 15min to ensure full hybridisation between the poly-A tail mRNA and oligo-dT beads. The mRNA/beads complex was separated by the magnetic rack and then washed by 500 µl of Washing Buffer A for 3 times and 500 µl of Washing Buffer B twice in the same practice. Afterwards, 18 µl of elution solution was transferred into the tube to mix with the mRNA/beads complex, and it was then placed in a heating block at 80℃ for 2 min. After incubation, it was immediately placed on a magnetic rack and the supernatant containing mRNA was transferred into a new RNase-free 1.5 ml tube on ice as quickly as possible.

2.2.2 cDNA library construction

A BD SMART™ RACE cDNA Amplification Kit (BD Bioscience Clontech, UK) was applied in the first strand cDNA library construction and primary DNA amplification. For preparing both 3'-RACE ready cDNA library and 5'-RACE ready cDNA library, the following components (Table 2.1 and 2.2) were added into each new PCR tube before a brief vortex and centrifugation.

Table 2.1 The templates and primers used in 3'-RACE cDNA reactions

Component	Final Volume	Final concentration
RNA sample	4 µl	40%
3'-RACE CDS Primer (10 µM)*	1 µl	1 µM

Table 2.2 The templates and primers used in 5'-RACE cDNA reactions

Component	Final Volume	Final concentration
RNA sample	3 µl	30%
5'-RACE CDS Primer (10µM)**	1 µl	1 µM
BD SMART oligo (dT) (10 µM)***	1 µl	1 µM

*3'-RACE CDS Primer sequence:

5'–AAGCAGTGGTATCAACGCAGAGTAC$(T)_{30}$V N–3' (N = A, C, G, or T; V = A, G, or C)

**5'-RACE CDS Primer sequence:

5'–$(T)_{25}$V N–3' (N = A, C, G, or T; V = A, G, or C)

***BD SMART oligo (dT) sequence:

5'–AAGCAGTGGTATCAACGCAGAGTACGCGGG–3'

All the tubes were mixed well and centrifuged briefly for 10 s. Next, they were placed in a heating block at 70℃ for 2 min, then placed in an ice bath for 2 min. Then, additional reagents (Table 2.3) were added into the tube and mixed completely then the tube was flicked and centrifuged briefly to collect all contents at the bottom without bubbles.

Table 2.3 Additional reagents used in cDNA library construction

Reagent	Final volume	Final concentration
5×First-Strand Buffer	2 µl	1×
DTT (20 mM)	1 µl	2 mM
dNTP Mix (10 nM)	1 µl	1 mM
BD RTase (100 Uint/ µl)	1 µl	10 Uint/ µl

After adding all reagents, tubes were incubated in the Thermal Cycler (Applied Biosystems, UK) at 42℃ for 90 min to complete the reverse transcription reaction followed by dilution through adding 50 µl PCR water to each tube when the incubation was finished. Then, the mixture was subjected to additional heat at 72℃ for 7 min to correct faults in the reaction. At this point, 3'- and 5'- RACE ready cDNA libraries were obtained and stored in a -20℃ freezer.

2.2.3 Rapid amplification of cDNA ends (RACE) PCR

This procedure was performed by using the BD SMART^{TM} RACE cDNA Amplification Kit (BD Bioscience Clontech, UK). The following components (Table 2.4) were combined and mixed completely for the RACE-PCR reaction.

Table 2.4 The components of one RACE-PCR reaction

Component	Final Volume	Final concentration
PCR water	3.1 µl	-
dNTP Mix (10 mM)	0.2 µl	0.2 mM
Sense Primer (20 µM)*	0.5 µl	1 µM
Nested Universal Primer (NUP) (20 µM)	0.5 µl	1 µM
10× Advantage 2 PCR Buffer	1.5 µl	1.5×
50× Advantage 2 Polymerase Mix	0.2 µl	1×
3'-RACE ready cDNA library**	5 µl	-

* The sequence of the degenerate Sense Primer was:

5'-GAWYYAYYHRAGCCYAAADATG-3'

** 3'-RACE ready cDNA library was substituted with the same volume of PCR water in the negative control group.

All the reagents were pipetted completely and micro-centrifuged to collect all contents at the bottom without bubbles. Finally, the RACE-PCR programme with a gradient temperature was set and commenced in the thermal cycler (ThermoFisher Scientific, USA), choosing the 'RACE PCR' programme as below. Afterwards, the products were stored at 4°C.

Stage 1 initial denaturation at 96 °C for 1 min.

Stage 2 40 cycles (denaturation at 96 °C for 20 s, primer annealing at 55 °C for 10 s, extension at 60 °C for 4 min).

Stage 3 final extension at 72 °C for 10 min.

2.2.4 Gel analysis

One litre of 1× Tris/Borate/EDTA (TBE) buffer was prepared by using 100 ml of UltraPure™ 10× TBE Buffer (Invitrogen), and 900 ml of ddH_2O. 35 ml of TBE Buffer and 0.45g agarose (Sigma-Aldrich, catalogue number: A9536) were mixed into a 100ml flask. Then, the mixture was heated in a microwave oven until the liquid was clear and then it was cooled down to around 50℃. Next, 2.5 µl of the Ethidium bromide (EB), 10 mg/ml, was transferred to the flask and mixed well. The melted agarose gel was poured into the casting tray in an electrophoresis tank, and a comb was placed on the gel to form the wells. The comb and the gel gates were removed when the gel was cool and solidified. Then, tank was filled by 1× TBE Buffer. 1.75 µl of each RACE PCR reaction was mixed with 0.35 µl of 6× DNA Gel Loading Dye (Thermo Scientific), and subsequently added into the wells in the gel. Next, the electrophoresis tank was turned on set at 95 V for 20 min. Finally, the gel was analysed by using a UV- light transilluminator (BioDoc® Imaging System, UVP).

2.2.5 PCR products purification

An E.Z.N.A.® Cycle Pure Kit (Omega Bio-Tek, USA) was employed to purify PCR product, in which DNA was bound to a bsilica-based filter membrane during washing steps and eluted for collection.

The CP Buffer of 5 times volume of PCR products in total was added to one positive sample and mixed well. A cartridge was placed into a 2 ml wash tube. Then the positive sample was transferred to a HiBind DNA Mini Colum and centrifuged at 10,000 ×g for

1 min and the flow-through liquid was then discarded. Next, the cartridge was placed back into a 2 ml wash tube and 700 µl of DNA Wash Buffer was added into the cartridge. Then it was centrifuged at 10,000 ×g for 1 min and the flow-through liquid was discarded. The cartridge was placed back as before and 500 µl of DNA Wash Buffer was added into the cartridge, and it was centrifuged as before. The flow-through liquid was discarded as well. Then it was centrifuged again at 10,000 ×g for 2 min to remove all the residual wash buffer. After that, the sample was placed into a 1.5 ml recovery tube and 30 µl of PCR Grade water was transferred to the centre of the cartridge. It was placed at room temperature for 2 min and the elution was collected after centrifugation at 10,000 ×g for 1 min. The DNA sample was subsequently dried in a concentrator (Eppendorf, UK) for 1h and then was sealed with Parafilm M® for protection.

2.2.6 Ligation

A pGEM®-T Easy Vector system (Promege, USA) was utilised to finish the ligation of RACE PCR purified product. The DNA with A at both ends of the strand could bind to and insert into the site of the pGEM®-T Easy Vector with T via A-T base pairing.

The dried DNA sample was resuspended into 8 µl of PCR Grade Water and vortexed for 1 min without keeping the tube on the vortex consistently. Then, the tube was centrifuged briefly. Next, the following prepared reagents (Table 2.5) were combined in a new DNase-free PCR tube, after which, the complex was incubated at 4°C overnight (16-20h) for maximum number of transformants.

Table 2.5 The components of the ligation reaction

Component	Final volume	Final concentration
2× Rapid Ligation Buffer*	2.5 µl	1×
pGEM®-T Easy Vector (50ng/ µl)**	0.5 µl	5 ng/µl
Prepared resuspended PCR product	1.5 µl	-
T4 DNA Ligase (3 Unit/ µl)	0.5 µl	0.3 Unit/ µl

* 2× Rapid Ligation Buffer was vigorously vortexed without centrifugation because ATP involved was unstable to heat resulted from spinning and ions in the buffer may precipitate during this process.

* *Due to fragmentation of their circular structures, pGEM®-T Easy Vectors should not be mixed by vortexing but by centrifugation.

2.2.7 Transformation

The LB Agar gel was prepared in the ratio of 3.2 g LB Agar/100 ml ddH_2O. The LB Agar, ddH_2O and a sterile magnetic rotor was added to the flask. The mixture was mixed well using an auto-stirrer. The flask with cap was sealed and sent to the autoclave. Then, it was cooled down to about 65°C. 255 µl of ampicillin (200 µl/100 ml) was transferred to the flask and it was shaken gently for mixing. Then the mixture was poured into 8 Petri dishes, and each dish was shaken gently with the lid closed. 100 µl of IPTG (0.1 M) was added to each dish when the gels had solidified, and it was spread by an L-spreader. Then, 20 µl of X-gal (500mg/L) was transferred to each LB plate and it was spread immediately. After that, the plates were put upside down and placed into the incubator for 20-30 min to activate.

A volume of 2.3 µl of Ligation product was transferred to a 1.5 ml tube in the ice bath.

Then 50 µl of semi-thawed JM109 *E.coli* cells were added into the tube rapidly and gently flicked. The tube was kept in the ice bath for 20 min. After 20 min, the tube was heat-shocked in the heating-block at 42°C for 47s and removed immediately from block to the ice bath for 2 min without shaking. Then 950 µl of SOC medium was added into the tube and the mixture was placed in the swing bed at 37°C for 2.5h (at 60 ×g). After incubation, 110 µl of the transformation products were added to each LB plate for 5 plates in total and it was spread with L- spreader. Then the 5 plates were put upside down in the incubator at 37°C for about 20h.

2.2.7 Blue-White colony screening

After the colonies were incubated, the white colonies were streaked onto the fresh LB/AMP/IPTG/X-gal plate by drawing a continuous line resembling a 'Z'. Then, the plates were placed in the incubator at 37°C overnight.

2.2.8 Isolation of recombinant plasmid DNA

After the overnight incubation, the pure white colonies were harvested by 200 µl pipette tips and transferred into the tube containing 20 µl of ddH_2O. After resuspending the cells, all the tubes were heated in the heating block at 100°C for 5 min, and then placed in the ice bath for 5 min. After those steps, the tubes were vortexed for 30s, then centrifuged for 5 min at 10,000 ×g. The plasmid DNA was in the supernatant.

2.2.9 Cloning PCR

The isolated products of recombinant DNA in section 2.2.8 were thawed and centrifuged at 10,000 × g for 5 min to collect the supernatant. In order to validate and amplify the plasmids extracted from competent *E. coli* cells, another PCR reaction was performed and each reaction PCR tube contained the reagents shown in Table 2.6. All the reaction PCR tube contents were mixed, flicked and centrifuged briefly to collect all contents at the bottom without bubbles, after which, they were subjected to the following PCR programme (Table 2.7). The cloning PCR products were placed in -20℃ storage afterwards and needed to be thawed and centrifuged briefly before use.

Table 2.6 The components of the cloning PCR reaction

Component	Final volume	Final concentration
5× Cloning Buffer	10 µl	1×
dNTP Mix (10 mM)	1 µl	0.2 mM
M13 Forward Primer (20 µM)	2.5 µl	1 µM
M13 Reverse Primer (20 µM)	2.5 µl	1 µM
PCR Water	31 µl	-
Taq Polymerase (5 Unit/µl)	0.25 µl	0.025 Unit/µl
DNA supernatant	2.5 µl	-

Table 2.7 The cycles of cloning PCR

Number of cycles	Procedure	Temperature	Time
1 cycle	Initial denaturation	94 ℃	1 min
31 cycles	Denaturation	94 ℃	30 s
	Annealing	55 ℃	30 s
	Extension	72 ℃	3 min
1 cycle	Final extension	72 ℃	3 min
1 cycle	Preservation	4 ℃	7 min

2.2.10 Gel electrophoresis & selected cloning PCR products purification

The products of cloning PCR were subjected to gel analysis as described in section 2.2.4. The selected PCR products were then purified and washed according to the same protocol as described for 3'-RACE PCR products in section 2.2.5.

2.2.11 DNA cycle sequencing reaction

A BigDye® Terminator v3.1 Cycle Sequencing Kit (Applied Biosystems, USA) was utilised in the DNA sequencing reaction in which the sequence was detected by fluorescence during DNA extension and termination processes.

The following components (Table 2.8) were mixed for each sequencing PCR reaction and were subjected to the PCR programme (Table 2.9). Finally, the sequencing products were stored at -20℃.

Table 2.8 The components of the sequencing PCR reaction

Component	Final volume	Final concentration
PCR Water	12.4 µl	-
M13 Forward or Reverse Primer (3.2 µM)	1.14 µl	0.16 µM
2.5× Ready Mix	2.86 µl	0.33 ×
5× Sequencing Buffer	3.57 µl	0.81 ×
DNA template	1.8-2.5 µl	-

Table 2.9 The cycles of sequencing PCR

Number of cycles	Procedure	Temperature	Time
1 cycle	Initial denaturation	96 ℃	1 min
	Denaturation	96 ℃	20 s
30 cycles	Annealing	55 ℃	10 s
	Extension	60 ℃	4 min
1 cycle	Preservation	4 ℃	7 min

2.2.12 Ethanol purification

Firstly, 10 µl of PCR Grade Water were added into each 1.5 ml tube. Then, 72 µl of 95% ethanol were added to each sample and then transferred to the tube directly. The tubes was vortexed for 30 s and placed at room temperature for 20 min before centrifuged at 13,000 ×g for 20 min. Then the ethanol was discarded very carefully. After that, 260 µl of 70% ethanol were added to each tube and vortexed for 10 s before centrifugation at

13,000 ×g for 10 min. The supernatant was removed again as completely as possible. The residual ethanol was then fully removed by the concentrator (Eppendorf, UK) by being vacuum-dried for 3-4 h.

2.2.13 Sequencing

The dried DNA sample was dissolved in 10.3 µl of highly-deionised formamide (HiDi) and vortexed for 30 s before being centrifuged briefly. All the tubes were heated at 95°C for 4.5 min in a heating block and transferred immediately on ice for another 3.5 min. Then all the samples were transferred into a 96-well sequencing plate and sequenced by an ABI 3730 automated sequencer (Applied Biosystems, USA).

2.3 Solid Phase Peptide Synthesis (SPPS)

2.3.1 Peptide synthesis

All the peptides were synthesised efficiently by the Tribute^{TM} Peptide Synthesiser (Protein Technologies, USA). All dry amino acids required were used in a 4-fold molar excess over the desired molar quantity in order to assure the purity and accuracy of product.

In detail, 1.2 mmol for every amino acid was weighed separately into acetone-cleaned amino acid vials, each mixed with 2-(1H-benzotriazol-1-yl)-1,1,3,3-tetramethyluronium hexafluorophosphate (HBTU) in equal proportion. The rink amide resin was utilised as the solid phase due to amidation at the C-terminus, weighed in the same molar quantity as the final product (0.3 mmol) and transferred into the reaction vessel.

After loading the carousel with amino acids, a reaction vessel start and stop position were selected as were coupling programmes for each amino acid. The process and reagents involved in SPPS are illustrated in Table 2.10. Nitrogen, a vortex and a vacuum are indispensable during the whole synthetic procedure. In detail, the Fmoc amino acids were dissolved in Dimethylformamide (DMF), and the Fmoc groups were removed from the amine group using 20% piperidine in DMF. Then, the amino acid was coupled with a free carboxyl group of the former amino acid in the presence of HBTU and 1M of N-Methylmorpholine (NMM) in DMF. After fully washing away the remaining amino acid and other reagents from the previous reaction, another deprotection process was carried out for preparing the next amino acid coupling reaction. Finally, degassed dichloromethane (DCM) was employed for washing the peptide/resin complex after the synthetic reaction, which was followed by drying the complex in a vacuum desiccator overnight.

Table 2.10 The main synthetic cycles of SPPS

Step	Action	Reagent
1	Wash resin	DMF
2	Deprotect N-terminus	Piperidine/DMF(1:4)
3	Wash resin	DMF
4	Activate C-terminus, mix and couple	NMM/DMF(11:89)

2.3.2 Cleavage and deprotection of peptides

After synthesis, the product was weighed and transferred into a 50 ml round bottomed flask. Next, the cleavage cocktail was prepared as (25ml/g: 94% Trifluoroacetic acid (TFA), 2% Thioanisole (TIS), 2% 1,2-Ethanedithiol (EDT), 2% water). Then the cocktail was added into the flask with a stirring bar and the flask was placed at room temperature

for at least 2 h.

The cleavage mixture was filtered into a 50ml round-bottomed flask by using the Buchner funnel, and the resin was washed by 3 ml DCM 3 times. Next the filtrate was concentrated by rotary evaporation to nearly dryness. 45 ml of the ice-cold diethyl ether was added to the flask then the mixture was transferred to a 50ml tube, and refrigerated at -20ºC overnight to complete the peptide precipitation.

2.3.3 Washing and drying

The next day, the 50 ml tube was shaken to mix contents well and centrifuged at 5,000 ×g for 5 min. Then the supernatant was removed and 45 ml of ice-cold diethyl ether was added into the tube for washing the peptide. After the washing step was repeated 3 times, the peptide was air-dried, and the remaining ether was evaporated at room temperature.

The dried peptide was dissolved in an appropriate volume of Buffer A (99.95% H_2O and 0.05% TFA) and Buffer B (80% acetonitrile, ACN, 19.95% H_2O and 0.05% TFA). Only when the peptide was hard to dissolve completely was Buffer B added and the final volume was about 15-20 ml, followed by lyophilisation.

2.4 Reverse Phase High Performance Liquid Chromatography HPLC (RP-HPLC)

2.4.1 Preparation of RP-HPLC mobile phase

The mobile phase of RP-HPLC consisted of two buffers. Buffer A was prepared using 99.95% H_2O and 0.05% TFA. Buffer B was prepared as 80% acetonitrile, ACN, 19.95% H_2O and 0.05% TFA. Both buffers were freshly-prepared and thoroughly degassed prior to use.

2.4.2 RP-HPLC analysis of amphibian skin secretion

The Waters Dual Pump HPLC system assembled with a Phenomenex® Jupiter® C5 300A LC Column (25 × 1 cm) was employed to separate the bioactive peptides in the skin secretion. In detail, 5 mg of crude lyophilised frog skin secretion was dissolved by 1 ml of buffer A. After that the sample was thoroughly mixed by vortexing and centrifuged at 13,000 × g for 5 min in an Eppendorf Centrifuge 5424 (Eppendorf, Germany), the supernatant from which was transferred into a 2 ml sample vial. The sample vial was placed on the Waters autosampler and subsequently injected into the HPLC column. The detection wavelength was set as 214 nm. The flow rate was 1 ml/min. The linear gradient method was programmed from 0% buffer B to 100% buffer B within a running time of 240 min. The HPLC fraction was collected every minute in a 3 ml test tube. The RP-HPLC system was equilibrated with 100% buffer A before use and washed by 100% buffer B for 30 min. The C5 column was stored in 65% ACN in water without any TFA.

2.4.3 RP-HPLC purification of synthetic peptides

The purification of the crude synthetic peptide was carried out by a Cecil Adept^{TM} CE4200 system fitted with a Phenomenex® Jupiter® C5&C18 300A LC Column (25 × 2.1 cm). At first, 4 mg of crude lyophilised peptide was dissolved in a 1.5ml tube with 500 µl buffer A and 500 µl buffer B. Then after a 5-min vortexing, the tube was centrifuged at 18,000 ×g for 5 min in an Eppendorf Centrifuge 5424 (Eppendorf, Germany) and the clear supernatant was the analyte. The HPLC system also equilibrated with 100% buffer A for 30 min before use. Then the analyte was injected into the column and eluted with a linear gradient from 0% B to 100% B in 80 min at a flow rate of 4 ml/min with a simultaneous 214 nm wavelength detection. The fractions at each peak were collected separately in tubes and utilised for identification. Finally, Buffer B was pumped to wash the column for 30 min.

2.5 Mass Spectrometry

2.5.1 Matrix-assisted laser desorption, ionization, time-of-flight (MALDI-TOF) mass spectrometry

A MALDI-TOF mass spectrometer (Voyager DE, PerSeptive Biosystems, USA) was used to analyse the masses of peptides. The matrix used in this experiment was α-cyano-4-hydroxycinnamic acid (CHCA), and it was prepared as 10 mg of CHCA dissolved in an acetonitrile/H2O/TFA (50%/49.95%/0.05%, v/v/v) solution. 2 µl of each sample was added onto the MALDI plate for testing. After the sample was air-dried, 1 µl of the matrix was added onto each sample and left to dry as well. Next, the sample plate was loaded into the mass spectrometer and the substances in the HPLC fraction were analysed by

MALDI-TOF MS.

2.5.2 LCQ Fleet™ Ion Trap Mass Spectrometer Sequencing

An LCQ Fleet™ ion-trap mass spectrometer (Thermo, USA) was used for the determination of the peptide sequences from the frog skin secretion. In detail, the fractions containing the corresponding molecular masses to those predicted from the cDNA precursor encoded peptides were subjected to LCQ analyses. The data-dependent "triple play" method was employed and defined as "Full scan/Zoom in/MS2". The scan range for full scan was set as 300 to 2000 m/z. The top 2 intensive ions were subjected to zoom scan to determine the charge state of the ion. Finally, the ions were fragmented under a Normalised collision energy (NCE) of 30. The MS2 spectra were subjected to Protein Discoverer 1.0 software (Thermo, USA) against the house-defined database. The sample was ionised under the spray voltage of 4.5 kV with capillary temperature of 320ºC. The flow rate of the LC pump was 100 μl/min.

2.6 Determination of Peptide Secondary Structures

2.6.1 Circular Dichroism (CD) analysis of synthetic peptides

Secondary structures of the synthesised peptides were determined using a JASCO J-815 CD spectrometer (Jasco, Essex, UK). The peptides were dissolved initially in 10 mM ammonium acetate and 50% TFE in 10 mM ammonium acetate to reach a concentration of 100 μM and then were added into a 1-mm high-precision quartz cell (Hellma Analytics, Essex, UK). CD spectra were obtained at 20°C from 190 nm to 250 nm at a scanning speed of 100 nm/min with 1 nm bandwidth and 0.5 nm data pitch. The data were further

analysed using online software K2D2 (http://cbdm-01.zdv.uni-mainz.de/~andrade/k2d2/) to calculate the percentage of α-helicity.

2.6.2 Computational analysis of synthetic peptides

The secondary structures of bioactive peptides were also analysed by online software. Their physiochemical properties and distribution of amino acid side chains were performed using the HeliQuest project (http://heliquest.ipmc.cnrs.fr/). Additionally, the secondary structures and 3D modules were predicted by the I-TASSAR server (https://zhanglab.ccmb.med.umich.edu/I-TASSER/). The interaction between peptides and molecular targets were examined using AutoDock (http://autodock.scripps.edu/).

2.7 Antimicrobial Assays

2.7.1 Viable cell counting

At first, 100 μl adjusted bacterial suspension was mixed with 900 μl phosphate-buffered saline (PBS) solution (pH 7.4) and ten-fold dilutions were made another five times. 20 μl of each diluted cell suspension with 3 replicates were spotted separately onto the prepared Mueller Hinton Agar (MHA) plate. Prior to incubation at 37 ℃ overnight, all liquid drops were air-dried. Finally, the microorganism colonies at countable dilution concentrations were counted in each drop, and the exact concentrations of bacteria were calculated using the following formula:

$$C=N/3\times50\times D,$$

where N represented the total quantity of the bacteria at a particular concentration while

D represented the dilution factor.

2.7.2 Minimum inhibitory concentration (MIC) assays

The reference strains including *Staphylococcus aureus* (NCTC 10788), *Escherichia coli* (NCTC 10418), *Candida albicans* (NCYC 1467), and *Pseudomonas aeruginosa* (ATCC 27853) were employed in this assay. Each strain was cultured separately with 100 ml of Mueller Hinton Broth (MHB) in the flasks. All the flasks were placed in a shaking incubator at 37 ºC and 200 rpm overnight. After incubation, 500µl of cell cultures were transferred into 20ml of pre-warmed sterilised MHB medium and incubated at 37℃ until the subcultured organisms reached their respective logarithmic growth phases, which could be measured by a UV spectrophotometer (λ=550 nm) when the optical densities (OD) of the subcultured suspensions reached the desired values below (Table 2.11). Subsequently, each suspension was diluted by an appropriate volume of pre-warmed MHB and mixed evenly to achieve the acquired concentration of 5×10^5 cfu/ml (cfu represents colony forming units).

Table 2.11 The desired OD values of the three microorganism cultures used

Microorganism	OD value	Concentration (cfu/ml)
S. aureus	0.23	10^8
E.coli	0.41	10^8
P. aeruginosa	0.40	10^8
C.albicans	0.15	5×10^6

The peptide was dissolved in the DMSO first and then mixed with diluted microorganism suspension to achieve final concentrations from 1-512 mg/L in 2-fold dilutions in 96-well test plates. Three control groups were set up as below:

- Vehicle Control 99 μl culture + 1 μl DMSO
- Negative Control 100 μl culture
- Blank Control 100 μl sterile MHB

The 96-well plate was transferred to the 37 ºC incubator overnight after mixing in the shaking incubator for 15 min. The plate was then observed perpendicularly and slots containing clear liquid represented no bacterial growth. On the other hand, for further detection, the absorbance of each well was monitored by the Synergy HT plate reader (Biotek, USA) at 550 nm wavelength and the viability of cells was calculated according the formula:

$$(OD_{Sample}-OD_{Sterile})/ (OD_{Growth}-OD_{Sterile}) \times 100\%$$

2.7.3 Minimum bactericidal concentration (MBC) assays

The clear solutions in sample groups of MIC assays at different concentrations, were chosen for the assessment of MBCs. 20 μl solution from each clear well was spotted onto a spare dried MHA plate, followed by incubation for about 6-8h. The MBC value was the lowest concentration where no colonies grew.

2.7.4 Biofilm assays

MBIC and MBEC testing was performed, with minor modifications, according to

(Knezevic and Petrovic, 2008; Sabaeifard et al., 2014), using the colorimetric indicator 2, 3, 5,-triphenyl tetrazolium chloride (TTC) to estimate microbial cell viabilities. Overnight bacterial cultures were washed once with pre-warmed PBS and diluted with fresh medium to 10^7 CFU/ml. For the MBIC assay, the peptide stock solutions were prepared in the same way and over the same concentration range as for the MIC assays and then incubated at 37°C for 24 h. Thereafter, the plates were washed twice with PBS followed by the addition of 200 µl fresh MHB with 2% glucose and 50 µl 1% TTC (w/v) solution per well. After 5 h incubation, 200 µL of the supernatant from each well were transferred to a new plate and its absorbance at 470 nm was determined using a Synergy HT plate reader (BioTek, Winooski, VT, USA). For the MBEC assay, 200 µL of the same diluted inoculum was dispersed into each well in a flat-bottomed 96-well plate for 48 h to form mature biofilms. After an appropriate time, the plates were washed three times with PBS to remove the planktonic cells and incubated with the same concentration range of peptide solutions as above at 37°C for 24 h. Thereafter, each well was washed, refilled with fresh medium, stained with TTC, and incubated for a further 5 h. Absorbance was measured in the same way as for the MBIC assays. MBICs and MBECs were determined as the lowest concentrations at which no colorimetric metabolites were formed by the bacteria.

The biofilm initial attachment (IA) inhibition assay was performed using *P. aeruginosa,* a strong biofilm-producing bacterium, using a slightly modified version of the method of (Zhang et al., 2016). Briefly, different concentrations of the peptide solutions and diluted bacterial inoculum were loaded in the same way as with the MBIC assays, but with an incubation time of only 1 h and also without agitation to facilitate bacterial binding. Thereafter, the wells were washed with PBS, fixed with methanol, air-dried and stained

with 0.1% (w/v) crystal violet, and washed with tap water before being air-dried. Finally, the crystal violet was solubilised in 33% acetic acid and the absorbance at 550 nm was measured in a plate reader to calculate the IC_{50} of biofilm initial attachment inhibition.

2.7.5 Cytoplasmic material leakage assays

As an indicator of the potential lysis of the microbial cell membranes in the presence of the peptides, cytoplasmic material leakage assays were performed (Samanta et al., 2013; Sahu et al., 2009). Briefly, overnight microbial cultures of *S. aureus*, *E. coli* and *C. albicans* were washed with pre-warmed PBS and diluted to 5×10^5 CFU/ml in PBS. The synthesised peptides to be tested were dissolved in PBS and two-fold diluted as described above to achieve a final concentration range from 512 to 1 mg/L. Triton-X 100 (0.2%) in PBS was used as a positive control, with 100 µl of different concentrations of the peptide in PBS (512 to 1 mg/L) being used as blank controls. The plates were incubated at 37°C for 2 h before the contents in each well were filtered through 0.22-µm syringe filters (Sigma-Aldrich, St. Louis, MO, USA) into new plates. A volume of 100 µl of the supernatant was transferred into a new 96-well plate and the absorbance at 260 nm was measured using a plate reader.

2.8 Haemolysis assays

Firstly, 2 ml of fresh defibrinated horse blood (TCS Bioscience ltd, UK) were transferred into a 50 ml universal tube and centrifuged at 930 ×g for 5 min to discard the supernatant and harvest erythrocytes at the bottom. These blood cells were washed with 30 ml autoclaved PBS solution (pH 7.4) by gentle orbital shaking and then centrifuged (930 ×g,

5 min) to discard the supernatant. This washing step was repeated until the supernatant was clear. Then, the universal tube was refilled with PBS solution (pH 7.4) to the final volume of 50 ml to obtain an even 4% (v/v) erythrocyte suspension after gentle shaking.

The stock solution of peptide was prepared in PBS solution (pH 7.4), and a two-fold dilution was used to obtain a series of gradient concentrations from 1024 to 2 mg/L. Then, 200 μl of the peptide solutions at different concentrations with five replicates were transferred into corresponding 1.5 ml tubes and an equal volume of 4% erythrocyte suspension was added slowly into each tube, making up sample groups. The other two groups utilised in this assay are shown in Table 2.12. Subsequently, all tubes were incubated at 37 ℃ for 2h (Genlab Limited, UK).

Table 2.12 The components of the additional experimental groups (each n=5)

Group name	Composition
Negative control group	200 μl PBS and 200 μl erythrocyte suspension
Positive control group	200 μl 2% Triton X-100 and 200 μl erythrocyte suspension

After incubation, all tubes were centrifuged at 930 ×g and 100 μl supernatant from each tube was transferred into corresponding wells of the 96-well plate. Finally, the absorbance of supernatants was detected at 570 nm wavelength by the Synergy HT plate reader (Biotek, USA) and the percentage haemolysis was calculated according the formula:

$$\% \text{ Haemolysis} = (A - A_0) / (A_X - A_0) \times 100\%$$

(A = absorbance of test solution, A_0 = absorbance of negative control and A_X = absorbance of positive control.)

2.9 Anti-cancer cell proliferation assays

2.9.1 Thawing frozen samples of cells

All the cell lines used in this study were stored at -80ºC, and the cells were cultured by the following process. The cryovials containing frozen cells were removed from the freezer and transferred into a pre-warmed 37 ºC water bath immediately. 1 ml of the thawed cells was transferred from the vials into a culture flask containing 15 ml pre-warmed growth medium and then placed into an incubator at 37 ºC 5% CO_2 overnight.

2.9.2 Sub-culturing of adherent cells

The medium in the flask was removed and then the cells were washed with 10 ml of pre-warmed PBS. Next, 1 ml of trypsin was added onto the cells and the flask was incubated at 37 ºC 5% CO_2 for 5 min. After that, the cells was detached from the flask and 10 ml of warmed growth medium were then transferred into the flask and pipetted to ensure the cells was separated from the bottom of the flask. The medium containing cells was transferred into a 15 ml tube and centrifuged at 920 ×g for 5 min and then the supernatant was removed. 4 ml of fresh growth medium were transferred into the 15 ml tube and the tube was vortexed.

2.9.3 Seeding of cell culture

A volume of 50 µl of the cell suspension was mixed with 50 µl of Trypan Blue solution in a small well by gently pipetting. A coverslip, covering a haemocytometer, was filled with the cell suspension and then observed under a microscope. Cell counts were obtained by the following formula:

$$T = Q \times 10^4 \times 2,$$

where T is the total cell number/ml, Q is the number of living cells in each square.

The cell suspension was diluted to 50 cells/ µl and then 100 µl of diluted medium was added to each well in a 96-well plate. The plate was placed in an incubator at 37 ºC under 5% CO_2 for 24 h.

2.9.4 MTT assay

The next day, the medium in the 96-well plate was discarded and 100 µl of pre-warmed serum-free medium was added to each well. Then it was incubated at 37 ºC 5% CO_2 for 12 h. After starvation, the peptides were prepared in different concentrations with serum-free medium from 10^{-4} to 10^{-9} M. The medium in the 96-well plate was removed and 100 µl of peptide solutions were added to each well. Then it was placed in an incubator at 37 ºC 5% CO_2 for 24 h. On the following day, 10 µl of MTT was added to each well and incubated for 4 h at 37 ºC 5% CO_2. Then, the medium was discarded and 100 µl of DMSO was transferred into all the wells. The absorbance of each well was measured at 550nm by using a BioTek ELx808^{TM} Absorbance Microplate Reader.

2.10 Statistical Analyses

For all assays, all peptide concentrations and controls were tested in three independent experiments of five replicates each. The statistical analyses employed t-test and one-way ANOVAs, with the statistical significance of the differences being indicated as * ($p < 0.05$), ** ($p < 0.01$), and *** ($p < 0.001$). The dose-response curves were constructed using a "best-fit" algorithm and HC50 and IC50 values were calculated through the data-analysis package in GraphPad Prism 6 (GraphPad Software, La Jolla, CA, USA).

Chapter 3

Biological activities of cationicity-enhanced and hydrophobicity-optimized analogues of an antimicrobial peptide, dermaseptin-PS3, from the skin secretion of *Phyllomedusa sauvagii*

Published online 2018 August 08. Toxins. 2018; 10(8), pii: E320.

doi: 10.3390/toxins10080320 PMID: 30087268

Abstract

In the process of evolution, amphibian skin has played an important role in self-defence. The skin secretions of frogs from the subfamily Phyllomedusinae have long been known to contain a number of compounds with antimicrobial potential. Herein, a biosynthetic dermaseptin precursor-encoding cDNA was obtained from a *Phyllomedusa sauvagii* skin secretion-derived cDNA library, and thereafter, the presence of the mature encoded peptide, namely dermaseptin-PS3 (DPS3), was confirmed by LC-MS/MS. Moreover, this naturally-occurring peptide was utilized to design two analogues, $K^{5,\ 17}$-DPS3 (introducing two lysine residues at position 5 and 17 to replace acidic amino acids) and $L^{10,\ 11}$-DPS3 (replacing two neutral amino acids with the hydrophobic amino acid, leucine), improving its cationicity on polar/unipolar faces and hydrophobicity in highly conserved sequence motifs, respectively. The results with regard to the two analogues, showed that either increasing cationicity, or hydrophobicity, enhanced the antimicrobial activity. Also, the latter analogue had an enhanced anticancer activity, with pre-treatment of H157 cells with 1 μM $L^{10,\ 11}$-DPS3 decreasing viability by approximately 78%, even though this concentration of peptide exhibited no haemolytic effect. However, it must be noted that in comparison of the initial peptide, both analogues demonstrated higher membrane-rupturing capacities towards mammalian red blood cells.

3.1 Introduction

Of the many anuran skin-derived peptides known, dermaseptin and dermaseptin-like peptides from Hylidae frogs are the candidates with highest potential for developing new antibiotics (Nicolas and El Amri, 2009, Nicolas and Ladram, 2013, Huang et al., 2017). Although there is much heterogeneity in peptide sequences and lengths, among dermaseptins, the family nevertheless share several common structural characteristics, including a Trp residue at position 3 and a conserved sequence motif - AA(G)KAALG(N)A - in the mid-region (Amiche et al., 2008). In addition, dermaseptins commonly possess a high propensity to adopt an α-helical conformation in hydrophobic media, since the first dermaseptin peptide with 80% α-helical conformation was isolated from Hylidae frogs (Huang et al., 2017, Mor et al., 1991, Strahilevitz et al., 1994). Pharmacologically, apart from broad-spectrum antimicrobial activity (e.g, dermaseptin S4 and B), haemolytic activity and anticancer activity have also been reported (dermaseptin-PH and B2) (Huang et al., 2017, Kustanovich et al., 2002, Dos Santos et al., 2017).

Numerous studies indicate the net charge is a key factor influencing the binding of AMPs to membranes, as AMPs bind to the membrane by electrostatic interaction and competitively replace the divalent cations (Brown and Hancock, 2006, Schmidtchen et al., 2014, Zhang, et al., 2018) Therefore, it is believed changing the number of positive charges present in an AMP can likely change its membrane binding ability, resulting in a change in antimicrobial activity. Also, in general, approximately half of AMP amino acid residues are hydrophobic, and their hydrophobicity and their activity can be altered by changing the number of Leu, Ile, and Val residues in these peptides. However, both antibacterial and haemolytic activities of these AMPs tend to increase simultaneously by

increasing the hydrophobicity, due to the fact that the hydrophobic groups play a key role in their insertion into the cell membrane (Schmidtchen et al., 2014).

Herein, we describe the discovery of a biosynthetic dermaseptin-encoding precursor, preprodermaseptin, encoding an antimicrobial peptide, DPS3, from the skin secretion of *Phyllomedusa sauvagii* by using a combination of "shotgun" cloning and mass spectrometry. The corresponding chemically synthetic replicate exerted weak antibacterial activity towards pathogenic microorganisms and weak cytotoxic activity towards tumour cells. Therefore, two analogues of this naturally occurring peptide were designed, $K^{5,\ 17}$-DPS3 and $L^{10,\ 11}$-DPS3, to potentially optimize its cationicity on polar/unipolar faces and hydrophobicity in conserved sequence motifs, respectively.

3.2 Materials and Methods

3.2.1 Acquisition of *Phyllomedusa sauvagii* Dermal Secretions

Three specimens of *Phyllomedusa sauvagii* (4–6 cm snout-to-vent length) obtained from a commercial source in the United States, were exposed to 12-hours of light at 20-25 °C daily and multivitamin-loaded crickets were provided as the fodder three-time/week. The procedure of harvesting of amphibian skin secretion was referred to Section 2.1.

3.2.2 "Shotgun" cloning of a cDNA Encoding DPS3 Peptide Biosynthetic Precursor

The "shotgun" of skin-derived cDNA was referred to Section 2.2. The sense primer (5'-

ACTTTCYGAWTTRYAAGMCCAAABATG-3') was designed from a highly-conserved segment of the 5'-untranslated regions of *Phyllomedusa* species.

3.2.3 Identification and Analysis of Amino-acid Sequence

The isolation of mature peptide was referred to Section 2.4, and the identification of the primary sequence by MS/MS fragmentation sequencing was referred to Section 2.5.

3.2.4 Design and Synthesis of DPS3 and its Two Analogues

To investigate the effect of the increasing cationicity and hydrophobicity, the peptide DPS3 was used as the framework to design two analogues where the two acidic amino acids (at position 5 and 17) and two neutral amino acid residues (at position 10 and 11) were substituted with lysine and leucine residues, respectively. Accordingly, these analogues were named K5,17-DPS3 (ALWKKILKNAGKAALNKINQIVQ-NH_2) and L10,11-DPS3 (ALWKDILKNLLKAALNEINQIVQ-NH_2). Sufficient quantities to evaluate the bioactivities of all three peptides were obtained using the automatic PS4 peptide synthesizer (Protein Technologies, USA) along with Rink amide resin and standard Fmoc-chemistry. Cleavage of the primary products from the resin and subsequent deprotection used a mixture of trifluoroacetic acid (TFA), ethanedithiol (EDT), triisopropylsilane (TIPS) and water (94:2:2:2 (v/v)). Finally, each synthetic peptide was purified using RP-HPLC (Phenomenex C-5 column, 0.46 cm × 25 cm) and the corresponding fractions were pooled and lyophilized again before biological assays.

3.2.5 CD Analysis of Synthetic Peptides

The secondary structure of each peptide was estimated using a CD spectrometer (Jasco J851, USA), which was referred to Section 2.6.1.

3.2.6 Antimicrobial Assays

The minimal inhibitory concentrations (MICs) of all three synthetic peptides were determined against *S. aureus* (NCTC 10788*), E. coli* (NCTC 10418) and *C. albicans* (NCTC 1467), which was referred to Section 2.7.

3.2.7 Assessment of Cytotoxic Effects of Peptides on Human Cancer Cells Using MTT Assay

Two cancer cell lines, non-small cell lung cancer H157 and human prostate carcinoma PC-3, and the normal human cell line, dermal microvascular endothelium cell line, HMEC-1, were seeded onto a 96-well plate at densities of 5000 cells/well respectively. The detailed procedure was referred to Section 2.9.

3.2.8 Haemolysis Assay

The experimental method was referred to Section 2.8.

3.2.9 Statistical Analyses

Statistical analyses were referred to Section 2.10.

3.3 Results

3.3.1 Molecular Cloning of a DPS3 Precursor cDNA from a Skin Secretion-Derived cDNA Library

Using the 'shotgun' cloning strategy, the nucleotide sequence of a full-length biosynthetic precursor-encoding cDNA was consistently cloned from the artificially reconstructed cutaneous secretion-derived cDNA library from *Phyllomedusa sauvagii*. A degenerate sense primer (S1; 5'- ACTTTCYGAWTTRYAAGMCCAAABATG-3') that was designed to a segment of the 5'-untranslated regions of phylloxin cDNA from *Phyllomedusa bicolor* (EMBL Accession no. AJ251876) and the opioid peptide cDNA from *Pachymedusa dacnicolor* (EMBL Accession no. AJ005443) was employed. More specifically, the domain architecture of this preprodermaseptin transcript (Figure 3.1), compromises 70 amino acid residues, encoding a single copy of a peptide termed DPS3, where the C-terminus was subjected to post-translational modification with carboxyl-terminal amide formation. From the translated open-reading-frame, the KR is a typical convertase processing site *in vivo* and the resulting mature peptide consisted of 23 amino acid residues (ALWKDILKNAGKAALNEINQIVQ-amide). The cDNA encoding the precursor was deposited in GenBank database under an accession number, MH536746.

```
 M  A  F  L   K  K  S   L  F  L   V  L  F  L   G  L  V
ATGGCGTTCC TAAAGAAATC TCTTTTCCTT GTACTATTCC TTGGATTGGT
TACCGCAAGG ATTTCTTTAG AGAAAAGGAA CATGATAAGG AACCTAACCA
  S  L  T   I  C  E  EE  K  R   E  N  E   D  E  M  E
CTCTCTTACT ATCTGTGAAG AAGAGAAAAG AGAAAATGAA GATGAAATGG
GAGAGAATGA TAGACACTTC TTCTCTTTTC TCTTTTACTT CTACTTTACC
   Q  D  DD  E  Q   S  E  M  K   R  A  L   W  K  D
AACAAGATGA TGATGAGCAA AGTGAAATGA AGAGAGCTCT GTGGAAAGAT
TTGTTCTACT ACTACTCGTT TCACTTTACT TCTCTCGAGA CACCTTTCTA
 I  L  K  N   A  G  K   A  A  L   N  E  I  N   Q  I  V
ATATTAAAAA ATGCAGGAAA GGCTGCTTTA AATGAAATTA ATCAAATAGT
TATAATTTTT TACGTCCTTT CCGACGAAAT TTACTTTAAT TAGTTTATCA
  Q  GG   *
ACAAGGAGGA TAATAAAGTA AGGAAGATAT AAAATGTAAT TAAATCAATT
TGTTCCTCCT ATTATTTCAT TCCTTCTATA TTTTACATTA ATTTAGTTAA
ATCAATAATT GTGCCAACCC TATATTAAAG CATGCTGAAC CGAAAAAAAA
TAGTTATTAA CACGGTTGGG ATATAATTTC GTACGACTTG GCTTTTTTTT
AAGAAAAAAA AAAAAAAAAA AAAAAAA
TTCTTTTTTT TTTTTTTTTT TTTTTTT
```

Figure 3.1 Nucleotide and translated open-reading frame amino acid sequence of the cDNA encoding the biosynthetic precursor of a novel peptide, DPS3, from the skin secretion of *Phyllomedusa sauvagii*. The putative N-terminal signal peptide sequence was double-underscored, putative mature peptide sequence was single-underscored and an asterisk indicates the stop codon.

3.3.2 Isolation and Structural Characterisation of DPS3

The predicted amino acid sequence identified via cDNA cloning, suggested the existence of a peptide in the skin secretion of *Phyllomedusa sauvagii*, so the lyophilized skin secretion was directly analysed to determine if this peptide was present. The presence of the mature DPS3 peptide was confirmed by RP-HPLC isolation, with the retention time at approximately 108 min, and MS/MS fragmentation sequencing (Figure 3.2 and Table 3.1).

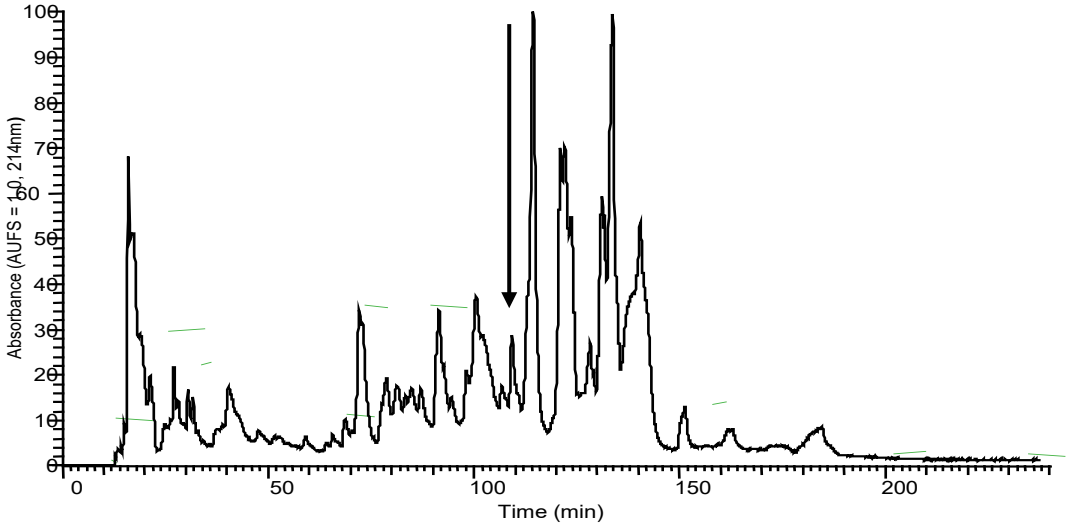

Figure 3.2 Region of RP-HPLC chromatogram of *Phyllomedusa sauvagii* skin secretion indicating the absorbance peak by an arrow which corresponding to DPS3.

Table 3.1 Predicted b-ion and y-ion MS/MS fragment ion series (Singly- and doubly-charged) of DPS3.

#1	b(1+)	b(2+)	Seq.	y(1+)	y(2+)	#2
1	72.04440	36.52584	A			23
2	185.12847	93.06787	L	2478.41923	1239.71325	22
3	371.20779	186.10753	W	2365.33516	1183.17122	21
4	499.30276	250.15502	K	2179.25584	1090.13156	20
5	614.32971	307.66849	D	2051.16087	1026.08407	19
6	727.41378	364.21053	I	1936.13392	968.57060	18
7	840.49785	420.75256	L	1823.04985	912.02856	17
8	968.59282	484.80005	K	1709.96578	855.48653	16
9	1082.63575	541.82151	N	1581.87081	791.43904	15
10	1153.67287	577.34007	A	1467.82788	734.41758	14
11	1210.69434	605.85081	G	1396.79076	698.89902	13
12	1338.78931	669.89829	K	1339.76929	670.38828	12
13	1409.82643	705.41685	A	1211.67432	606.34080	11
14	1480.86355	740.93541	A	1140.63720	570.82224	10
15	1593.94762	797.47745	L	1069.60008	535.30368	9
16	1707.99055	854.49891	N	956.51601	478.76164	8
17	1837.03315	919.02021	E	842.47308	421.74018	7
18	1950.11722	975.56225	I	713.43048	357.21888	6
19	2064.16015	1032.58371	N	600.34641	300.67684	5
20	2192.21873	1096.61300	Q	486.30348	243.65538	4
21	2305.30280	1153.15504	I	358.24490	179.62609	3
22	2404.37122	1202.68925	V	245.16083	123.08405	2
23			Q-Amidated	146.09241	73.54984	1

3.3.3 Physicochemical Properties and Secondary Structures of DPS3 and its Analogues

Both DPS3 and $L^{10, 11}$-DPS3 possessed the same net positive charge of +2, which increased to +6 in the case of the cationicity-enhanced analogue (Table 3.2). Additionally, DPS3 and $K^{5, 17}$–DPS3 had a similar degree of hydrophobicity, which was increased in $L^{10, 11}$-DPS3. The helical wheel projects showed that DPS3 and its analogues have the same direction of summed vectors of hydrophobicity (Figure 3.3). Meanwhile, $K^{5, 17}$–DPS3 had one more positive charge on both hydrophilic and hydrophobic phase than the other two analogues, and $L^{10, 11}$-DPS3 showed enlarged hydrophobic face. Also, although these three peptides existed in random coil in aqueous solution, they all adopted α-helical conformations in membrane-mimicking solution, presenting obviously negative peaks at 222 nm and 208 nm, with the natural peptide presenting the largest proportion of α-helical domain (44.9% of its secondary structure) (Figure 3.3 and Table 3.2).

Table 3.2 Physicochemical properties of DPS3 and its two analogues.

Peptide	Hydrophobicity (H)	Hydrophobic Moment (μH)	% Helix[1]	Net charge
ALWKDILKNAGKAALNEINQIVQ-NH_2	0.373	0.437	44.9	+2
ALWKKILKNAGKAALNKINQIVQ-NH_2	0.349	0.437	39	+6
ALWKDILKNLLKAALNEINQIVQ-NH_2	0.508	0.517	28.8	+2

1 In 50% 2,2,2-trifluoroethanol (TFE)/10mM ammonium acetate (NH4AC) solution

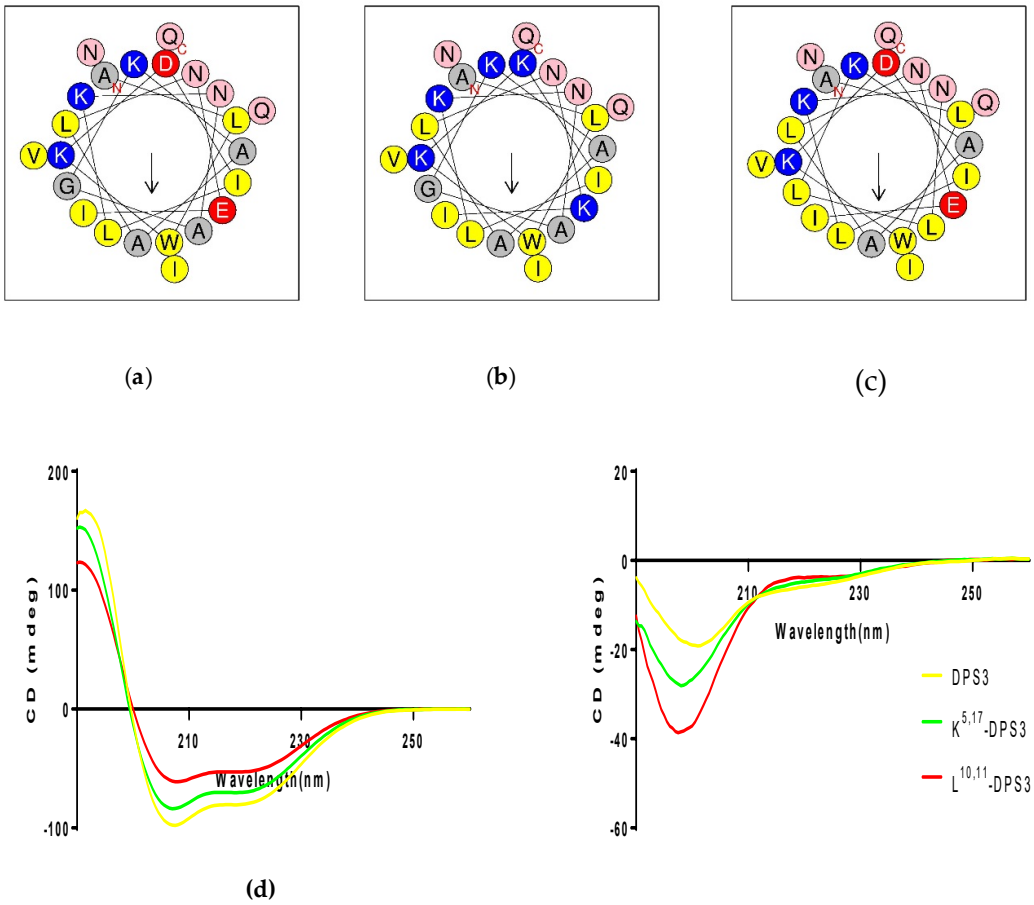

Figure 3.3 Predicted helical wheel projections of the three peptides, (a) DPS3, (b) $K^{5,17}$-DPS3 and (c) $L^{10,11}$-DPS3; CD spectra recorded for 100 μM of DPS3 (yellow), $K^{5,17}$-DPS3 (green) and $L^{10,11}$-DPS3 (red) peptides in (d) 10 mM NH_4AC/water solution and in (e) 50% TFE/10 mM NH_4AC/water solution.

3.3.4 Antimicrobial Activity

The parent peptide, DPS3, generally showed weak antimicrobial activity, although it did exhibit better activity against Gram negative bacteria. As expected, when compared to the parent peptide, both artificial analogues displayed enhanced antimicrobial activity against all the microorganisms examined (Table 3.3). In particular, $K^{5,17}$-DPS3 displayed MIC values of 8 μM or less against Gram positive (*S. aureus*) and Gram negative (*E. coli*) bacteria, as well as yeast (*C. albicans*).

Table 3.3 Antimicrobial activity of the parent DPS3 peptide and its two analogues against various microorganisms.

Microorganisms	DPS3	$K^{5,17}$-DPS3	$L^{10,11}$-DPS3
	MIC (mg/L)		
S. aureus (NCTC 10788)	512	16	16
E. coli (NCTC 10418)	64	16	32
C. albicans (NCTC 1467)	128	8	32

3.3.5 Cytotoxicity of Peptides on Human Cancer Cells

DPS3 and its two artificial analogues all exhibited inhibitory effects on the proliferation of the two tested human cancer cell lines (Figure 3.4). Increasing the cationicity of the parent peptide had no significant influence on its antiproliferative activity, whereas, altering its hydrophobicity markedly enhanced its antiproliferative activity, with this peptide exhibiting an IC_{50} value more than 10-fold lower than either of the other peptides

(Table 3.4).

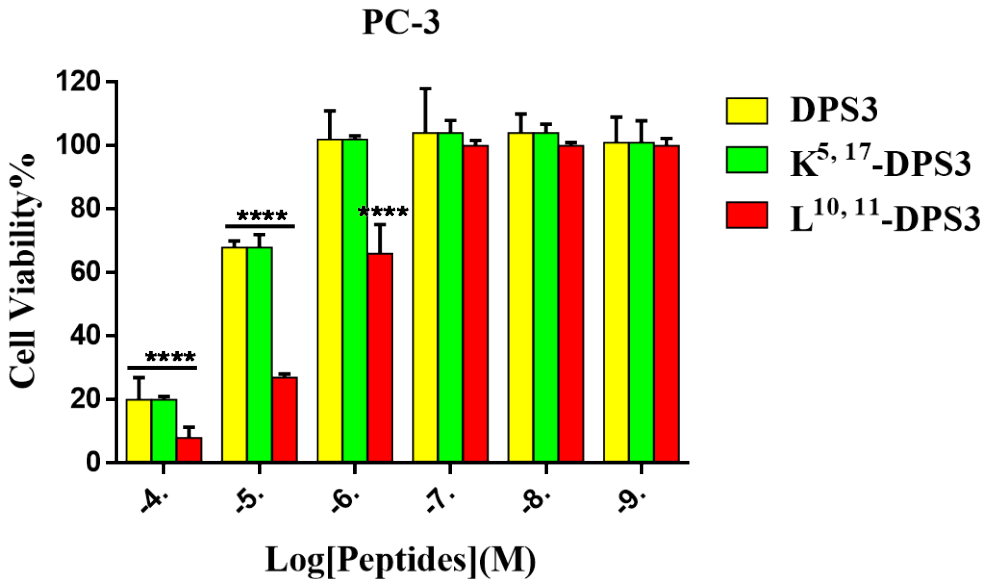
PC-3
Cell Viability%
120
100
80
60
40
20
0
****
****
****
-4
-5
-6
-7
-8
-9
Log[Peptides](M)
DPS3
K5, 17-DPS3
L10, 11-DPS3

(a)

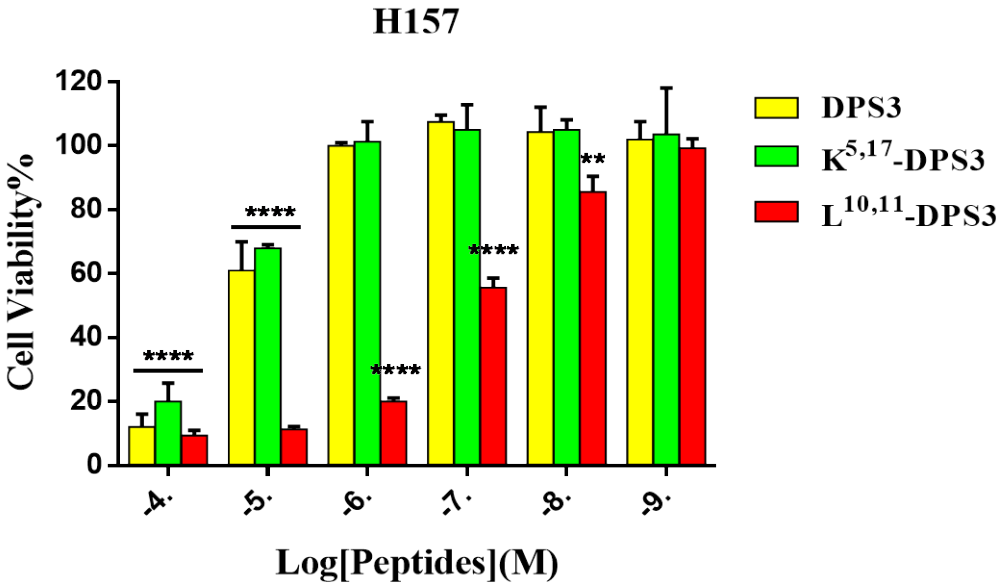
H157
Cell Viability%
120
100
80
60
40
20
0
****
****
****
****
**
-4
-5
-6
-7
-8
-9
Log[Peptides](M)
DPS3
K5,17-DPS3
L10,11-DPS3

(b)

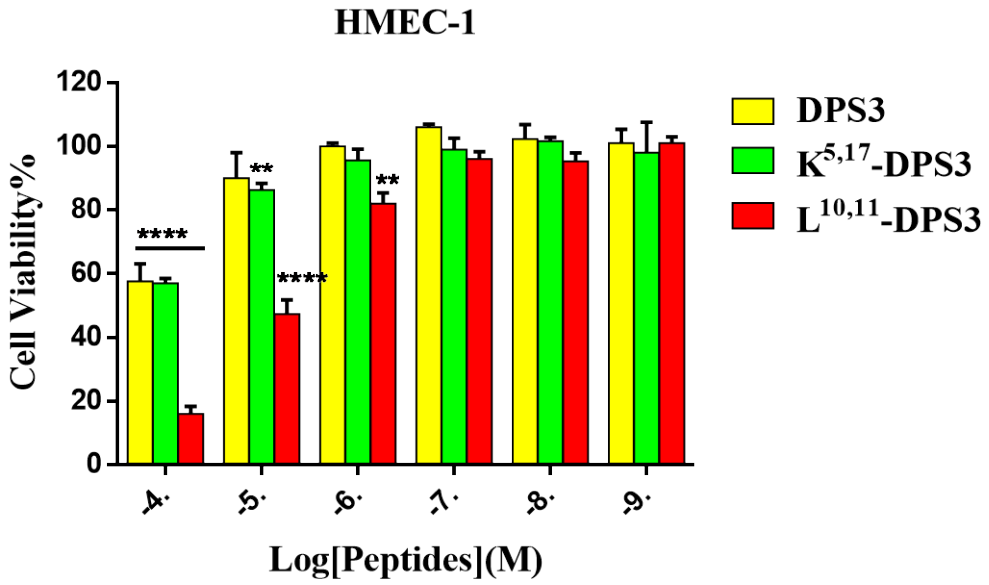

(c)

Figure 3.4 The cytotoxic effect of DPS3 (yellow), $K^{5,17}$-DPS3 (green) and $L^{10,11}$-DPS3 (red) on the cancer cell lines (a) H157, (b) PC-3 and (c) the normal human cell line HMEC-1. The significance is given as ** $p<0.01$ and **** $p<0.0001$. Each concentration was compared to growth control.

Table 3.4 Induced cytotoxicity of DPS3 and analogues on the human cancer cells. IC_{50}s were calculated from the normalized curves in Figures 4 using GraphPad Prism 6 (GraphPad Software, USA).

Peptide	IC_{50} for H157 (**μM**)	IC_{50} for PC3 (**μM**)	IC_{50} for HMEC-1 (**μM**)
DPS3	15.67	18.20	132.10
$K^{5,17}$-DPS3	18.20	18.20	123.00

$L^{10, 11}$-DPS3	0.12	1.85	8.76

3.3.6 Haemolysis Activity

All three peptides exhibited some haemolytic activity against healthy red blood cells (Figure 3.5). However, both artificial analogues exhibited a greater effect than the parent peptide, with the $L^{10, 11}$-DPS3 analogue showing marked haemolysis even at lower concentrations. The HC_{50}s of DPS3, $K^{5, 17}$-DPS3 and $L^{10, 11}$-DPS3 are 138.1, 14.98 and 3.44 mg/L, respectively.

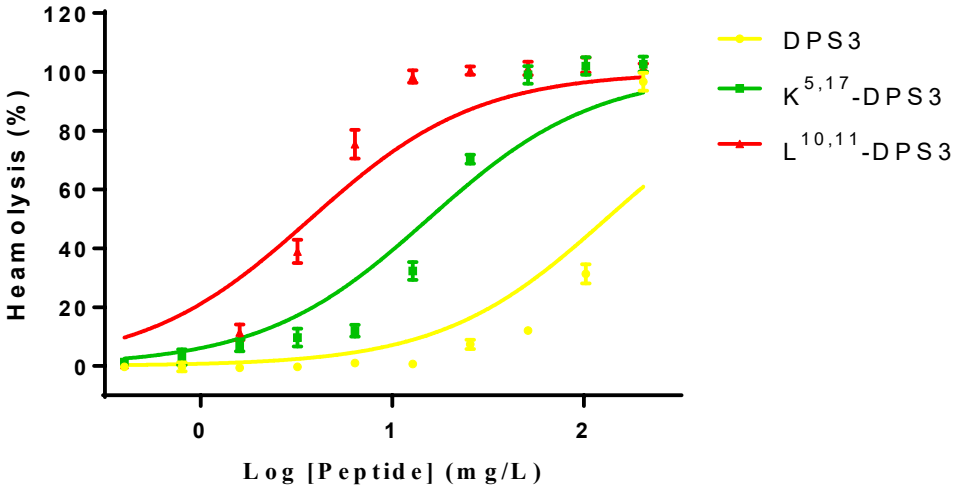

Figure 3.5 Haemolytic activity of DPS3 (yellow), $K^{5, 17}$-DPS3 (green) and $L^{10, 11}$-DPS3 (red) against horse red blood cells.

3.4 Discussion

Typically, most naturally-occurring dermaseptins are 28 to 34 amino acid residues in length (Galanth et al., 2008, Silva et al., 2008, Hoskin and Ramamoorthy, 2008), therefore the 23-mer DPS3 reported here is relatively short for this family. Huang and colleagues have previously isolated a similar length dermaseptin, dermaseptin-PH (Huang et al., 2017). Compared with other similar dermaseptins, the antimicrobial activity of DPS3 and dermaseptin-PH indicate these two native truncated dermaseptins are less potent as AMPs than other longer dermaseptin peptides, possibly suggesting increasing peptide length in this family is potentially related to higher antimicrobial activity. Besides other physicochemical properties, charge and hydrophobicity are the main factors affecting antimicrobial activity, therefore they are considered as one of the design parameters to optimize in AMPs (Giangaspero et al., 2001, Kustanovich et al., 2002, Timofeeva and Kleshcheva, 2011, Fjell and Hiss 2012). In terms of the antibacterial mechanism of action of AMPs, it is mostly thought to concern the electrostatic interaction and hydrophobic engagement between AMPs and bacterial cell membranes (Schweizer, 2009). In particular, the polycationic properties, as well as the large number of hydrophobic amino acids in the primary structure, and conformational alternation from random coil to helical frame among dermaseptins, along with their membrane-lytic activity, suggest their mechanism of action is likely to involve membrane disruption. Indeed, previous studies have found leakage and morphological alterations in artificial bacterial membranes after treatment with fluorescently-labelled dermaseptins (Riedl et al., 2011, van Zoggel 2012). More recently, using electron microscopy, a dermaseptin peptide, DS1, was found to distort the cell wall surface, proposing that the cytolysis or cell membrane disruption of *C.albicans* eventually causes cell death (Belmadani et al.,

2018).

Early research had revealed a strong correlation between α-helical domain and antimicrobial activity, involving the local fusion of the membrane leaflets, pore formation, cracks, as well as the depth of membrane insertion (Mor and Nicolas, 1994, Hancock and Chapple, 1999, Lequin et al., 2006). Also, the α-helical conformation of dermaseptins is normally considered as one of the main factors in the hydrophobic interaction of AMPs and lipid layers (Mor and Nicolas, 1994, Lequin et al., 2006). In our investigation, the CD spectra of the three peptides showed that the amount of helical conformation is similar across all three. Our results indicate that an increase in antimicrobial activity can be achieved via optimization of cationic or hydrophobic properties of the dermaseptin peptides through residue substitution. However, both artificial analogues induced more haemolysis than the parent peptide, though $K^{5, 17}$-DPS3 showed minimal haemolysis at the concentrations which exhibited antimicrobial activity, indicating it could still represent an interesting AMP. As the electrical attraction of these peptides to the membrane is important for their antimicrobial activity, this could explain why the cationicity-enhanced analogue shows more potent antimicrobial activity than L10,11 – DPS3, but less haemolysis. Similarly, K4K20-S4, a dual lysine-substituted dermaseptin-S4, also shown increased antimicrobial activity, along with 2-fold haemolytic potency and it was found higher lipophilic affinity (Miltz et al., 2006). Previously, 2D-NMR has shown that the consensus motif AA(G)KAALG(N) among dermaseptins adopts a well-defined α-helical structure (Nicolas and El Amri, 2009, Kustanovich et al., 2002). Herein, we enhanced the hydrophobicity in this highly conserved motif within the amphipathic α-helix and found more potent cytolytic action towards mammalian erythrocytes. On the other hand, as the hydrophobicity is important for membrane disruption, increasing the

hydrophobicity could improve the peptides ability to disrupt membranes, but not in a way that favours microorgansim selectivity. In this regard, we proposed it possibly results from stronger hydrophobic interaction within the core of the bacterial membrane. Taken together, the data presented indicates it is possible to improve the membrane-lytic activity of these AMPs without increasing the peptide length.

DPS3, and its analogues, all exhibit anti-proliferative effects on the tested cancer cells, although $L^{10, 11}$ -DPS3 exhibited an enhanced anti-proliferative impact. Recent studies have shown that cancer cell membranes, similar to the bacterial membrane, carry a negative charge due to overexpression of anionic molecules, such as phosphatidylserine, sialic acid and glycosaminoglycans (GAGs) (Kustanovich et al., 2002, Fjell and Hiss, 2012, Schweizer, 2009). Therefore, although it is unclear how the dermaseptins mediate their anticancer activity, it could result from their interaction with and disruption of the cell membrane, similar to their antimicrobial action. However, dermaseptins have been found to interact with, and aggregate on, the surface of cancer cells, as well as being able to penetrate into cancer cells, without compromising the cell membrane (Dos Santos et al., 2017, Hoskin and Ramamoorthy, 2008, van Zoggel et al., 2012, Schweizer, 2009). Also, Dos Santos and colleagues found that a biotin- labelled version of the dermaseptin peptide, DRS-B2, could internalise into cancer cells, and implicated its non-protein binding partner GAGs, suggesting GAGs are possibly involved in dermaseptin internalization (Dos Santos et al., 2017). Notably, the viability of H157 cells pre-treated with $L^{10, 11}$-DPS3 (1 μM) decreased by approximatley 78%, whilst no membrane-lysis was observed in mammalian erythrocytes exposed to the same concentration of peptide, possibly suggesting a non-lytic mechanism may be involved, at least at lower concentrations. At higher peptide concentrations (>1μM), the higher anti-cancer cell

impact is consistent with increasing haemolysis activity, suggesting this is possibly due to cell membrane disruption. However, further investigations will be needed to confirm this.

Chapter 4

Isolation and Identification of a novel dermaseptin, Dermaseptin-PC1, from skin secretion of *Phyllomedusa camba.*

Abstract

Dermaseptins are a remarkable antimicrobial peptide family discovered in the skin secretions of Phyllomedusinae tree frogs. They possess a potent and broad antimicrobial activity, especially against Gram-negative bacteria. Additionally, they exhibit antiproliferative effects against several cancer cell lines. In this study, a novel dermaseptin from the skin secretion of *Phyllomedusa camba,* namely dermaseptin-PC1 (DPC1), is reported. The peptide precursor encoding cDNA was obtained through "shotgun" cloning with degenerate primers. The presence of DPC1 in the skin secretion was confirmed using MS/MS fragmentation sequencing, which determined an amide at the C-terminus. Subsequently, DPC1 was chemically synthesised and purified via RP-HPLC. CD analysis revealed that it can form an α-helical structure in a membrane-mimicking environment. DPC1 exhibited antimicrobial activity against Gram-positive bacteria, *S. aureus*, Gram-negative bacteria, *E. coli*, and the yeast, *C. albicans,* with MIC values of 64, 16 and 64 mg/L, respectively. However, it was not able to inhibit the growth of *P. aeruginosa* at concentrations up to 512 mg/L. Additionally, DPC1 exhibited a moderate effect on the cell viability of cancer cells, MB435S, H157, MCF-7 and U251MG. Notably, it showed more potent efficacy against MB435S and H157. Along with such potent biological activities, DPC1 induced a mild haemolytic effect at concentrations up to 512 mg/L (less than 30% haemolysis), which indicates that DPC1 has a potential higher therapeutic index when developed as an antibiotic or anticancer drug.

4.1 Introduction

Bioactive peptides are widely found in many organisms, with the biological functions of resisting foreign pathogens and eliminating mutant cells *in vivo* (Hess et al., 2017; Weide et al., 2017). They are non-specific immune response products with defensive activity (Morchikh et al., 2017). As an integral part of the natural immune system, these, together with interferon and complement, etc. constitute the host's natural immune defence system (Yang et al., 2017; Webb, 2016; Mishra et al., 2017).

Antimicrobial peptides (AMPs) as the organism's first line of defence, are natural immune system effector molecules (Li et al., 2015). They have been proven to inhibit and kill a variety of pathogenic microorganisms, such as Gram-negative bacteria, Gram-positive bacteria, viruses and fungi (Garten et al., 2015; Santos et al. 2017). In addition to their direct anti-bacterial function, they also have inflammatory functions in the role of intermediates (Kim et al., 2017; Fuente-Núñez et al., 2017). The sources of AMPs isolated from nature covers almost all species from single-celled organisms, insects, invertebrates, plants, amphibians, birds, fish, mammals and humans (Fuente-Núñez et al., 2017). The expression of the AMPs is divided between constitutive gene expression and inducible gene expression by infection or inflammatory stimuli such as pro-inflammatory cytokines, bacteria and lipopolysaccharides (Panteleev et al., 2017; Holstein et al., 2017; Wangkahart et al., 2016). With further study, it has been found that some AMPs also have anticancer activity (Rady et al., 2017; Hicks et al., 2016; Mechkarska et al., 2014).

Dermaseptins from frog skin secretion have been considered as one of the most promising groups of antibiotic peptides from nature. They usually consist of 18-34 amino acid residues including multiple basic amino acids, a conserved Trp residue at position 3

and a motif sequence −AA(A/G)KAAL(G/N)A−, in their mid-regions (Amiche et al., 2008). They show not only broad-spectrum antibacterial activity but also can inhibit filamentous fungi, protozoans as well as some human viruses (Mor et al., 1991; Hernandez et al., 1992; Brand et al., 2002; Brand et al., 2006). Research indicates that dermaseptins can fold into amphipathic α-helical structures in membranes and then disrupt their integrity, which results in the permeabilisation of cells (Huang et al., 2017).

Here, a novel dermaseptin from the skin secretion of *Phyllomedusa camba,* has been identified through the combination of "shot-gun" cloning and MS/MS fragmentation sequencing and named dermaseptin-PC1 (DPC1). The peptide was replicated by solid phase peptide synthesis and its secondary structure was determined using circular dichroism. Antimicrobial and anticancer assays were employed to evaluate the biological activities of DPC1. Furthermore, antibiofilm effects were also tested.

4.2 Materials and Methods

4.2.1 "Shotgun" cloning of cDNAs encoding novel peptide biosynthetic precursors

The experimental method was referred to Section 2.2. The highly conserved degenerate primers (5 '- ACTTTCYGAWTTRYAAGMCCAAABATG - 3') was designed from previously identified peptide encoding cDNAs from *Phyllomedusinae* frogs.

4.2.2 Identification and structural analysis of the novel peptide

The isolation of mature peptide was referred to Section 2.4. The sample was then analysed by LCQ-Fleet ion trap MS for sequencing. The detailed processes have been described in section 2.5.

The Circular Dichroism (CD) method was employed to analyse the secondary structure of the peptide. CD spectra were obtained at a scanning speed of 100 nm/min from 190 nm to 250 nm at 20° C with 1nm bandwidth and the data interval of 0.5 nm. The detailed processes have been described in section 2.6.

4.2.3 Solid-phase peptide synthesis

The mature peptide sequence was synthesized via solid phase peptide synthesis. In the process of synthesis, F-moc groups protected amino acid, resin, HBTU, N-methyl morpholine (NMM), piperidine, N, N-dimethyl formamide (DMF) and dichloromethane (DCM) were employed. The peptide and resin were separated through use of the TFA

cocktail solution. The detailed processes have been described in section 2.3.

4.2.4 Assays of antimicrobial activity

Four microorganisms, *S. aureus*, *E. coli*, *P. aeruginosa* and *C. albicans*, were employed in this study. They were each subcultured in MHB overnight before use. A 96-well plate was used to incubate the peptide with microbes. Each well of the plate contained 50,000 cfu of organisms and the peptide over the concentration range of 1 to 512 mg/L. The negative control was 100% microbial culture and 100% pure MHB was used as the blank control. After loading, the sample was placed in the incubator at 37°C about 16-18 h. Next, the sample was analysed by a UV light detector. The detailed processes have been described in section 2.7.2.

The biofilm assay was performed after the determination of the MIC. Both *S. aureus* and *E. coli* were employed to study the antibiofilm activity of DPC1. The detailed processes have been described in section 2.7.4.

4.2.5 Haemolysis assay

The experimental method was referred to Section 2.8.

4.2.6 MTT cell viability assay

Four cancer cell lines, non-small cell lung cancer H157 and human breast carcinoma, MCF-7, human melanoma, MB435S and human glioblastoma cell, U251MG were

seeded onto a 96-well plate at densities of 5000 cells/well respectively. The detailed procedure was referred to Section 2.9.

4.2.7 Statistical Analyses

Statistical analyses were referred to Section 2.10.

4.3 Results

4.3.1 Molecular cloning of the peptide precursor and analysis of the primary and secondary structure

The cDNA encoding a novel prepropeptide was repeatedly cloned from the skin secretion of *Phyllomedusa camba* with an open reading frame including a signal peptide terminating in a cysteine residue; an acidic amino-acid residue-rich spacer peptide; and a predicted putative mature peptide. The predicted mature peptide appeared after a lysine-arginine (KR) motif, which is a typical propeptide convertase cleavage processing site (Figure 4.1). A BLAST search showed that the natural peptide belonged to the dermaseptin peptide family, therefore it was named as dermaseptin-PC1 (DPC1). The alignment of full length translated open reading frame amino acid sequences of DPC1, preprodermaseptin S13 (Assession No. Q1EN11) and preprodermaseptin S12 (Assession No. Q1EN12) showed that they are all highly-conserved (Figure 4.2). The signal peptide domain and acidic spacer peptide domain only had 4 amino acid differences between

these three sequences. The -AAKA(T)A- motif is also observed in the mid-region of the mature peptide sequence. Except for preprodermaseptin S13, the other two proteins display a typical Trp residue at position 3.

Figure 4.1 The nucleotide and translated open-reading frame amino acid sequence of the cDNA encoding the biosynthetic precursor of a novel peptide from the skin secretion of *Phyllomedusa camba.* The putative N-terminal signal peptide sequence was double-underscored, the putative mature peptide sequence was single-underscored, and an asterisk indicates the stop codon.

```
DPC1       MAFLKKSLFLVLFLGLVSLSICEEEKRENEDEEEQEDDEQSEMKRGLWSKIKEAAKTAGK    60
S11        MAFLKKSLFLVLFLGLVSLSICDEEKRENEDEENQEDDEQSEMRRGLRSKIKEAAKTAGK    60
S12        -ASLKKSLFLVLFLGLVSLSICEEEKRENEDEENQEDDEQSEMRRGLWSKIKEAAKTAGK    59
            * ****************** ********** ********* *** ************

DPC1       AAMGFVNEMVGEQ   73
S11        MALGFVNDMAGEQ   73
S12        MAMGFVNDMVGEQ   72
            * **** * ***
```

Figure 4.2 The alignment of the translated open reading frame amino acid sequences of DPC1, preprodermaseptin S13 (Assession No. Q1EN11) and preprodermaseptin S12 (Assession No. Q1EN12). The identical amino acid residues are indicated by asterisks.

4.3.2 Identification and structural analysis of DPC1

An RP-HPLC chromatogram for the skin secretion of *Phyllomedusa camba* was successfully obtained (Figure 4.3). The HPLC fractions were first analysed by MALDI-TOF MS to determine the molecular masses in each fraction. Then the fraction containing the molecular mass consistent with putative DPC1 was subjected to LCQ MS. The MS/MS spectrum confirmed the primary structure of DPC1 as well as the presence of an amide at the C-terminus. The database search results for DPC1 are shown in Table 4.1. The observed b-ions and y-ions are indicated by single-underlines. The retention time of DPC1 in the skin secretion chromatogram was 137 min.

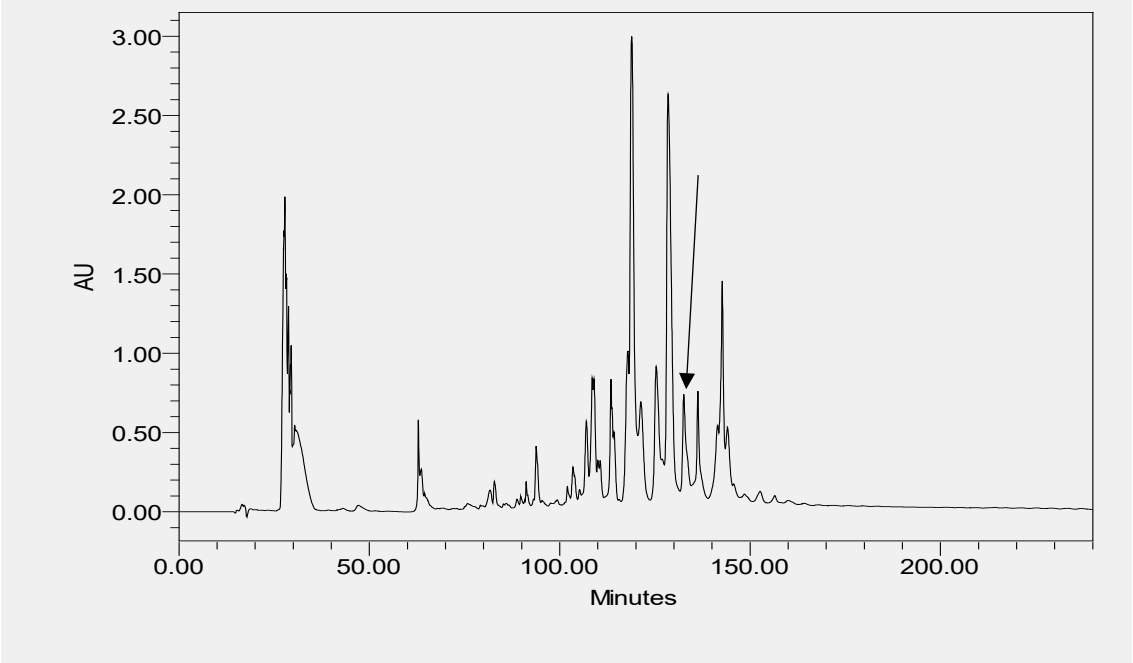

Figure 4.3 Full RP-HPLC chromatogram of the skin secretion of *Phyllomedusa camba*. The retention time of DPC1 was at 137 min, indicated by an arrow.

Table 4.1 Predicted singly-charged and doubly-charged b-ions and y-ions produced by MS/MS fragmentation of DPC1 identified in skin secretion. Observed ions following MS/MS fragmentation are underlined.

#1	b(1+)	b(2+)	Seq.	y(1+)	y(2+)	#2
1	58.02875	29.51801	G			25
2	171.11282	86.06005	L	2579.38381	1290.19554	24
3	357.19214	179.09971	W	2466.29974	1233.65351	23
4	444.22417	222.61572	S	2280.22042	1140.61385	22
5	572.31914	286.66321	K	2193.18839	1097.09783	21
6	685.40321	343.20524	I	2065.09342	1033.05035	20
7	813.49818	407.25273	K	1952.00935	976.50831	19
8	942.54078	471.77403	E	1823.91438	912.46083	18
9	1013.57790	507.29259	A	1694.87178	847.93953	17
10	1084.61502	542.81115	A	1623.83466	812.42097	16
11	1212.70999	606.85863	K	1552.79754	776.90241	15
12	1313.75767	657.38247	T	1424.70257	712.85492	14
13	1384.79479	692.90103	A	1323.65489	662.33108	13
14	1515.83529	758.42128	M	1252.61777	626.81252	12
15	1643.93026	822.46877	K	1121.57727	561.29227	11
16	1714.96738	857.98733	A	993.48230	497.24479	10
17	1786.00450	893.50589	A	922.44518	461.72623	9
18	1843.02597	922.01662	G	851.40806	426.20767	8
19	1900.04744	950.52736	G	794.38659	397.69693	7
20	2047.11586	1024.06157	F	737.36512	369.18620	6
21	2146.18428	1073.59578	V	590.29670	295.65199	5
22	2260.22721	1130.61724	N	491.22828	246.11778	4
23	2389.26981	1195.13854	E	377.18535	189.09631	3
24	2520.31031	1260.65879	M	248.14275	124.57501	2
25			V-Amidated	117.10225	59.05476	1

4.3.3 Purification of synthetic DPC1

Solid phase peptide synthesis of DPC1 was performed successfully using the Tribute

automated peptide synthesiser. The crude peptide was further purified by RP-HPLC and the MS spectrum of pure peptide exhibited a high degree of purity for DPC1 (Figure 4.4). The observed molecular mass of DPC1 was 2637.3 Da.

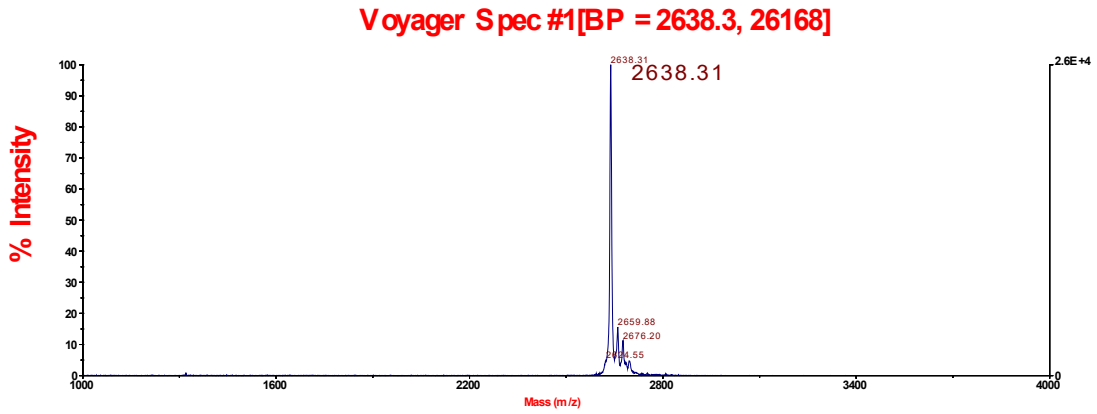

Figure 4.4 MALDI-TOF MS spectrum of purified DPC1. The observed [M+H] ion is 2638.3 m/z.

4.3.4 Prediction of Secondary Structure and Physiochemical Properties

The CD analysis showed that DPC1 formed a typical α-helical structure with negative bands at 208 nm, 222 nm and a positive band at 190 nm in the membrane-mimetic 50% TFE solution (Figure 4.5), though it forms a random coil structure in the aqueous environment (data not shown). The calculated proportions of α helix and β strand contents of the peptide were 35.46% and 13.24%, respectively. Subsequently, the helical wheel plot of DPC1 showed that it had a sizeable hydrophobic face as -AALFAIMAAWV- (Figure 4.6). The hydrophobic moment was calculated as 0.447.

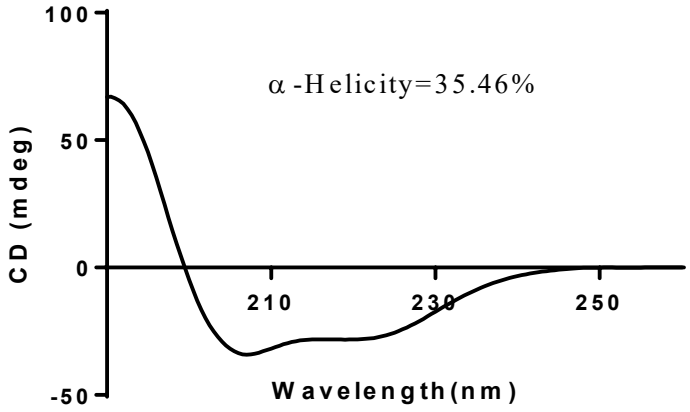

Figure 4.5 CD spectrum of peptide DPC1 (100 μM) in 50% 2,2,2-trifluoroethanol (TFE)/10 mM ammonium acetate/water solution. The peptide formed a typical α-helix in membrane-mimetic solution. The calculated α-helical content was 35.46%.

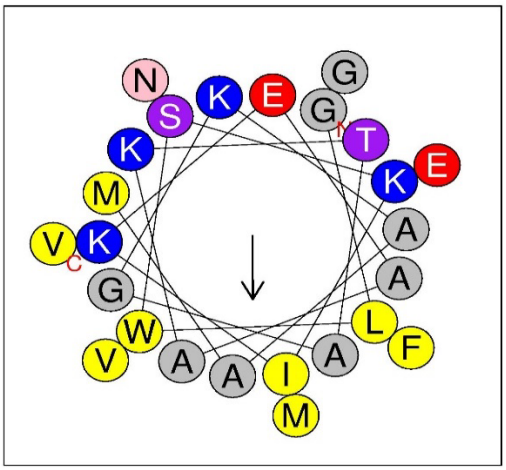

$_{1}$GLWSKIKEAAKTAGKAAMGFVNEMV$_{25}$		
Physico-chemical properties	**Polar residues + GLY**	**Nonpolar residues**
Hydrophobicity <H>	**Polar residues + GLY (n / %)**	**Nonpolar residues (n / %)**
0.335	12 / 48.00	13 / 52.00
Hydrophobic moment <μH>	**Uncharged residues + GLY**	**Aromatic residues**
0.447	SER 1, THR 1, ASN 1, GLY 3	TRP 1, PHE 1,
Net charge z	**Charged residues**	**Special residues**
2	LYS 4, GLU 2,	CYS 0, PRO 0
Hydrophobic face : A A L F A I M A A W V		

Figure 4.5 The helical wheel projection of DPC1. The hydrophobic moment is indicated by an arrow.

4.3.5 Antimicrobial Assay

By incubation with a gradient concentration of peptide from 1 to 512 mg/L, the minimum inhibitory concentration of synthetic replicate DPC1 was performed using a microdilution assay. The results of the antimicrobial activity showed that the peptide exhibited a significant inhibitory effect against the growth of the Gram-negative bacterium, *E.coli*, whilst it showed a higher inhibitory concentration against the growth of the yeast, *C. albicans* and the Gram-positive bacterium, *S. aureus,* compared to the potency against *E. coli*. The antimicrobial activity against *P. aeruginosa* was also evaluated but no effect was observed at concentrations up to 512 mg/L (Table 4.2). Interestingly, DPC1 showed anti-biofilm activity against *E. coli* and *S. aureus* biofilms at concentrations of 64 mg/L and 256 mg/L, respectively (Figure 4.6).

Table 4.2 The antimicrobial activity of DPC1 against four microorganisms.

Peptide	MIC (mg/L)			
	S. aureus	*E. coli*	*P. aeruginosa*	*C. albicans*
Dermaseptin-PC1	64	16	>512	64

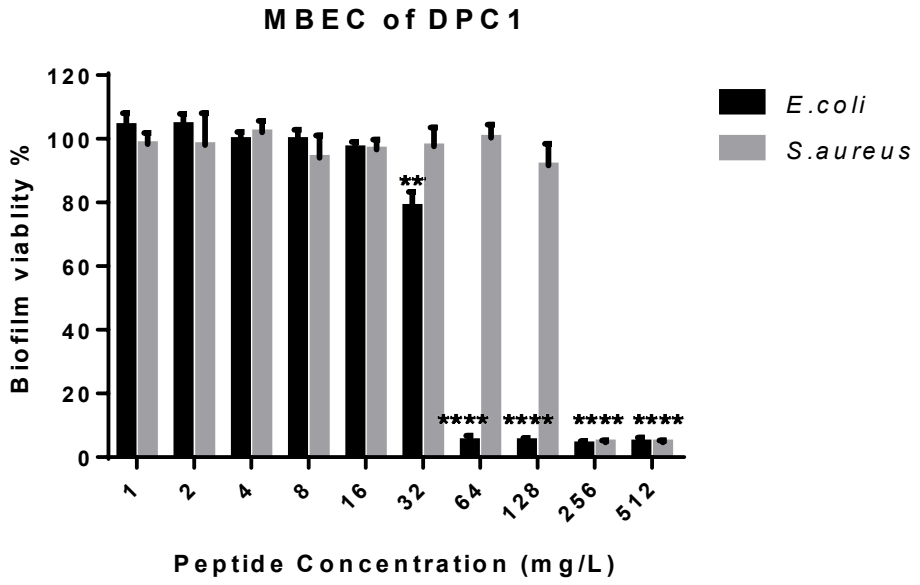

Figure 4.6 The biofilm eradication effect of DPC1 against the biofilm of *E. coli* and *S. aureus*. The percentage of biofilm viability was compared with the absorbance of TTC of the growth control, which contains bacteria only. The significance is given as ** $p<0.01$ and **** $p<0.0001$. Each concentration was compared to growth control.

4.3.6 Haemolytic activity of DPC1

DPC1 showed a low degree of haemolytic activity on horse erythrocytes (Figure 4.7). Even at the highest concentration of 512 mg/L, DPC1 only induced around 30% haemolysis. At the corresponding MIC and MBEC values, the haemolysis of DPC1 was less than 20%.

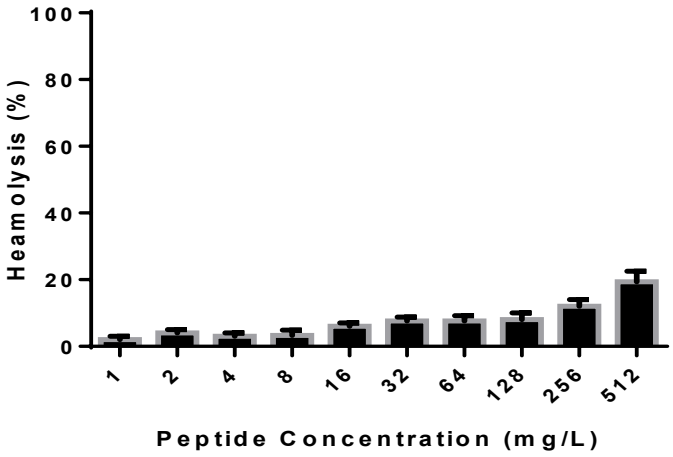

Figure 4.7 Haemolytic activity of DPC1. The percentage was calculated using the haemolysis induced by 1% TritonX-100.

4.3.7 Cancer cell viability following treatment with DPC1

DPC1 exhibited different potencies against the tested cancer cell lines. Although it resulted in a similar degree of cell viability at 100 μM, the effect was significantly stronger on H157 and MCF-7 cells than on MB435S and U251MG cells, at the concentration of 10 μM. Specifically, DPC1 significantly decreased the cell viability of MCF-7 cells at an even lower concentration, 1 μM (Figure 4.8).

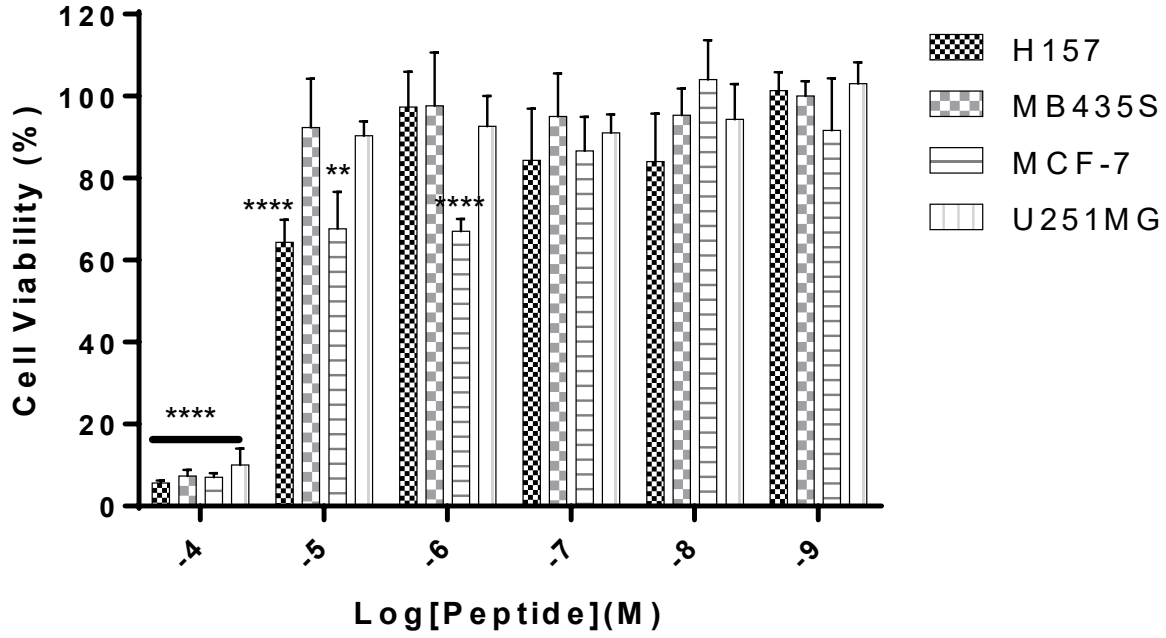

Figure 4.8 Cell viability of four human cancer cell lines following treatment with DPC1 in the concentration range of 10^{-9} to 10^{-4} M. The error bar represents the SD for five replicates. The significance is given as ** $p<0.01$ and **** $p<0.0001$. Each concentration was compared to growth control.

4.4 Discussion

It is nearly 30 years since the first dermaseptin peptide was discovered in the skin secretion of a phyllomedusinae tree frog (Mor et al, 1991). Since then, around 80 dermaseptin sequences have been identified and recorded in the Uniprot database (access date: July 2018). Although the primary structure of dermaspetin has a high degree of variation, some common motifs have been observed such as the Trp residue at position 3. In this Chapter, another dermaseptin peptide was identified and named DPC1. It is expressed in the skin secretion of *Phyllomedusa camba*. The precursor of DPC1 was very

similar to the two precursors discovered in the skin secretion of *Phyllomedusa sauvagii.* This indicates that these two species may be closely-related.

The activity of AMPs depends on the physicochemical parameters of amino acids (Pane et al., 2017; Zhang et al., 2017) The results show that several parameters are closely related to the activity of antimicrobial peptides as follows: secondary structure, cationicity, amphiphilicity, hydrophobic moment, hydrophobicity and polar angle (Hollmann et al., 2016; Hädicke et al., 2016; Rice and Wereszczynski, 2017; Mahindra et al., 2014). Any of these parameters which undergo change are likely to change the activity of the bioactive peptides (Manzor et al., 2017).

The mechanism of antimicrobial peptides acting on cell membranes is well known. Antimicrobial peptides have a tremendous number of positive charges and strong hydrophobic and amphiphilic structures (Nguyen et al., 2011). A variety of phospholipids, phosphatidic acid and lipopolysaccharides have many negative charges. The metal ions on the surface of the cell membrane could be replaced by antimicrobial peptides which can then be adsorbed onto the membrane by electrical attraction (Dannehl et al., 2013). The hydrophobic surface of the antimicrobial peptide interacts with the phospholipid on the cell membrane to form a complex which inserts into the cell membrane; the hydrophilic surface forms a transmembrane pathway with the phospholipid (Wang et al., 2014). Finally, the bacteria are killed as their internal environments are damaged and the osmotic pressure is decreased.

Like the other dermaseptin peptides, DPC1 shows the typical structural motif at the mid-region of the peptide which unsurprisingly adopts the α-helix conformation in the membrane-mimicking environment. Similarly, it demonstrated remarkable antimicrobial activity against *E.coli*, *S. aureus* and *C. albicans*, while it did not inhibit the growth of *P.*

aeruginosa. This latter result was unexpected because dermaseptin Q2 (DDQ2), which has only three amino acids differences, demonstrated an inhibitory effect against *P. aeruginosa* (Figure 4.9) (Batista et al., 1999). As the data shows, the order of antimicrobial activity of DDQ2 against the bacteria is *E. coli* > *S. aureus*, which is quite similar to that of DPC1. Moreover, the potency of the antimicrobial activity of the two peptides against *E. coli* and *S. aureus* are almost at the same degree (Table 4.3). According to the peptide sequences, DPC1 contains one more positive charge, which is considered to be an essential factor in the bacteria-killing mechanism. However, it did not help the membrane permeabilisation of DPC1 on *P. aeruginosa*. While, within the same segment, DDQ2 contains two hydrophobic amino acids, Leu and Met, which increases the hydrophobicity and amphipathicity of DDQ2. On the other hand, the constitution of lipopolysaccharide (LPS) in the outer membrane of Gram-negative bacteria is usually different in different bacteria. For instance, the *P. aeruginosa* LPS cores have been found to be uncapped in about 80% of the cases, while for *E. coli*, only ~10% of LPS molecules are uncapped. Even in the different strains of the same bacterium, like *E. coli*, the structure of LPS could vary considerably (Ivanov et al., 2010). Therefore, we assume that the sensitivity of Gram-negative bacteria to dermaseptin could be affected by the form of LPS. Bello's study showed that the length of LPS only has a slightly steric barrier against AMP penetration (Bello et al., 2016). In the meantime, dermaseptin has been proven to interact with LPS of Gram-negative bacteria to exert the killing effect, and the hydrophobic amino acid residue, Trp, plays an essential role during this interaction (Navon-Venezia et al., 2002; Rydlo et al., 2006). However, it is still not clear which part of LPS has the critical effect on the antimicrobial activity of dermaseptins. Here, it is speculated that the shifting and complicated outer cores and O-antigen could be the potential binding targets on LPS for dermaseptins.

```
DPC1       GLWSKIKEAAKTAGKAAMGFVNEMV   25
DDQ2       GLWSKIKEAAKTAGLMAMGFVNDMV   25
           **************  ****** **
```

Figure 4.9 The alignment of the mature peptide sequences of DPC1 and dermaseptin Q2 (DDQ2). The identical amino acid residues are indicated by asterisks.

Table 4.3 The comparison of antimicrobial activity of DPC1 and DDQ2 against *E. coli* *S. aureus* and *P. aeruginosa*.

Peptide	MIC (mg/L)		
	E. coli	*S. aureus*	*P. aeruginosa*
DPC1	16	64	>512
DDQ2	14.9	58.7	58.7

Interestingly, DPC1 did not lyse the membranes of red blood cells but decreased the cell viability of four cancer cells. Particularly, the cell viability of MCF-7 cells was significantly decreased. Previous studies showed that dermaseptin B2 has antiproliferative effects against the human prostate cancer cell line, PC3, via necrosis and apoptosis, which is mediated by its interaction with negatively-charged molecules on the surface of cancer cells, like glycosaminoglycans (Dos Santos et al., 2017). DPC1 contains 2 net positive charges that makes it interact with the negatively-charged molecules, while, the appropriate hydrophobicity and amphipathicity ensure that DPC1 induce a low degree of haemolysis.

In summary, this is the first time report of the discovery of a dermaspetin peptide from the skin secretion of *Phyllomedusa camba*. DPC1 exerted remarkable antimicrobial activity and moderate anticancer activity, while it showed low haemolytic effects. These data suggest that DPC1 has a high degree of therapeutic index for applications in both anti-infection and anticancer chemotherapy.

Chapter 5

Discovery of Distinctin-Like-Peptide-PH (DLP-PH) from the Skin Secretion of *Phyllomedusa hypochondrialis*, a Prototype of a Novel Family of Antimicrobial Peptides

Published online 2018 Mar 23. Front Microbiol. 2018; 9: 541.

doi: 10.3389/fmicb.2018.00541 PMCID: PMC5876494 PMID: 29628917

Abstract

Amphibian skin secretions are an important treasure house of bioactive antimicrobial peptides (AMPs). Despite having been the focus of decades of research in this context, investigations of phyllomedusine frogs continue to identify new AMPs from their skin secretions. In this study, the prototype of a novel family of AMP distinctin-like-peptide-PH (DLP-PH) was identified from the skin secretion of the otherwise well-studied Tiger-Legged Tree Frog *Phyllomedusa hypochondrialis* through cloning of its precursor-encoding cDNA from a skin secretion-derived cDNA library by a 3'-rapid amplification of cDNA ends (RACE) strategy. Subsequently, the mature peptide was isolated and characterised using reverse-phase HPLC and MS/MS fragmentation sequencing. DLP-PH adopted an α-helical conformation in membrane mimetic solution and demonstrated unique structural features with two distinct domains that differed markedly in their physiochemical properties. Chemically synthesised replicates of DLP-PH showed antimicrobial activity against planktonic bacterial and yeast cells, but more potent against Escherichia coli at 32 mg/L. Furthermore, DLP-PH inhibited the growth of sessile cells of gram-negative bacteria in biofilms. In addition, DLP-PH exhibited anti-proliferative activity against human cancer cell lines, H157 and PC3, but with no major toxicity against normal human cell, HMEC-1. These combined properties make DLP-PH deserving further study as an antimicrobial agent and the further investigations of its structure-activity relationship could provide valuable new insights into drug lead candidates for antimicrobial and/or anti-cancer purposes.

5.1 Introduction

Not even a century after the discovery of penicillin marked a new era in the treatment of bacterial infectious agents, modern medicine is quickly reaching a crossroads with respect to the utility of antibiotics in health care. Two trends are especially apparent and worrisome in what is an evolutionary arms race. The first is the recent, rapid increase in the emergence of drug-resistant infectious agents ("superbugs") caused, in part, through the inappropriate prescribing of conventional antibiotics (Poole, 2011). The second is the natural ability of diverse bacterial species to form biofilms. These biofilms, which are derived from the hydrated polymeric matrices of sessile bacterial cells, are potently resistant to conventional treatment because of their thick, slimy and slippery coating and can thus cause persistent, serious infections. Evidence is also growing that the biofilms represent a natural defensive strategy on the part of the bacteria, in part in response to sub-inhibitory antibiotic doses (Karatan and Watnick, 2009). Whereas recent efforts have been directed to some extent at modifying existing antibiotics to increase their potency (e.g., vancomycin; Okano et al., 2017), a useful alternative strategy might be the discovery and application of novel antibiotic compounds with a different mode of action to conventional antibiotics.

In this second context, antimicrobial peptides (AMPs) have attracted the attention of many researchers because of their numerous, unique advantages, such as potent effects against a variety of pathogens, including many superbugs, their ability to suppress biofilm formation (Pletzer and Hancock, 2016; Reffuveille et al., 2014), and that their apparent primary mechanism of action (degradation of the microbial membrane) might prove to be more resistant to the development of antibiotic resistance. Moreover, in addition to their direct antimicrobial activities, AMPs have been recently discovered to

possess beneficial, secondary actions such as mediating the immune response and enhancing both wound healing and angiogenesis (Habets and Brockhurst, 2012; Samy et al., 2011).

An important natural resource for AMPs, are the skin secretions of amphibians, which, in addition to AMPs, also contain a cocktail of other chemically complex bioactive molecules displaying a wide range of activities. Indeed, amphibians AMPs have attracted much attention over the past decades (Xu and Lai, 2015), with over one-third of the nearly 3000 naturally occurring AMPs listed in the Antimicrobial Peptide Database (http://aps.unmc.edu/AP) coming from amphibians and 90% of those from frogs and toads. Nevertheless, the potential of amphibian skin secretions as a source of AMPs and of the AMPs themselves as a source of novel antibiotics has barely been tapped. Many new amphibian AMPs remain to be discovered and the AMPs that are already known either possess potent antimicrobial activities that deserve further study or can be used as templates for computer-aided drug design to enhance their efficacy.

Within this latter context, we describe a novel AMP precursor that we identified from the skin secretion of *Phyllomedusa hypochondrialis*. The mature peptide, which we called distinctin-like-peptide-PH (DLP-PH), displayed a number of interesting characteristics deserving of further investigation, including an evaluation of its bioactivities.

5.2 Materials and Methods

5.2.1 Secretion Acquisition and Maintenance of Experimental Specimens

Four adult specimens of *P. hypochondrialis* were obtained from a commercial source in

Peru (PeruBiotech E.I.R.L., Lima, Santiago de Surco, Peru). The frogs were kept in a tropical frog vivarium at 25°C and 85% humidity under a 12 h/12 h day/night cycle and were fed multivitamin-loaded crickets three times per week. The skin secretions were sampled referred to Section 2.1.

5.2.2 Construction of A Skin Secretion-derived cDNA Library and "Shotgun" Cloning

Five milligrams of lyophilized *P. hypochondrialis* skin secretion were used to perform the experiment, which was referred to Section 2.2 with a degenerate primer (5'-ACTTTCYGAWTTRYAAGMCCAAABATG-3') that we designed to bind to a highly-conserved segment of the 5'-untranslated region of bioactive peptide cDNAs from phyllomedusine frogs (Pierre et al., 2000; Wechselberger et al., 1998).

5.2.3 Identification and Primary Structure Analysis of Mature Peptide in Crude Skin Secretion

The isolation of mature peptide was referred to Section 2.4, and the identification of the primary sequence by MS/MS fragmentation sequencing was referred to Section 2.5.

5.2.4 Solid-Phase Peptide Synthesis

The mature peptide sequence was synthesized via solid phase peptide synthesis. In the process of synthesis, F-moc groups protected amino acid, resin, HBTU, N-methyl

morpholine (NMM), piperidine, N, N-dimethyl formamide (DMF) and dichloromethane (DCM) were employed. The peptide and resin were separated through use of the TFA cocktail solution. The detailed processes have been described in section 2.3.

5.2.5 Determination and Visualization of Peptide Secondary Structures

The secondary structure of each peptide was estimated using a CD spectrometer (Jasco J851, USA), which was referred to Section 2.6.1.

Additionally, we used several modeling methods to further elucidate secondary structures as well as to investigate possible mechanisms of action of the peptides. Helical Wheel Projection (http://rzlab.ucr.edu/scripts/wheel/wheel.cgi) was used to visualize the α-helical peptide and the I-TASSER online server (Yang et al., 2015) was employed to predict the secondary structures of the native peptide and its derivatives and to infer their 3-D structural models. The overall quality of these models were quantified by Ramachandran plots using RAMPAGE (Lovell et al., 2003) and by z-scores using ProSA (Wiederstein and Sippl, 2007). The physiochemical parameters of the AMPs were predicted using HeliQuest (Gautier et al., 2008).

As DLP-PH was more effective against the growth of *E. coli*, we aimed to simulate the antimicrobial mechanism using the *E. coli* membrane model (Pandit and Klauda, 2012), which has been fit to experimentally determined results and consists of six different lipids, was reconstructed through CHARMM-GUI (Jo et al., 2008). We then adopted the water-removed model to simulate AMP-membrane interaction. Molecular docking was performed using AutoDock Tools and AutoDock Vina (Trott and Olson, 2010). The aforementioned water-removed membrane model was used as the receptor molecule, the

absent polar hydrogens were added to this molecule through AutoDock Tools and then saved as a formatted pdbqt file. The grid box was set to cover the outer leaflet with the centre in 0, 0, 14 (x, y, z); and its size was set to 69 for each of the three axes, the optimal box size 69 for DLP-PH as determined by the eBoxSize script (Feinstein and Brylinski, 2015). The DLP-PH model file was input to AutoDock Tools as the ligand molecule. The Gasteiger charges were added and the nonpolar hydrogens were merged automatically. Then the missing polar hydrogens were added, the chemical bonds torsions were adjusted and the molecule was output to a pdbqt formatted file. Exhaustiveness was set to 20 given that the volume of the search space was larger than 27000 $Å^3$. All of the information was written into a configuration file and was calculated by AutoDock Vina. The calculated molecular docking result with the best affinity score was rendered with the PyMol (PyMOL Molecular Graphics System, Version 1.8 Schrödinger, LLC).

5.2.6 Antimicrobial Susceptibility Assays

The antimicrobial activities of the synthetic peptides were assayed against both planktonic microbial cells as well as sessile cells in biofilms. In the former case, we quantified both the minimal inhibitory (MIC) and minimal bactericidal concentrations (MBC) against planktonic cells of the gram-positive bacterium *Staphylococcus aureus* (NCTC 10788), the gram-negative bacteria *Escherichia coli* (NCTC 10418) and *Pseudomonas aeruginosa* (ATCC 27853), and the yeast *Candida albicans* (NCYC 1467) using the micro broth dilution method (Wu et al., 2016; Yitian et al., 2016).

Susceptibility assays against sessile cells in biofilms were conducted by quantifying the minimal biofilm inhibition (MBIC) and the minimal biofilm eradication concentrations

(MBEC) as well as the biofilm initial attachment inhibition against the same strains of gram-negative bacteria used above (*E. coli* and *P. aeruginosa*). MBIC and MBEC testing was performed, with minor modifications, according to (Knezevic and Petrovic, 2008; Sabaeifard et al., 2014), using the colorimetric indicator 2,3,5,-triphenyl tetrazolium chloride (TTC) to estimate microbial cell viabilities.

The biofilm initial attachment (IA) inhibition assay was performed using *P. aeruginosa*, a strong biofilm-producing bacterium, using a slightly modified version of the method of (Zhang et al., 2016). Briefly, different concentrations of the peptide solutions and diluted bacterial inoculum were loaded in the same way as with the MBIC assays, but with an incubation time of only 1 h and also without agitation to facilitate bacterial binding. Thereafter, the wells were washed with PBS, fixed with methanol, air-dried and stained with 0.1% (w/v) crystal violet, and washed with tap water before being air-dried. Finally, the crystal violet was solubilised in 33% acetic acid and the absorbance at 550 nm was measured in a plate reader to calculate the IC50 of biofilm initial attachment inhibition.

5.2.7 Cytoplasmic Materials Leakage Assay

As an indicator of the potential lysis of the microbial cell membranes in the presence of the peptides, we performed a cytoplasmic material leakage assay (Samanta et al., 2013; Sahu et al., 2009). Briefly, overnight microbial cultures of *S. aureus*, *E. coli* and *C. albicans* were washed with pre-warmed PBS and diluted to 5×10^5 CFU/ml in PBS. The synthesised peptides to be tested were dissolved in PBS and two-fold diluted as described above to achieve a final concentration range from 512 to 1 mg/L. Triton-X 100 (0.2%) in PBS was used as a positive control, with 100 µl of different concentrations of the peptide

in PBS (512 to 1 mg/L) being used as blank controls. The plates were incubated at 37°C for 2 h before the contents in each well were filtered through 0.22-μm syringe filters (Sigma-Aldrich, St. Louis, MO, USA) into new plates. A volume of 100 μl of the supernatant was transferred into a new 96-well plate and the absorbance at 260 nm was measured using a plate reader.

5.2.8 Haemolysis Assay

The experimental method was referred to Section 2.8.

5.2.9 Assessment of Anti-proliferation Effect and Cytotoxicity on Human Cancer and Normal Cell Lines

Possible anti-cancer activities of the novel peptide were investigated against a range of five human cancer cells lines: human prostate carcinoma cell line PC-3 (ATCC-CRL-1435) and human non-small cell lung cancer cell line H-157 (ATCC-CRL-5802) were cultured in RPMI-1640 medium (Gibco, Invitrogen, Paisley, UK) with 10% fetal bovine serum (FBS) (Sigma-Aldrich, St. Louis, MO, USA) and 1% Penicillin-Streptomycin (PS) (Invitrogen, Paisley, UK), whereas human breast melanoma cell line MDA-MB-435s (ATCC-HTB-129), human breast adenocarcinoma cell line MCF-7 (ATCC-HTB-22) and human neuronal glioblastoma cell line U251MG (ECACC-09063001) were cultured in DMEM medium (Invitrogen, Paisley, UK) with 10% FBS and 1% PS. As a control, human microvessel endothelial cell line HMEC-1 (ATCC-CRL-3243), which was cultured in 10% FBS, 10 ng/ml epidermal growth factor (EGF) (Invitrogen, Paisley, UK),

10 mM L-glutamine (Invitrogen, Paisley, UK) and 1% PS loaded MCDB131 medium (Invitrogen, Paisley, UK), was used to evaluate the cytotoxicity of the synthetic peptides on normal human cell line. The detailed procedure was referred to Section 2.9.

Cell cytotoxicity activity was assessed using the LDH assay (Pierce LDH cytotoxicity assay kit, Thermo Scientific), and the experiment was followed the instruction provided with the kit. The cells were seeded in a 96 well plate as described above and synchronised for a further 4 h. Afterwards, the cells were treated with DLP-PH same concertation range as MTT assay and incubated for 45 min. Lysis solution and ddH_2O were applied as positive and negative control, respectively. After incubation, 50 µl of each sample medium were transferred into another 96-well plate and mixed with 50 µl of LDH reaction mixture. Each sample was further mixed with 50 µl of stop solution after a 30 min incubation period from light at room temperature. The LDH activity was measured by the absorbance at 490 nm, which subtracted the absorbance at 680 nm.

5.2.10 Statistical Analyses

Statistical analyses were referred to Section 2.10.

5.3 Result

5.3.1 Identification and Characterization of a DLP-PH Precursor cDNA from a Skin Secretion-derived cDNA Library

Through shotgun cloning of the *P. hypochondrialis* skin secretion derived cDNA library,

we consistently retrieved a cDNA encoding the precursor of a novel peptide (DLP-PH) with an open reading frame of 80 amino-acid residues, including a signal peptide terminating in a cysteine residue; an acidic amino-acid residue-rich spacer peptide; and a predicted putative mature peptide of 36 amino-acid residues. The predicted mature peptide appeared after a lysine-arginine (KR) motif, which is a typical propeptide convertase cleavage processing site (Figure 5.1a). The nucleotide sequence of the entire cDNA encoding DLP-PH has been deposited in the EMBL sequence database under the accession number LT718215. An NCBI BLAST analysis, showed that the DLP-PH precursor exhibited a high degree of structural identity with another distinctin-like peptide precursor from *Phyllomedusa azurea*, including an identical mature peptide region and highly-conserved signal/spacer peptide regions (Tompson, 2006) (unpublished data). Additionally, the DLP-PH peptide precursor demonstrated strong similarity to the B-chain peptide (distinctin-B) precursor of the heterodimeric AMP distinctin from *Phyllomedusa distincta*(Batista et al., 2001; Evaristo et al., 2013) along most of the entire precursor-encoding cDNA of the latter. Noticeable dissimilarity only arose in the C-terminal domain of the mature peptides, with DLP-PH also being much longer than distinctin-B (Figure 5.1b, c).

MALDI-TOF mass spectrometry analyses of the fractionated skin-secretion samples from RP-HPLC (Figure 5.2a) identified a peptide coincident in molecular mass to that of the mature peptide predicted from the cloned cDNA (4196.9) in fraction #118. MS/MS fragmentation sequencing of a sample of this fraction (Figure 5.2b) confirmed the primary structure of the mature peptide.

Figure 5.1 The biosynthetic precursor of DLP-PH and the comparison with Distinctin-B. **(A)** Nucleotide and translated open-reading frame amino acid sequence of a cDNA encoding the DLP-PH precursor cloned from a *P. hypochondrialis* skin secretion library. The predicted mature peptide is single underlined, the signal peptide is double-underlined and the stop codon is indicated by an asterisk. **(B)** The alignment of amino acid sequences of distinctin-B and DLP-PH precursors. **(C)** The alignment of corresponding precursor-encoding cDNA sequences. Conserved residues/bases are indicated in red with a yellow highlight. Similar residues are highlighted in green.

A

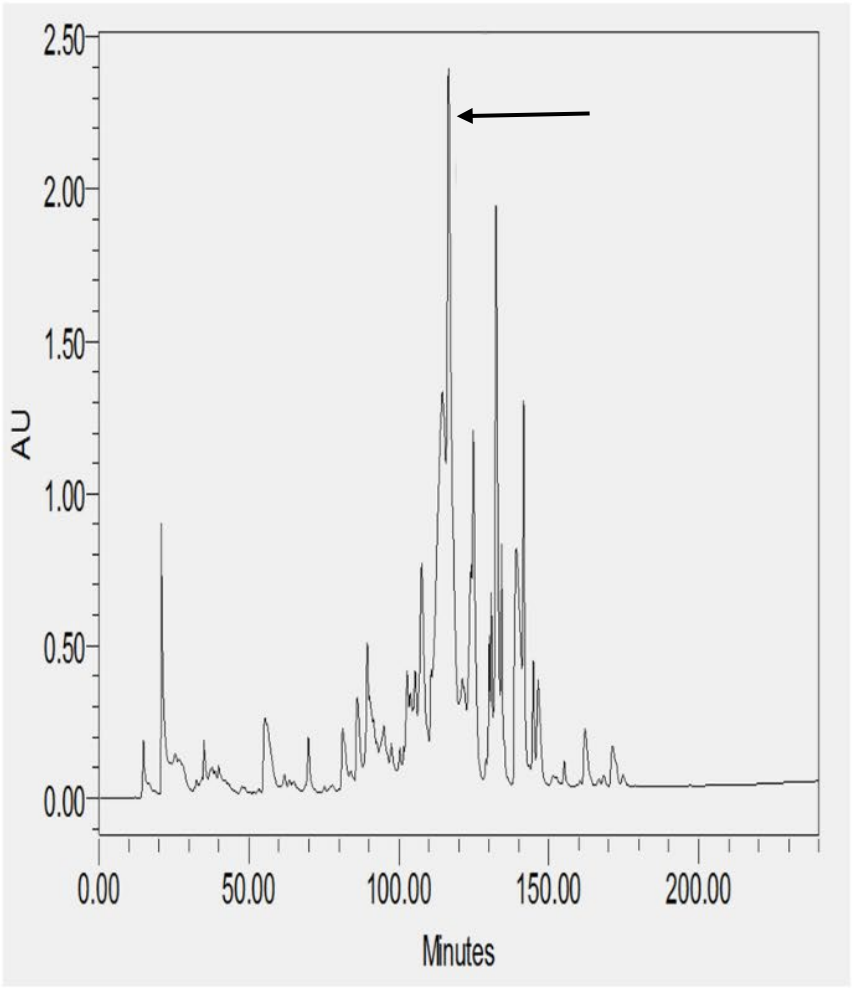

B

#1	b(1+)	b(2+)	b(3+)	Seq.	y(1+)	y(2+)	y(3+)	#2
1	115.050	58.029	39.022	N				36
2	228.134	114.571	76.716	L	4081.409	2041.208	1361.141	35
3	327.203	164.105	109.739	V	3968.325	1984.666	1323.446	34
4	414.235	207.621	138.750	S	3869.256	1935.132	1290.424	33
5	485.272	243.140	162.429	A	3782.224	1891.616	1261.413	32
6	598.356	299.682	200.123	L	3711.187	1856.097	1237.734	31
7	711.440	356.224	237.818	I	3598.103	1799.555	1200.039	30
8	840.483	420.745	280.832	E	3485.019	1743.013	1162.344	29
9	897.504	449.256	299.840	G	3355.976	1678.492	1119.330	28
10	1053.605	527.306	351.873	R	3298.955	1649.981	1100.323	27
11	1181.700	591.354	394.572	K	3142.854	1571.930	1048.289	26
12	1344.763	672.885	448.926	Y	3014.759	1507.883	1005.591	25
13	1457.848	729.427	486.621	L	2851.695	1426.351	951.237	24
14	1585.943	793.475	529.319	K	2738.611	1369.809	913.542	23
15	1699.985	850.496	567.333	N	2610.516	1305.762	870.844	22
16	1799.054	900.031	600.356	V	2496.473	1248.740	832.829	21
17	1912.138	956.573	638.051	L	2397.405	1199.206	799.807	20
18	2040.233	1020.620	680.749	K	2284.321	1142.664	762.112	19
19	2168.328	1084.668	723.447	K	2156.226	1078.617	719.413	18
20	2281.412	1141.210	761.142	L	2028.131	1014.569	676.715	17
21	2395.455	1198.231	799.156	N	1915.047	958.027	639.020	16
22	2551.556	1276.282	851.190	R	1801.004	901.006	601.006	15
23	2664.640	1332.824	888.885	L	1644.903	822.955	548.972	14
24	2792.735	1396.871	931.583	K	1531.819	766.413	511.278	13
25	2921.778	1461.392	974.597	E	1403.724	702.366	468.579	12
26	3049.873	1525.440	1017.296	K	1274.681	637.844	425.565	11
27	3163.916	1582.461	1055.310	N	1146.586	573.797	382.867	10
28	3292.011	1646.509	1098.008	K	1032.543	516.775	344.853	9
29	3363.048	1682.027	1121.687	A	904.448	452.728	302.154	8
30	3491.143	1746.075	1164.386	K	833.411	417.209	278.475	7
31	3605.186	1803.096	1202.400	N	705.316	353.162	235.777	6
32	3692.218	1846.612	1231.411	S	591.273	296.140	197.763	5
33	3820.313	1910.660	1274.109	K	504.241	252.624	168.752	4
34	3949.355	1975.181	1317.123	E	376.146	188.577	126.054	3
35	4063.398	2032.203	1355.138	N	247.104	124.055	83.039	2
36				N	133.061	67.034	45.025	1

Figure 5.2 (A) RP-HPLC chromatogram at 214 nm of *P. hypochondrialis* skin secretion indicating elution position/retention time of DLP-PH (arrow). (B) MS/MS fragmentation datasets of fragment ions corresponding to those of DLP-PH. Expected singly- and doubly-charged b-ion and y-ion fragment m/z ratios were predicted and observed fragment ions are indicated in red and blue coloured typefaces.

5.3.2 Prediction of Secondary Structure and Physiochemical Properties

The z-score of -1.34 for the 3D model of DLP-PH predicted using I-TASSER is within the range of scores typically found for protein/peptide native folds identified by NMR with similar size (Figure 5.3). Moreover, assessment of stereo-chemical backbone of the DLP-PH model via the Phi and Psi dihedral angles of the Ramachandran plot showed that all residues were in the favored regions (Figure 5.3). The model revealed that the peptide should adopt an α-helical conformation, which was verified by CD assays. Whereas the mature peptide existed as a random coil in aqueous solution, it did indeed form a typical α-helical structure with negative bands at 208 nm, 222 nm and a positive band at 190 nm in the membrane-mimetic TFE solution (Figure 5.3).

The best molecular docking model between DLP-PH and the model of the *E. coli* cytoplasmic membrane showed a binding affinity of -3.5 kcal/mol, with DLP-PH bonding to the hydrophilic heads of the phospholipid molecules. Parallel to this, most of the cationic charged residues (Lys and Arg) of DLP-PH were predicted to face the cell membrane through electrostatic attraction (Figure 5.4a). Both the binding model and the DLP-PH helical wheel projection plot of DLP-PH (Figure 5.4b) indicated that the N-terminal (inner circle in Figure 5.4b) and C-terminal domains of the mature peptide (outer

circle) possess distinctly different physiochemical properties, with the former being amphipathic and the latter hydrophilic. We confirmed this by synthesizing two additional peptides corresponding to the two domains of the full peptide (DLP-PHn and DLP-PHc, respectively). Thus, whereas the entire peptide is hydrophilic (H = -0.031) and cationic (+8) nature because of the high proportion of polar residues, DLP-PHn is amphipathic (μH = 0.487) with a high hydrophobicity (H = 0.358) and an outstanding hydrophobic face (-YAVGLLLL-) and DLP-PHc with its comparative lack of nonpolar residues shows poor hydrophobicity (H = -0.480) and amphipathicity (μH = 0.158) (Table 5.1). A third peptide, DLP-PHt, was designed by truncating the native peptide at Asn^{15} according to that portion of DLP-PH that shows distinctly reduced homology with the B-chain of distinctin (Lys^{14} to Asn^{36}) while avoiding Lys^{14}, which might be enzymatically sensitive. Compared with DLP-PHc, DLP-PHt displayed a higher hydrophobicity (H = -0.283) and amphipathicity (μH = 0.270), but with values that were still distinctly lower than those for DLP-PH and DLP-PHn.

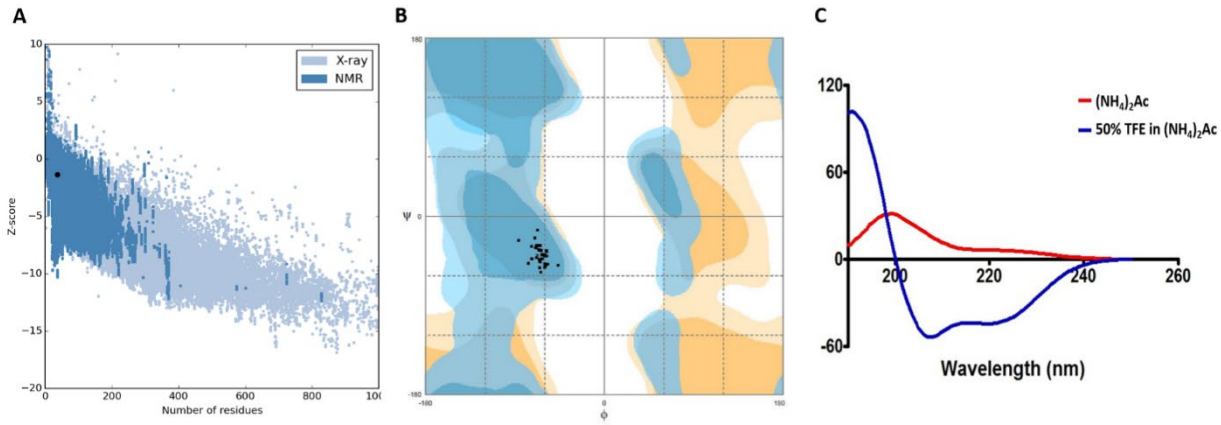

Figure 5.3 (A) The validation of the predicted DLP-PH 3D model by z-score using ProSA. **(B)** The validation of the predicted DLP-PH 3D model by Ramachandran plot using RAMPAGE. All residues were in the favored regions. **(C)** CD spectra recorded for

DLP-PH (100 μM) in 10 mM ammonium acetate/water solution (red) and in 50% 2,2,2-trifluoroethanol (TFE)/10 mM ammonium acetate/water solution (blue). The peptide was existed in random coli in aqueous solution while was induced to a typical α-helix in membrane-mimetic solution.

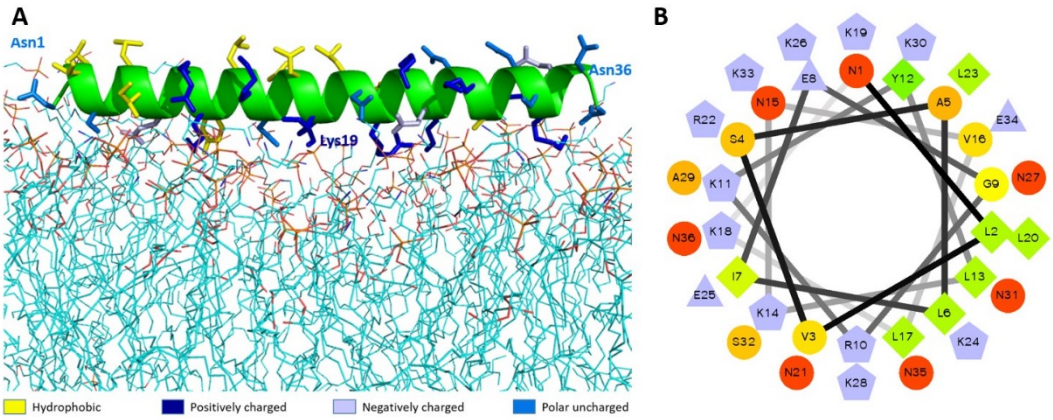

Figure 5.4 The molecular modelling of DLP-PH structures. **(A)** Theoretical docking study of DLP-PH with *E. coli* model membrane. The secondary structure of DLP-PH is showing in green cartoon, the main chain is hided and side chains are representing in sticks with different colors (designated in the figure according to the properties of the residues). The phospholipids are presenting in lines with carbon atoms in cyan, oxygen atoms in red, nitrogen atoms in blue and phosphorus atoms in orange. **(B)** Helical wheel projection of DLP-PH with the N-terminal domain in the inner circle and the C-terminal domain in the outer circle.

Table 5.1 Sequences of DLP-PH, its derivatives, distinctin and distinctin-B

Peptide	Sequence
DLP-PH	NLVSALIEGRKYLKNVLKKLNRLKEKNKAKNSKENN
DLP-PHn	NLVSALIEGRKYLKNVLK
DLP-PHc	KLNRLKEKNKAKNSKENN
DLP-PHt	NVLKKLNRLKEKNKAKNSKENN
Distinctin-B	NLVSGLIEARKYLEQLHRKLKNCKV
Distinctin	ENREVPPGFTALIKTLRKCKII (A)
	|
	NLVSGLIEARKYLEQLHRKLKNCKV (B)

5.3.3 Antimicrobial Activities

The naturally occurring peptide DLP-PH exhibited activity against planktonic cells of all four tested microorganisms, albeit with noticeably less potency against the gram-positive bacterium *S. aureus* or in the presence of divalent cations (Table 5.2). Most of this activity appears to derive from the N-terminal domain of the peptide, with DLP-PHc and DLP-PHt being devoid of effective antimicrobial effects. Only DLP-PHn showed any noteworthy efficacy, which was at least 2-fold more effective than that of DLP-PH in the case of *S. aureus*. (However, because the molecular mass of DLP-PHn (2059 Da) is nearly half of that of DLP-PH (4197 Da), their MICs against *S. aureus* were quite similar when viewed in terms of molarity: 62.2 μM versus 61.0 μM, respectively). The efficacy of DLP-PH against sessile cells of either *E. coli* or *P. aeruginosa* in biofilm was strongly reduced compared to the analogous values against planktonic cells (four- and eight-fold reduced, respectively; Table 5.3). The inhibition of biofilm initial attachment (IA) against *P. aeruginosa* showed an IC_{50} value of 96 mg/L (22.8 μM) (Figure 5.5b).

The cytoplasmic materials release experiment revealed that DLP-PH lysed nearly 100% of the microbial cells at high concentrations of peptide (512 mg/L; Figure 5.5a). Effects at lower concentrations were organism-specific. Thus, whereas strong cell lysis was also observed at the MIC of DLP-PH against *S. aureus* (256 mg/L), barely any cells of *E. coli* were lysed at its MIC of 32 mg/L. By contrast, DLP-PH continued to result in >50% cell lysis of *C. albicans* even at concentrations well below its MIC (64 mg/L) against this organism.

Table 5.2 Antimicrobial activity of DLP-PH and its derivatives against planktonic cells of four reference microorganisms. (Unit: mg/L; values in brackets were the MICs tested in divalent cation supplemented medium.)

	S. aureus		***E. coli***		***P. aeruginosa***		***C. albicans***	
	MIC	**MBC**	**MIC**	**MBC**	**MIC**	**MBC**	**MIC**	**MBC**
DLP-PH	256	512	32(128)	32	64(>512)	128	64	64
DLP-PHn	128	128	128	128	>512	>512	64	64
DLP-PHc	>512	>512	>512	>512	>512	>512	512	>512
DLP-PHt	512	>512	>512	>512	>512	>512	256	256

Table 5.3 Anti-biofilm activity of DLP-PH against gram-negative bacteria. (mg/L, molarity was calculated and shown in the brackets.)

	E. coli		***P. aeruginosa***		
	MBIC	**MBEC**	**MBIC**	**MBEC**	**IA-IC_{50}**
DLP-PH	128 (30.5)	256 (61.0)	512 (122.0)	512 (122.0)	96 (22.8)

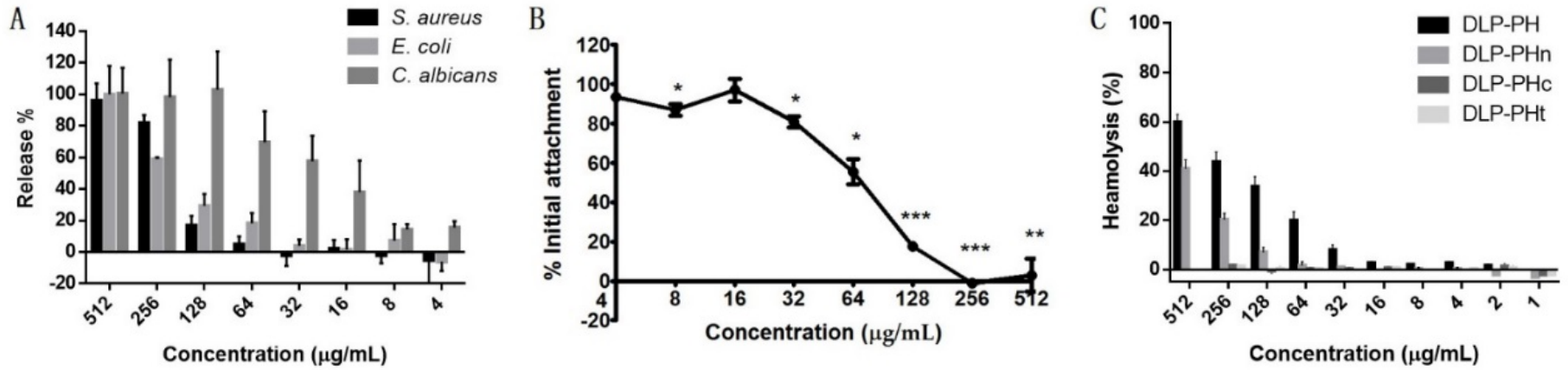

Figure 5.5 (A) Effect of DLP-PH on cytoplasmic material release of *S. aureus*, *E. coli* and *C. albicans* at 260 nm.The error bar represents the standard error for three repeats (ANOVA, P<0.05). **(B)** Effect of DLP-PH on the *P. aeruginosa* biofilm initial attachment.The error bar represents the standard error for three repeats. The significance is given as * p<0.05; ** p<0.01; *** p<0.001.**(C)** Relative haemolysis of DLP-PH and its deviates on horse red blood cells.The 100% haemolysis was defined using haemolytic effect induced by 1% Triton X-100 (ANOVA, P<0.05).

5.3.4 Bioactivity of DLP-PH on Mammalian Cells

Only DLP-PH and DLP-PHn showed any haemolytic activity against horse blood red cells, but 100% haemolysis was never observed even at the highest tested concentration of 512 mg/L. The remaining designed peptides, DLP-PHc and DLP-PHt, showed no haemolytic activity whatsoever, thereby mirroring their weak antimicrobial activities (Figure 5.5c).

Of the five different cancer cell lines used to screen the anti-proliferation activity of DLP-PH, evident activity (defined as a growth inhibition concentration ≥4.197 μM) was only shown against the two cell lines H-157 and PC-3, with IC_{50} values 15.41 mg/L and 32.25 mg/L, respectively (Figure 5.3.4A). By contrast, DLP-PH showed significant cytotoxicity against the normal human cell line HMEC-1 only at the highest concentration tested (419.7 mg/L), with the IC_{50} of 287.2 mg/Lalso being much higher than the corresponding values for the two cancer lines above (Figure 5.6a). The LDH assay confirmed that DLP-PH resulted in low degree of cytotoxicity on mammalian cells, especially HMEC-1, while it exhibited more toxic on cancer cell lines (Figure 5.6b).

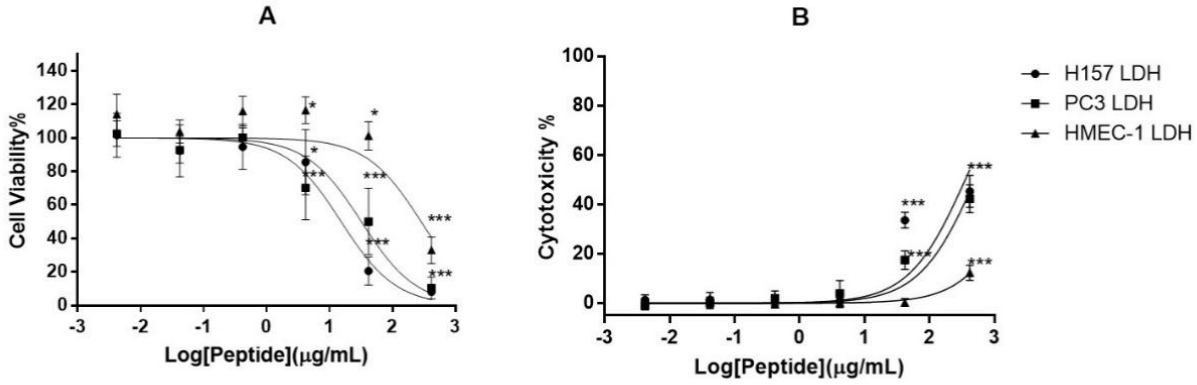

Figure 5.6 (A) The anti-proliferation effect and **(B)** cytotoxicity of DLP-PH on human cancer cell lines**,** H-157 and PC-3, and the normal human endothelial cell line**,** HMEC-1 within the concentration range of 419.7 to 4.197×10^{-3} mg/L. The error bar represents the standard error for three repeats. The significance is given as * $p<0.05$; ** $p<0.01$; *** $p<0.001$.

5.4 Discussion

Phyllomedusa hypochondrialis represents a well-studied frog species with respect to its skin secretions, with the Antimicrobial Peptide Database listing at least 36 AMPs that have been isolated from this species. Our study identified another novel AMP for the species, with the mature peptide, DLP-PH, First, as the name suggests, showing high identity to the 25-residue B-chain of the AMP distinctin from *Phyllomedusa distincta*(Batista et al., 2001), which itself is unusual among AMPs because of its heterodimeric structure. Furthermore, DLP-PH possessed an intriguing structure consisting of an N-terminal amphiphilic region and a C-terminal hydrophilic region.

Altogether, these unique characteristics of DLP-PH argue for it representing the prototype of a novel AMP family. Compared to the majority of amphibian AMPs, DLP-PH is unusual because of the extremely heterogeneous properties of its N- and C-terminal domains, with only the former displaying the characteristics typical of amphibian AMPs (i.e., high amphiphilicity and hydrophobicity) and thus seemingly contributing most to the antimicrobial activity of the entire peptide. By contrast, the C-terminal end was hydrophilic, less amphiphilic and, as evidenced by the DLP-PHc peptide that we designed, devoid of any antimicrobial activity on its own. However, some possible synergistic effects between the two domains of DLP-PH might have been observed in that the entire peptide showed stronger activity against the Gram-negative bacteria tested than did either domain alone, and notably the N-terminal domain, in isolation (Table 5.1). By contrast, the N-terminal domain alone showed better activity against the gram-positive *S. aureus* than did the complete peptide.

Based on these results, we hypothesise that the amphiphilic α-helical N-terminal domain is responsible for the actual bioactivity of DLP-PH, probably by membrane lysis via pore formation. However, the importance of the latter mechanism remains uncertain to some degree, as it does for most amphibian AMPs. Although our cytoplasmic leakage assays did indicate cell lysis against all tested organisms, cell lysis for *E. coli* was minimal at the empirically determined MIC (32 mg/L) for this organism, implying some other mechanism for the observed bioactivity (e.g., translocation of DLP-PH through the non-lethal pores to instead target intracellular structures or interfere with bacterial metabolism or growth cycles). Similarly, the high leakage of cytoplasmic contents that was inferred for *C. albicans* below its observed MIC (64 mg/L), indicates that cell lysis alone appears to be insufficient for antimicrobial action and that an additional, possibly intracellular,

mechanism is also required.

By contrast, the highly cationic-charged C-terminal domain would appear to be nonobligatory with respect to actual bioactivity, but could facilitate the initial attachment of DLP-PH onto the negatively charged bacterial cell membrane through electrostatic attraction. Evidence for the latter comes from molecular docking model, which clearly showed that the cationic charged residues, especially those in the C-terminal domain, mostly faced the negatively charged phospholipid head groups of the *E. coli* model membrane. Additionally, the loss of function of DLP-PH in the divalent cation supplemented medium indicates inhibition of the electrostatic attraction to the microbial membrane through competition from the additional cations. This proposed function of the C-terminal domain might also explain why DLP-PH was able to inhibit the growth of at least two human cancer cells without showing other significant cytotoxic effects given that the cell membranes of cancer cells are known to be more negatively charged than those of normal cells (Gaspar et al., 2013). Again, it is unclear if anti-cancer activity results solely primarily cellular membrane lysis (Papo and Shai, 2005) and/or if interacting with cell surface receptors and influencing intercellular signaling pathways (Scott et al., 2000) are also involved. For example, gene microarray studies indicate that some cationic peptides can regulate the expression of a number of genes related to cell apoptosis and cell proliferation (Scott et al., 2000).

Through its heterogeneous nature, DLP-PH structurally somewhat resembles the AMP distinctin, which was isolated from the congeneric frog *Phyllomedusa distincta* (Batista et al., 2001). Distinctin itself is unusual in being a disulphide-bridged, heterodimeric AMP. AMPs with disulphide bridges are known and include human beta-defensins (HBDs) from human leukocytes and epithelial cells (Schneider et al., 2005) and cysteine-

rich peptides (CRPs) from plants (Tam et al., 2015), both of which adopt β-sheet structures that are stabilised by two or more intramolecular disulphide bonds. They are also present in the skin secretions of frogs, such as some AMPs from *Rana* spp., which contain a disulphide-bridged cyclic domain of varying size (six or seven residues; the "Rana box" (Conlon, 2011)) and the Bowman-Birk inhibitor (BBI) like peptides, which contain a canonical disulphide BBI loop with 11 residues (Song et al., 2008). However, in all these cases, the disulphide bridge is intramolecular, whereas the bridge in distinctin is found between the heterodimers, with each chain being encoded by separate mRNAs (Evaristo et al., 2013) as well as having distinct physiochemical properties, albeit not as extreme as we found for the two domains of DLP-PH. The resemblance between DLP-PH and distinctin is further strengthened by the extremely high degree of similarity between the primary structures of the N-terminal domain of DLP-PH and the B-chain of distinctin. However, the exact relationship between the two peptides remains unclear given the complete lack of similarity between the remainder of DLP-PH and any part of distinctin.

A functional similarity between DLP-PH and distinctin also exists insofar as distinctin shows a broad-spectrum antimicrobial activity against both gram-positive and gram-negative bacteria and a generally doubled potency compared to the B-chain in isolation (Table 5.4). In this study, distinctin was more broad-spectrum than DLP-PH, which showed less efficacy against the gram-positive *S. aureus*; however, the antimicrobial activity of DLP-PH against gram-negative bacteria was as good as or even better than distinctin or Pexiganan, an antibiotic in late stage clinical trial that is derived from a frog skin AMP. Notably, all AMPs or AMP-derived products were much more effective against the gram-negative bacteria tested than was the conventional antibiotic ampicillin.

Considering that DLP-PH is more potent against *E. coli* without damaging erythrocytes, it might benefit the treatment for *E. coli* induced bacteremia. Furthermore, as AMPs have been reported to have the ability of neutralizing a broad range of bacterial toxins (Kudryashova et al., 2017), the further investigation on the inactivation of *E. coli* toxins, like Shiga toxin, by DLP-PH might be carried out for the drug discovery in the treatment of hemolytic uremic syndrome.

Table 5.4 Comparative study of the antimicrobial activities of DLP-PH, distinctin, the B-chain of distinctin in isolation, Pexiganan and conventional antibiotic ampicillin.

(Unit: μM; ND: not determined.)

	MIC		
	S. aureus	***E. coli***	***P. aeruginosa***
DLP-PH[a]	61.0	7.6	15.2
Distinctin[b]	23.4	11.7	23.4
Distinctin, B-chain[b]	43.3	24.7	43.3
Pexiganan[c]	6.5	12.9	12.9
Ampicillin[a]	0.06	45.8	>366.3

[a] Determined using the type strains mentioned in this study.

[b] MIC_{90} values at which 90% of the isolates tested were inhibited (Dalla Serra et al., 2008).

[c] Determined using the same type strains mentioned in this study (Ge et al., 1999).

Chapter 6

General discussion

6.1 The Significance of AMPs

AMPs are immunologically active peptides produced by the animal immune defence system under the stimulation of external conditions. Antimicrobial peptides have the characteristics of low molecular weight, good water solubility, low antigenicity, and substantial thermal stability. Most AMPs have antibacterial or fungal activities, and some also have antiprotozoal, viral, or tumour cell functions, while having fewer effects on normal animal cells.

It is generally believed that antimicrobial peptides kill the cell by forming pores in the cell membrane, thereby altering cell membrane permeability or causing leaking of the contents. The action model of the process of AMPs killing bacteria is divided into the following three steps: Firstly, the antimicrobial peptide and the cell membrane attract each other to bind to the membrane. Next, the hydrophobic C-terminus has inserted into the membrane meanwhile the N-terminus forms α-helix and stays at the membrane interface. Finally, the amphipathic α-helix inserts into the plasma membrane and then forms a more extensive pore, thereby killing the bacterial cells (Zhu et al., 2007). The primary biochemical properties that affect the antimicrobial activity of antimicrobial peptides include helicity, hydrophobicity, amphiphilicity, and net charge.

Studies show that the α-helix domain of the N-terminus of dermaseptin plays a vital role to maintain antimicrobial activity (Mor & Nicolas, 1994). Chen et al. (2005) reported that replacing D-type amino acids with L-amino acids revealed that substitutions are not conducive to the formation of the helix structure in the peptide chain. Moreover, the net charge and hydrophobicity are not affected by reducing the helix content. It is an effective method for studying the relationship between the helicity of antimicrobial peptides and their antibacterial activity and haemolytic activity.

Antibacterial peptides contain nearly half hydrophobic amino acid residues, and effects of hydrophobicity on their activity can be studied by changing the number of Leu, Ile, and Val of peptides. Peptide chains can form multimers by interacting with a hydrophobic group which presents in solution, resulting in increasing their affinity for eukaryotic cell membranes, and also enhancing the ability of antimicrobial peptides to form α-helix. With the increasing of α-helix, the stability of antimicrobial peptides is improved as well (Lee et al., 2002). However, both antibacterial and haemolytic activities of AMPs are improved simultaneously by increasing the hydrophobicity, which is because the hydrophobic group plays a crucial role in the insertion of the antimicrobial peptide into the cell membrane.

Amphipathicity is an essential structural feature of α-helical antimicrobial peptides. In this structure, hydrophilic groups and hydrophobic groups are either concentrated at the N-terminus or C-terminus of antimicrobial peptides or distributed on both sides of AMPs to form hydrophilic and hydrophobic surfaces. The α-helix facilitates the binding of antimicrobial peptides to the surface of bacteria. When peptide binds to the cell membrane, its hydrophilic structure binds to the phospholipid head of the membrane by electrostatic attraction, and the hydrophobic part and the membrane phospholipid tail are combined with hydrophobic effect. The α-helical antimicrobial peptides with stronger lysis of membranes usually possess more hydrophobic regions and longer hydrophobic moments (Dathe, 1999).

The number of net charges of antimicrobial peptides is a key factor influencing the binding of antimicrobial peptides to membranes. The antimicrobial peptide binds to the membrane by electrostatic interaction and competitively replaces the divalent cation. Therefore, changing the number of positive charges of antimicrobial peptides can change the binding ability of AMPs to membranes, resulting in the change of antimicrobial activity (Hancock, 2001).

6.2 The Findings in This Thesis

Because of the significance of AMPs, in this thesis, we focused on the antimicrobial peptides from the phyllomedusinae tree frogs. In Chapter 3, we identified a 23-mer dermaseptin from the skin secretion of *Phyllomedusa sauvagii*, namely dermaseptin-PS3. According to the literature and the peptide database, the length of the amino acid sequence is the one of the shortest dermaseptin peptides identified so far (Huang et al., 2017). As the data shows, the antimicrobial activity is mild compared to other dermaseptins, such as dermaseptin S4 (Feder et al., 2000), while it possesses moderate haemolytic activity, which is quite distinct from the general description of "low cytotoxicity" of dermaseptins. The first thought is that the amino acid constitution results in remarkable membrane lytic effects without any specificity. Therefore, the subsequent amino acid substitution was carried out to confirm this. Firstly, as the cationicity could improve the affinity of AMP to bacteria, we introduced two positive charges to DPS3. The enhancement of antimicrobial activity was observed, but the haemolysis was also increased. To demonstrate non-specific membrane interaction of DPS3, two Leu were introduced to increase the hydrophobicity, which exhibited enhancement of all the activities. Notably, the haemolysis is more severe than the Lys-substituted analogue. It indicates that for DPS3, charges only improve the selectivity to a certain degree, while hydrophobicity ruined the selectivity completely. It suggests that the increase of charge improves the adhesion affinity but the increased hydrophobicity enhances the insertion affinity (Gaidukov et al., 2003). This hypothesis was also glimpsed in Chapter 4. Although dermaseptin-PC1 is just two-amino-acid-residues longer than DPS1, the cytolytic activity has been proven to be much less than DPS1.

Comparing the two peptides, they have similar hydrophobicity (0.373 verse 0.335) and hydrophobic moment (0.437 verse 0.447). Whereas, DPC1 possesses one more charge (2 verse 1), and exhibited a higher degree of therapeutic efficacy. In the meantime, we found that the mid-region motif of DPC1 is longer than that of DPS3, indicating the insertion affinity might be related to the unique structure. The mid-region motif mainly consists of neutral amino acid residues, Ala and Gly, and essential amino acid residue, Lys, which can form a relatively hydrophilic, positively-charged helical domain. This domain may only benefit the adhesion affinity through the electrostatic interaction between anionic phospholipid groups. Additionally, the domain may interfere with the continuously hydrophobic field, which could prevent the interaction with zwitterionic phospholipid of normal cell membranes (Gaidukov et al., 2003). Therefore, no matter which factor we adjusted (hydrophobicity or charge), the antimicrobial activity and cytotoxicity are hard to balance due to the short mid-region motif of DPS3.

In this thesis, a prototype peptide of a novel antimicrobial peptide family, is described. In Chapter 5, distinctin-like-peptide-PH was identified from the skin secretion of *Phyllomedusa hypochondrialis*. DLP-PH contains 36 amino acids, one-third of which are basic amino acids. The N-terminal segment of DLP-PH is similar to the chain B of distinctin, a 47-residue heterodimeric antimicrobial peptide from *Phyllomedusa distincta* (Batista et al., 2001). Unsurprisingly, the signal peptide domains of three peptide precursors in this thesis are highly conserved. Notably, the two of the dermaseptins showed only one amino acid difference. This phenomenon reveals the evolutionary processes on the skin defence system of *Phyllomedusa* species, which could be derived from one ancient gene for producing bioactive peptides. For

dermaseptin superfamily in phyllomedusinae tree frogs, the generation of such a peptide library is related to gene duplication, focal hypermutation, and diversifying selection (Nicolas and Amri, 2009). Especially in the case of DLP-PH, production of the prototype or heterodimer may just be caused by the site mutation of cysteine, resulting in the deficiency of disulphide bond formation. While, we demonstrated that the N-terminus and C-terminus of DLP-PH might work synergistically against the microorganisms. The two segments were recognised as amphipathic (N-terminus) and hydrophilic (C-terminus). The removal of the C-terminus resulted in activity reduction against *E. coli*. As the sequence shows, the C-terminus contains multiple positively-charged amino acid residues, and the function of such a segment could be speculated as cell penetration ability, similar to the Tat peptide, a cell penetrating peptide consisting of cationic amino acids (Richard et al., 2003). Therefore, the penetrating ability for the outer membrane of *E. coli* was decreased due to lack of the C-terminus, whereas the activity against *S. aureus* did not alter remarkably (comparison made in μM) because the peptidoglycan layer cannot be a further obstacle to peptide translocation on the plasma cell membrane.

In summary, the antimicrobial peptides investigated in this thesis not only disclosed the function-structure relationships at the sequence level but also provided new insights in using skin-derived antimicrobial peptides from phyllomedusinae tree frogs as drug candidates in the treatment of bacteria-related infections.

6.3 Things Which Need To Be Considered

AMPs are promising agents for treating bacterial infections, especially against those associated with antibiotic resistant strains. For instance, the current systematic nomenclature of AMPs is in a great mess. As Conlon indicated (2008), orthologous peptides from different species may be characterised by the initial letter of that species, set in the upper case, with paralogs belonging to the same peptide family being assigned letters set in the lower case, e.g. brevinin-1Pa, instead of using brevinin-1 only. We could not agree with Conlon on this point as the name was sometimes confusing. Another point is that the families of peptides should be classified more accurately. Particularly, for dermaseptins (*sensu stricto*), the structures display a high degree of variety, suggesting that subfamilies could be included, just like the brevinin-1 and brevinin-2 families, dermaseptins also could be divided into dermaseptin-A and dermaseptin-G, of which the first amino acid residue at the N-terminal is Ala or Gly.

Further investigations on reducing the cytotoxicity needs to be taken into consideration due to the severe cytotoxicity. Studies showed that polyethylene glycol (PEG) conjugated antimicrobial peptide could conserve the antimicrobial activity both *in vitro* and *in vivo*, as well as increasing the biocompatibility (Morris et al., 2012; Benincasa et al., 2015). Although studies showed that the PEGylation weakened the antimicrobial activity, the effect would vary based on the structure of parent peptide (Imura et al., 2007; Guiotto et al., 2003). Therefore, the site of PEGylation and the size of PEG should be investigated to optimise the activity of PEGylated antimicrobial peptide. On the other hand, avoiding enzymatic digestion is also essential for making antimicrobial peptides into drugs. Of course, PEGylation and D-form

structures are both excellent ways to maintain the integrity of peptide chains, while applying nanoparticle techniques which are becoming popular currently. Encapsulation of antimicrobial peptides into chitosan nanoparticles could increase antimicrobial activity while reducing the toxicity (Piras et al., 2015). Additionally, this could prolong the antimicrobial effect and protect from degradation.

As a preliminary stage of the study, heavy workloads remained for the development of new antibiotic drugs, especially the evaluation of *in vivo* activity of these peptides discussed here. We still feel encouraged and confident in the discovery of novel antimicrobial agents as the more antimicrobial peptides we find, the closer we are to find the best AMP to be manufactured. I hope that this study provides ideas for those who are studying AMPs in terms of design strategies and prototype templates.

References

Amiche, M.; Ladram, A.; Nicolas, P. A consistent nomenclature of antimicrobial peptides isolated from frogs of the subfamily Phyllomedusinae. Peptides 2008, 29, 2074-2082. DOI: 10.1016/j.peptides.2008.06.017

Apponyi, M. A., Pukala, T. L., Brinkworth, C. S., Maselli, V. M., Bowie, J. H., Tyler, M. J., Booker, G. W., Wallace, J. C., Carver, J. A., Separovic, F., Doyle, J. and Llewellyn, L. E. (2004). "Host-defense peptides of Australian anurans: structure, mechanism of action and evolutionary significance", *Peptides*, Vol. 25, No. 6: pp. 1035-1054.

Barra, D. and Simmaco, M. (1995). "Amphibian skin: A promising resource for antimicrobial peptides", *Trends in biotechnology*, Vol. 13, No. 6: pp. 205-209.

Batista, C. V. F., Scaloni, A., Rigden, D. J., Silva, L. R., Rodrigues Romero, A., Dukor, R., et al. (2001). "A novel heterodimeric antimicrobial peptide from the tree-frog Phyllomedusa distincta",*FEBS Lett*, Vol. 494: pp. 85-89.

Batista, C. V., da Silva, L. R. and Sebben, A. (1999). "Antimicrobial peptides from the Brazilian frog Phyllomedusa distincta", *Peptide*, Vol. 20, No. 6: pp. 679-686.

Belmadani, A.; Semlali, A.; Rouabhia, M. Dermaseptin-S1 decreases Candida albicans growth, biofilm formation and the expression of hyphal wall protein 1 and aspartic protease genes. Journal of applied microbiology 2018, 125, 72-83. DOI: 10.1111/jam.13745

Bello, G., Bodin, A., Lawrence, M.J., Barlow, D., Mason, A.J., Barker, R.D. and Harvey, R.D., 2016. The influence of rough lipopolysaccharide structure on molecular interactions with mammalian antimicrobial peptides. *Biochimica et Biophysica Acta (BBA)-Biomembranes*, 1858(2), pp.197-209.

Benincasa, M., Zahariev, S., Pelillo, C., Milan, A., Gennaro, R. and Scocchi, M., 2015. PEGylation of the peptide Bac7 (1–35) reduces renal clearance while retaining antibacterial

activity and bacterial cell penetration capacity. European journal of medicinal chemistry, 95, pp.210-219.

Brogden, K. A. (2005). "Antimicrobial peptides: pore formers or metabolic inhibitors in bacteria?", *Nature Reviews Microbiology*, Vol. 3: pp. 238-250.

Brogden, K. A., De Lucca, A. J., Bland, J. and Elliott, S. (2004). "Isolation of an ovine pulmonary surfactant-associated anionic peptide bactericidal for Pasteurella haemolytica", *Proceedings of the National Academy of Sciences of the United States of America*, Vol. 93, No. 1: pp. 412-416.

Brown, K. L.; Hancock, R. E. Cationic host defense (antimicrobial) peptides. Current opinion in immunology, 2006, 18, 24-30. DOI: 10.1016/j.coi.2005.11.004

Chapuisat, M., Oppliger, A., Magliano, P. and Christe, P. (2007). "Wood ants use resin to protect themselves against pathogens", *Proceedings of the Royal Society Biological Sciences*, Vol. 274, No. 2007: pp. 2013-2017.

Chen, J. G., Xu, X. M., Underhill, C. B., Yang, S. M., Wang L. P., Chen, Y. X., Hong,

Chen, T., Tang, L. and Shaw, C. (2003). "Identification of three novel *Phyllomedusa sauvagei dermaseptins* (sVI-sVIII) by cloning from a skin secretion-derived cDNA library", *Regulatory Peptides*, Vol. 116: pp. 139-146.

Chen, Y. X., Mant, C. T., Farmer, S. W., Hancock, R. E. W., Vasil, M. L. and Hodges, R. S. (2005). "Rational design of alpha-helical antimierubial peptides with Enhanced Activities and specificity/therapeutic index", *Journal of Biological Chemistry*, Vol. 280: pp. 12316-12329.

Choi, Y. S., Choo, Y. M., Lee, K. S., Yoon, H. J., Kim, I., Je, Y. H., Sohn, H. D. and Jin, B.R. (2008). **"**Cloning and expression profiling of four antimicrobial peptide genes from the

bumblebee*Bombus* ignites", *Comparative Biochemistry & Physiology Part B*, Vol. 150, No. 2: pp. 141-146.

Conlon, J. M. (2011). "Structural diversity and species distribution of host-defense peptides in frog skin secretions",*Cellular & Molecular Life Sciences Cmls*,Vol. 68: pp. 2303-2315.

Dagan, A., Efron, L., Gaidukov, L., Mor, A. and Ginsburg, H. (2002). "In vitro antiplasmodium effects of dermaseptin S4 derivatives", *Antimicrob Agents Chemother*.Vol. 46, No. 4: pp. 1059-1066.

Dalla Serra, M., Cirioni, O., Vitale, R. M., Renzone, G., Coraiola, M., Giacometti, A., et al. (2008). "Structural features of distinctin affecting peptide biological and biochemical properties", Biochemistry,Vol. 47: pp. 7888-7899.

Dannehl, C., Gutsmann, T. and Brezesinski, G. (2013). "Surface activity and structures of two fragments of the human antimicrobial LL-37", *Colloids and Surfaces B: Biointerfaces*, Vol. 109: pp. 129-135.

Dathe, M. and Wieprecht, T. (1999), "Structural feactures of helical antimicrobial peptides: their potential to modulate activity on model membranes and biologiacal cells", *Biochinica et Biophysica Acta*, Vol. 1462, No. 1: pp. 71-87.

Dathe, M., Nikolenko, H., Meyer, J., Beyermann, M. and Bienert, M. (2001). "Optimization of the antimicrobial activity of magainin peptides by modification of charge", *FEBS Letters*, Vol. 501, No. 2: pp. 146-150.

Dathe, M., Wieprecht, T.,Nikolenko, H.,Handel, L.,Maloy, W. L.,MacDonald, D. L.,Beyermann, M. and Bienert, M. (1997). "Hydrophobicity, hydrophobic moment and angle subtended by charged residues modulate antimicrobial and haemolytic activity of amphipathic helical peptides", *FEBS Letters*, Vol. 403, No. 2: pp. 208-212.

de la Fuente-Núñez, C., Silva, O. N., Lu, T. K. and Franco, O. L. (2017). "Antimicrobial peptides: Role in human disease and potential asimmunotherapies" *Pharmacology & Therapeutics*, Vol. 163-7258, No. 17: pp. 1-9.

Delfino, G., Giachi, F. and Nosi, D. (2001). "Secretory granule-cytoplasm relationships in serous glands of anurans: ultrastructural evidence and possible functional role", *Toxicon*, Vol. 39, No. 8 : pp. 1161-1171.

Dennison, S. R., Whittaker, M., Harris, F. and Phoenix, D. A. (2006). "Anticancer -Helical Peptides and Structure/Function Relationships Underpinning Their Interactions with Tumour Cell Membranes", *Current Protein and Peptide Science*, Vol. 7: pp. 487-499.

Dennisona, S. R., Harrisb, F. and Phoenix, D. A. (2007). "The interactions of aurein 1.2 with cancer cell membranes", *Biophysical Chemistry*, Vol. 127, No. 1-2: pp. 78-83.

Dhople, V., Krukemeyer, A. and Ramamoorthy, A. (2006). "The human beta-defensin-3, an antimicrobial peptide with multiplebiological functions", *Biochimica et Biophysica Acta(BBA)- Biomembrames*, Vol. 1758, No. 9: pp. 1499-1512.

Dos Santos C.; Hamadat S.; Le Saux K.; Newton C.; Mazouni M.; Zargarian L.; Miro-Padovani M.; Zadigue P.; Delbé J.; Hamma-Kourbali Y.; Amiche M. Studies of the antitumor mechanism of action of dermaseptin B2, a multifunctional cationic antimicrobial peptide, reveal a partial implication of cell surface glycosaminoglycans. PloS one 2017, 12, e0182926. DOI:10.1371/journal.pone.0182926

Dos Santos, L. A , Taveira, G. B., Ribeiro, S. F., Pereira, L. D., Carvalho, A. O., Rodrigues, R., Oliveira, A. E., Machado, O. L., Araújo, J. D., Vasconcelos, I. M. and Gomes, V. M. (2017). "Purification and characterization of peptides from Capsicum annuum fruits which are α-amylase inhibitors and exhibit high antimicrobial activity against fungi of agronomic

importance", *Protein Expression and Purification*, Vol. 132, pp. 97-107.

Evan, F. H., Howard, N. H., Katsumi, M. and Hans, J. V. (2009). "Solution NMR studies of amphibian antimicrobial peptides: Linking structure to function?", *Biochimica et Biophysica Acta (BBA) - Biomembranes*, Vol. 1788, No. 8: pp. 1639-1655.

Evaristo, G., Pinkse, M., Wang, L., Zhou, M., Wu, Y., Wang, H., et al. (2013). "The chains of the heterodimeric amphibian skin antimicrobial peptide, distinctin, are encoded by separate messenger RNAs",*Journal of Proteomics*, Vol. 78, No. 1: pp. 245-253.

Feinstein, W. P. and Brylinski, M. (2015). "Calculating an optimal box size for ligand docking and virtual screening against experimental and predicted binding pockets",*Journal of Cheminform*,Vol. 7, No. 1: p. 18.

Fernández-Carneado, J.,Kogan, M. J.,Pujals, S. andGiralt, E. (2004). "Amphipathic peptides and drug delivery", *Biopolymers*, Vol. 76, No. 2: pp. 196-203.

Fjell, C.D.; Hiss, J.A.; Hancock, R.E.;Schneider, G. Designing antimicrobial peptides: form follows function. Nature reviews Drug discovery 2012, 11(1), 37. DOI: 10.1038/nrd3591

Galanth, C.; Abbassi, F.; Lequin, O.; Ayala-Sanmartin, J.; Ladram, A.; Nicolas, P.; Amiche, M. Mechanism of Antibacterial Action of Dermaseptin B2: Interplay between Helix− Hinge− Helix Structure and Membrane Curvature Strain. Biochemistry 2008. 48, 313-327. DOI: 10.1021/bi802025a

Gao, Y. H., Rong, Y. L., Wang, Y. M., Xiong, H. T., Huang, X., Han, F. F., Feng, J. and Wang, Y. Z. (2014). "Expression pattern of porcine antimicrobial peptide PR-39 and its induction by enterotoxigenic Escherichia coli (ETEC) F4ac", *Veterinary Immunology and Immunopathology*, Vol. 160, No. 3-4: pp. 260-265.

Gao, Y., Wu, D., Xi, X., Wu, Y., Ma, C., Zhou, M., Wang, L., Yang, M., Chen, T. and Shaw, C. (2016). "Identification and Characterisation of the Antimicrobial Peptide, Phylloseptin-PT, from the Skin Secretion of Phyllomedusatarsius, and Comparison of Activity with Designed, Cationicity-Enhanced Analogues and Diastereomers", *Molecules*, Vol. 21, No. 12: pp. 1-14.

Garten, W., Braden, C., Arendt, A., Peitsch, C., Baron, J., Lu, Y., Pawletko, K., Hardes, K., Steinmetzer, T. and Böttcher-Friebertshäuser, E. (2015). "Influenza virus activating host proteases: Identification, localization and inhibitors as potential therapeutics", E*uropean Journal of Cell Biology*, Vol. 94, No.7-9: pp. 375-383.

Gaspar, D., Salomé Veiga, A. and Castanho, M. A. R. B. (2013). "From antimicrobial to anticancer peptides. A review",*Frontiers in Microbiology*,Vol. 4, No. 4: p. 294.

Gautier, R., Douguet, D., Antonny, B. and Drin, G. (2008). "HELIQUEST: A web server to screen sequences with specific α-helical properties",*Bioinformatics,*Vol. 24, No.18: pp. 2101-2102.

Ge, Y., MacDonald, D. L., Holroyd, K. J., Thornsberry, C., Wexler, H. and Zasloff, M. (1999). "In vitro antibacterial properties of pexiganan, an analog of magainin. Antimicrob",*Agents Chemother*, Vol. 43, No. 4: pp. 782-788.

Ghosh, A., Kar, R. K., Jana, J., Saha, A., Jana, B., Krishnamoorthy, J., Kumar, D., Ghosh, S., Chatterjee, S. and Bhunia, A. (2014), "Indolicidin Targets Duplex DNA: Structural and Mechanistic Insight through a Combination of Spectroscopy and Microscopy", *ChemMedChem*, Vol. 9, No. 9: pp. 2052–2058.

Giangaspero, A.; Sandri, L.; Tossi, A. Amphipathic α helical antimicrobial peptides. A systematic study of the effects of structural and physical properties on biological activity. European Journal of Biochemistry 2001, 268(21), 5589-5600. DOI: 10.1046/j.1432-

1033.2001.02494.x

Gibson, B. W., Tang, D., Mandrell, R., Kelly, M. and Spindel, E. R. (1991). "Bombinin-like peptides with antimicrobial activity from skin secretions of the Asian toad Bombina orientalis", *Journal of Biological Chemistry*,Vol. 266, No. 34: pp. 23103-23111.

Giovannini, M. G., Poulter, L., Gibson, B. W. and Williams, D. H. (1987). "Biosynthesis and degradation of peptides derived from Xenopus laevis prohormones", *Biochemistry Journal*, Vol. 243, No. 1: pp. 113-120.

Giuliani, A., Pirri, G. and Nicoletto, S. F. (2007). "Antimicrobial peptides: An overview of a promising class of therapeutics", *Central European Journal of Biology*, Vol. 2, No. 1: pp. 1-33.

Guiotto, A., Pozzobon, M., Canevari, M., Manganelli, R., Scarin, M. and Veronese, F.M., 2003. PEGylation of the antimicrobial peptide nisin A: problems and perspectives. Il Farmaco, 58(1), pp.45-50.

Habets, M. G. J. L. and Brockhurst, M. A. (2012). "Therapeutic antimicrobial peptides may compromise natural immunity", *Biology Lerrers*, Vol. 8, No. 3:pp. 416-418.

Hädicke, A. and Blume, A. (2016). "Binding of cationic peptides (KX)4K to DPPG bilayers. Increasing the hydrophobicity of the uncharged amino acid X drives formation of membrane bound β-sheets: A DSC and FT-IR study", *Biochimica et Biophysica Acta*, Vol. 1858, No. 6: pp. 1196-1206.

Hancock, R. E. (2001). "Cationic peptides: effectors in innate immunity and novel antimicrobials", The Lancet Infectious Diseases, Vol.1, No. 3: pp. 156-164.

Hancock, R. E. W. and Sahl, H. G. (2006). "Antimicrobial and host-defense peptides as new anti-infective therapeutic strategies", *Nature Biotechnology*, Vol. 24, No, 12: pp.1551-1557.

Hancock, R.E.; Chapple, D.S. Peptide antibiotics. Antimicrobial agents and chemotherapy 1999, 43(6), 1317-1323. PMID:10348745 PMCID:pmc89271

Hess, K. L., Andorko, J. I., Tostanoski, L. H. and Jewell, C. M. (2017). "Polyplexes assembled from self-peptides and regulatory nucleic acids blunt toll-like receptor signaling to combat autoimmunity", *Biomaterials*, Vol. 118: pp. 51-62.

Hicks, R. P. (2016). "Antibacterial and anticancer activity of a series of novel peptides incorporating cyclic tetra-substituted C(α) amino acids", *Bioorganic & Medicinal Chemistry*, Vol. 24, No. 18: pp. 4056-4065.

Hollmann, A., Martínez, M., Noguera, M. E., Augusto, M. T., Disalvo, A., Santos, N. C., Semorile, L. and Maffía, P. C. (2016). "Role of amphipathicity and hydrophobicity in the balance betweenhemolysis and peptide–membrane interactions of three relatedantimicrobial peptides", *Colloids and Surfaces B: Biointerfaces*, Vol. 141: pp. 528-536.

Holstein, J., Fehrenbacher, B., Brück, J., Müller-Hermelink, E., Schäfer I., Carevic, M. , Schittek, B., Schaller, M., Ghoreschi, K. and Eberle, F. C. (2017). "Anthralin modulates the expression pattern of cytokeratins and antimicrobial peptides by psoriatic keratinocytes", *Journal of Dermatological Science*, Vol. 923-1811, No. 17: pp. 30708-30709.

Hoskin, D. W. and Ramamoorthy, A. (2007). "Studies on Anticancer Activities of Antimicrobial Peptides", *Biochimica et Biophysica Acta (BBA) - Biomembranes*, Vol. 1788, No. 2: pp. 357-375.

Hoskin, D.W.; Ramamoorthy, A. Studies on anticancer activities of antimicrobial peptides. Biochimica et Biophysica Acta (BBA)-Biomembranes 2008, 1778, 357-375. DOI: 10.1016/j.bbamem.2007.11.008

Huang, L.; Chen, D.; Wang, L.; Lin, C.; Ma, C.; Xi, X.; Chen, T.; Shaw, C.; Zhou, M.

Dermaseptin-PH: A Novel Peptide with Antimicrobial and Anticancer Activities from the Skin Secretion of the South American Orange-Legged Leaf Frog, Pithecopus (Phyllomedusa) hypochondrialis. Molecules 2017, 22, 1805. DOI: 10.3390/molecules22101805

Huang, Y., Huang, J. and Chen, Y. (2010). "Alpha-helical cationic antimicrobial peptides: Relationships of structure and function", *Protein Cell*, Vol. 1, No. 2: pp. 142-152.

Hwang, J. S., Lee, J., Kim, Y. J., Bang, H. S., Yun, E. Y., Kim, S. R., Suh, H. J., Kang, B. R., Nam, S. H., Jeon, J. P., Kim, I. and Lee, D. G. (2009). "Isolation and characterization of a defensin-like peptide (Coprisin) from the dung beetle, Copris tripartitus", *International Journal of Peptides*, Vol. 2009, No. 2009: p. 136284.

Ivanov, I.E., Kintz, E.N., Porter, L.A., Goldberg, J.B., Burnham, N.A. and Camesano, T.A., 2011. Relating the physical properties of Pseudomonas aeruginosa lipopolysaccharides to virulence by atomic force microscopy. *Journal of bacteriology*, 193(5), pp.1259-1266.

Jeżowskabojczuk，M. and Stokowasołtys, K. (2018). "Peptides having antimicrobial activity and their complexes with transition metal ions", *European Journal of Medicinal Chemistry*, Vol. 143: pp. 997-1009.

Jiang, Z., Vasil, A. I., Hale, J. D., Hancock, R. E., Vasil, M. L. and Hodges, R. S. (2008). "Effect of net charge and the number of positively charged residues on the biological activity of amphipathic α-helical cationic antimicrobial peptides", *Biopolymers*, Vol. 90, No. 3: pp. 369-383

Jo, S., Kim, T., Iyer, V. G. and Im, W. (2008). "CHARMM-GUI: A web-based graphical user interface for CHARMM",*Journal of Computational Chemistry*, Vol. 29, No. 11: 1859-1865.

Karatan, E. and Watnick, P. (2009). "Signals, regulatory networks, and materials that build and

break bacterial biofilms",*Microbiology and Molecular Biology Reviews*, Vol. 73, No. 2: pp. 310-347.

Kim, E. Y., Rajasekaran, G. and Shin, S. Y. (2017), "LL-37-derived short antimicrobial peptide KR-12-a5 and its d-amino acid substituted analogs with cell selectivity, anti-biofilm activity, synergistic effect with conventional antibiotics, and anti-inflammatory activity", E*uropean Journal of Medicinal Chemistry*, Vol. 136: pp. 428-441.

Knezevic, P. and Petrovic, O. (2008). " A colorimetric microtiter plate method for assessment of phage effect on Pseudomonas aeruginosa biofilm", *Journal of Microbiological Methods*, Vol. 74, No. 2-3: pp. 114-118.

Knezevic, P. and Petrovic, O. (2008). "A colorimetric microtiter plate method for assessment of phage effect on Pseudomonas aeruginosa biofilm", J*ournal of Microbiology Methods*, Vol. 74: pp. 114-118.

Kudryashova, E., Seveau, S.M. and Kudryashov, D.S. (2017). "Targeting and inactivation of bacterial toxins by human defensins",*Biological Chemistry*, Vol. 398, No. 10: pp.1069-1085.

Kustanovich, I.; Shalev, D. E.; Mikhlin, M.; Gaidukov, L.; Mor, A. Structural requirements for potent versus selective cytotoxicity for antimicrobial dermaseptin S4 derivatives. Journal of Biological Chemistry 2002, 277, 16941-16951. DOI:10.1074/jbc.M111071200

Kustanovich, I.; Shalev, D.E.; Mikhlin, M.; Gaidukov, L.; Mor, A. Structural requirements for potent versus selective cytotoxicity for antimicrobial dermaseptin S4 derivatives. Journal of Biological Chemistry 2002, 277(19), 16941-16951. DOI: 10.1074/jbc.M111071200

Imura, Y., Nishida, M. and Matsuzaki, K., 2007. Action mechanism of PEGylated magainin 2 analogue peptide. Biochimica et Biophysica Acta (BBA)-Biomembranes, 1768(10), pp.2578-2585.

Lacombe, C., Carmen, C. D., Dunia, I., Auber-Thomay, M., Nicolas, P. and Amiche, M. (2000). "Peptide secretion in the cutaneous glands of south American tree frog *Phyllomedusa bicolor*: an ultrastructural study", *European Journal of Cell Biology*, Vol. 79, No. 9: pp. 631-641.

Lavine, M. D., Chen, G. and Strand, M. R. (2005). "Immune challenge differentially affects transcript abundance of three antimicrobial peptides in hemocytes from the moth *Pseudoplusia includes*", *Insect Biochemistry and Molecular Biology*, Vol. 35, No. 12: pp. 1335-1346.

Lee, D. G., Kim, H. N., Park, Y., Kim, H. K., Choi, B. H., Choi, C. and Hahm, K. (2002). "Design of novel analogue peptides with potent antibiotic activity based on the antimicrobial peptide, HP(2-20), derived from N-terminus of helicobacter pylorl ribosomal protein L1", *Biochimica et Biophysica Acta (BBA) - Biomembranes*, Vol. 1598, No. 1-2: pp. 185-194.

Lee, H. S., Park, C. B., Kim, J. M., Jang, S. A., Park, I. Y., Kim, M. S., Cho, J. H. and Kim, S. C. (2008). "Mechanism of anticancer activity of buforin lIb, a histone H2A-derived peptide", *Cancer Letters*, Vol. 271, No. 1: pp. 47-55.

Lehmann, J., Retz, M., Sidhu, S. S., Suttmann, H., Sell, M., Paulsen, F., Harder, J., Unteregger, G. and Stoeckle, M. (2006). "Antitumor Activity of the Antimicrobial Peptide Magainin II against Bladder Cancer Cell Lines", *European urology*, Vol. 50, No. 1: pp. 141-147.

Lequin, O.; Ladram, A.; Chabbert, L.; Bruston, F.; Convert, O.; Vanhoye, D.; Chassaing, G.; Nicolas, P.; Amiche, M. Dermaseptin S9, an α-helical antimicrobial peptide with a hydrophobic core and cationic termini. Biochemistry 2006, 45(2), 468-480. DOI: 10.1021/bi051711i

Li, C., Blencke, H. M., Haug, T. and Stensvåg, K. (2015). "Antimicrobial peptides in echinoderm host defense", *Developmental and Comparative Immunology*, Vol. 49, No. 1: pp. 190-197.

Li, Y. M., Xiang, Q., Zhang, Q. H., Huang, Y. D. and Su, Z. J. (2012). "Overview on the recent study of antimicrobial peptides: Origins, functions, relative mechanisms and application", *Peptides*, Vol. 37, No. 2: pp. 207-215.

Li, Y. M., Xiang, Q., Zhang, Q. H., Huang, Y. D. and Su, Z. J. (2012). "Overview on the recent study of antimicrobial peptides: Origins, functions, relative mechanisms and application", *Peptides*, Vol. 37, No. 2: pp. 207-215.

Lovell, S. C., Davis, I. W., Arendall, W. B., de Bakker, P. I. W., Word, J. M., Prisant, M. G., et al. (2003). "Structure validation by Cα geometry: ϕ, ψ and Cβ deviation", *Proteins Structure Function & Bioinformatics*, Vol. 50, No. 3: pp.437-450.

Lyu, P. C., Liff, M. I., Marky, L. A. and Kallenbach, N. R. (1990). "Side Chain Contributions to the Stability of Alpha-Helical Structure in Peptides", *Science*, Vol. 250: pp. 669-673.

Mahindra, A., Bagra, N., Wangoo, N., Jain, R., Khan, S. I., Jacob, M. R. and Jain, R. (2014). "Synthetically modified L-histidine-rich peptidomimetics exhibit potent activity against Cryptococcus neoformans", *Bioorganic & Medicinal Chemistry Letters*, Vol. 24, No. 14: pp. 3150-3154.

Manzor, K., Proinsias, K. and Kelleher, F. (2017). "Solid-phase peptide synthesis of analogues of the N-terminus A-ring fragment of the lantibioticnisin: Replacements for the dehydroalanine (Dha) residue at position 5 and the first incorporation of a thioamide residue", *Tetrahedron Letters*, Vol. 58, pp. 2959-2963.

Marshall, S. H. (2003). "Antimicrobial peptides: A natural alternative to chemical antibiotics and a potential for applied biotechnology", *The Electronic Journal of Combinatorics*, Vol. 6, No. 3: pp. 271-284.

Masayuki, K., Tomohisa, H., Mari, H., Yoshiaki, Y., Koji, O., Oumi, N., Katsumi, M. and Koji, K. (2011). "A novel hybrid peptide targeting EGFR-expressing cancers", *European Journal of Cancer*, Vol. 47, No. 5: pp. 773-783.

Matsuzaki, K. (2009). "Control of cell selectivity of antimicrobial peptides", *Biochimica et Biophysica Acta*, Vol. 1788, No. 8: pp. 1687-1692.

Mechkarska, M., Attoub, S., Sulaiman, S., Pantic, J., Lukic, M. L. and Conlon, J. M. (2014). "Anti-cancer, immunoregulatory, and antimicrobial activities of the frog skin host-defense peptides pseudhymenochirin-1Pb and pseudhymenochirin-2Pa", *Regulatory Peptides*, Vol. 194-195, pp. 69-76.

membrane-lytic peptides", *Biochimica et Biophysica Acta (BBA) - Biomembranes*, Vol. 1462, No. 1-2: pp. 55-70.

Miltz, J.; Rydlo, T.; Mor, A.; Polyakov, V. Potency evaluation of a dermaseptin S4 derivative for antimicrobial food packaging applications. Packaging Technology and Science: An International Journal 2006, 19(6), 345-354. DOI: 10.1021/bi034514x

Mishra, B., Reiling, S., Zarena, D. and Wang, G. (2017). "Host defense antimicrobial peptides as antibiotics: design and application strategies", *Current Opinion in Chemical Biology*, Vol. 38, pp. 87-96.

Mor A and Nicolas, P. (1994). "The NH2-terminal α-helical domain1-18 of dermaseptin is responsible for antimicrobial activity", *Journal of Biological Chemistry*, Vol. 269: pp. 1934-1939.

Mor, A. and Nicolas, P. (1994). "Isolation and structure of novel defensive peptides from frog skin", *The FEBS Journal,* Vol. 219, No. 1-2: pp. 145-154.

Mor, A., Amiche, M., and Nicolas, P. (1994). "Structure ,synthesis, and activity of dermaseptin b , a novel vertebrate defensive peptide from frog skin: relationship with adenoregulin", *Biochemistry*, Vol. 33, No. 21 : pp. 6642-6650.

Mor, A., Nguyen, V. H., Delfour, A., Migliore-Samour, D. and Nicolas, P. (1991). "Isolation, amino acid sequence, and synthesis of dermaseptin, a novel antimicrobial peptide of amphibian skin", *Biochemistry*, Vol. 30, No. 36: pp. 8824-8830.

Mor, A.; Nicolas, P. The NH2-terminal alpha-helical domain 1-18 of dermaseptin is responsible for antimicrobial activity. Journal of Biological Chemistry 1994, 269(3), 1934-1939. PMID:8294443

Mor, A.; Van Huong, N.; Delfour, A.; Migliore-Samour, D.; Nicolas, P. Isolation, amino acid sequence and synthesis of dermaseptin, a novel antimicrobial peptide of amphibian skin. Biochemistry 1991, 30, 8824-8830. DOI: 10.1021/bi00100a014

Morchikh, M1., Cribier, A., Raffel, R., Amraoui, S., Cau, J., Severac, D., Dubois, E., Schwartz, O., Bennasser, Y. and Benkirane, M. (2017). "HEXIM1 and NEAT1 Long Non-coding RNA Form a Multi-subunit Complex that Regulates DNA-Mediated Innate Immune Response", *Molecular Cell*, Vol. 67, No.3: pp. 387-399.

Morris, C.J., Beck, K., Fox, M.A., Ulaeto, D., Clark, G.C. and Gumbleton, M., 2012. Pegylation of antimicrobial peptide maintains the active peptide conformation, model membrane interactions and antimicrobial activity while improving lung tissue biocompatibility following airway delivery. Antimicrobial agents and chemotherapy, pp.AAC-06335.

Mulero, I.,Noga, E. J.,Meseguer, J.,García-Ayala, A. and Mulero, V. (2008). "The antimicrobial peptides piscidins are stored in the granules of professional phagocytic granulocytes of fish and are delivered to the bacteria-containing phagosome upon phagocytosis", *Developmental &*

Comparative Immunology, Vol. 32, No. 12: pp. 1531-1538.

Navon-Venezia, S., Feder, R., Gaidukov, L., Carmeli, Y. and Mor, A., 2002. Antibacterial properties of dermaseptin S4 derivatives with in vivo activity. Antimicrobial agents and chemotherapy, 46(3), pp.689-694.

Nguyen, L. T., Haney, E. F. and Vogel, H. J. (2011). "The expanding scope of antimicrobial peptide structures and their modes of action", *Trends in Biotechnology*, Vol. 29, No. 9: pp. 464-472.

Nicolas, P. and El Amri, C. (2009). "The dermaseptin superfamily: a gene-based combinatorial library of antimicrobial peptides",*Biochimica et Biophysica Acta (BBA) – Biomembranes*, Vol. 1788, No. 8: pp. 1537-1550.

Nicolas, P.; El Amri, C. The dermaseptin superfamily: a gene-based combinatorial library of antimicrobial peptides. Biochimica et Biophysica Acta (BBA)-Biomembranes 2009, 1788, 1537-1550. DOI: 10.1016/j.bbamem.2008.09.006

Nicolas, P.; Ladram, A. Dermaseptins. In Handbook of Biologically Active Peptides, 2nd ed.; Kastin, A.J.; Academic Press: Boston, 2013; Volume 3, 350-363 ISBN 9780123850959.

Okano, A., Isley, N.A. and Boger, D.L. (2017). "Peripheral modifications of [Ψ [CH2NH] Tpg4] vancomycin with added synergistic mechanisms of action provide durable and potent antibiotics",*PNAS*, Vol. 114, No. 26: pp. 5052-5061.

Oman, T. J. and van der Donk, W. A. (2009). "Insights into the Mode of Action of the Two-Peptide Lantibiotic Haloduracin", *ACS Chemical Biology*, Vol. 4, No. 10: pp. 865-874.

Pál, T.,Sonnevend, A., Galadari, S. andConlon, J. M. (2005) "Design of potent, non-toxic antimicrobial agents based upon the structure of the frog skin peptide, pseudin-2", *Regulatory*

Peptides, Vol. 129, No. 1: pp. 85-91.

Pandit, K. R. and Klauda, J. B. (2012). "Membrane models of E. coli containing cyclic moieties in the aliphatic lipid chain",*Biochimica Et Biophysica Acta*, Vol. 1818, No. 5: pp. 1205-1210.

Pane, K., Durante, L., Crescenzi, O., Cafaro, V., Pizzo, E., Varcamonti, M., Zanfardino, A., Izzo, V., Di Donato, A. and Notomista, E. (2017). "Antimicrobial potency of cationic antimicrobial peptides can be predicted from their amino acid composition: Application to the detection of 'cryptic' antimicrobial peptides", *Journal of Theoretical Biology*, Vol. 419, pp. 254-265.

Panteleev, P. V., Myshkin, M. Y , Shenkarev, Z. O., Ovchinnikova, T. V. (2017). "Dimerization of the antimicrobial peptide arenicin plays a key role in the cytotoxicity but not in the antibacterial activity", B*iochemical and Biophysical Research Communications*, Vol. 482, No. 4: pp. 1320-1326.

Papo, N. and Shai, Y. (2005). "Host defense peptides as new weapons in cancer treatment", *Cellular Molecular Life Science*, Vol. 62, No. 7-8: pp. 784-790.

Park, C. B., Yi, K. S., Matsuzaki, K., Kim, M. S. and Kim, S. C. (2000). "Structure-activity analysis of buforin II, a histone H2A-derived antimicrobial peptide: the proline hinge is responsible for the cell-penetrating ability of buforin II", *Proceedings of the National Academy of Sciences of the United States of America*, Vol. 97, No. 15: pp. 8245-8250.

Pierre, T. N., Seon, A. A., Amiche, M. and Nicolas, P. (2000). "Phylloxin, a novel peptide antibiotic of the dermaseptin family of antimicrobial/opioid peptide precursors", *European Journal of Biochemistry*, Vol. 267, No. 2: pp. 370-378.

Piras, A.M., Maisetta, G., Sandreschi, S., Gazzarri, M., Bartoli, C., Grassi, L., Esin, S., Chiellini, F. and Batoni, G., 2015. Chitosan nanoparticles loaded with the antimicrobial peptide temporin

B exert a long-term antibacterial activity in vitro against clinical isolates of Staphylococcus epidermidis. Frontiers in microbiology, 6, p.372.

Pletzer, D. and Hancock, R. E. W. (2016). "Antibiofilm Peptides: Potential as Broad-Spectrum Agents", *Journal of Bacteriology*, Vol. 198: pp. 2572-2578.

Poole, K. (2011)."Pseudomonas Aeruginosa: Resistance to the Max", *Frontiers in Microbiology*. Vol. 2, No.1: p.65.

Pouny, Y., Rapaport, D., Mor, A., Nocolas, P. and Shai, Y. (1992). "Interaction of antimicrobial dermaseptin and its fluorescently labeled analogs with phospholipid membranes", *Bopchemistry*, Vol. 31, No. 49: pp. 12416-12423.

Rady, I., Siddiqui, I. A., Rady, M. and Mukhtar, H. (2017). "Melittin, a major peptide component of bee venom, and its conjugates in cancer therapy", *Cancer Letters*, Vol. 402: pp. 16-31.

Reffuveille, F., De La Fuente-Nũnez, C., Mansour, S. and Hancock, R. E. W. (2014). "A broad-spectrum antibiofilm peptide enhances antibiotic action against bacterial biofilms",*Antimicrob Agents Chemother*,Vol. 58, No. 9: pp. 5363-5371.

Rice, A. and Wereszczynski, J. (2017). "Probing the disparate effects of arginine and lysine residues on antimicrobial peptide/bilayer association", B*iochimica et Biophysica Acta*, Vol. 1859, No. 10: pp. 1941-1950.

Riedl, S.; Zweytick, D.; Lohner, K. Membrane-active host defense peptides–challenges and perspectives for the development of novel anticancer drugs. Chemistry and physics of lipids 2011, 164, 766-781. DOI: 10.1016/j.chemphyslip.2011.09.004

Rydlo, T., Rotem, S. and Mor, A., 2006. Antibacterial properties of dermaseptin S4 derivatives

under extreme incubation conditions. Antimicrobial agents and chemotherapy, 50(2), pp.490-497.

S. G., Creswell, K. and Zhang L. R. (2001). "Tachyplesin Activates the Classic Complement Pathway to Kill Tumor Cells", *Cancer Research*, Vol. 65, No. 11: pp. 4614-4622.

Sabaeifard, P., Abdi-Ali, A., Soudi, M. R. and Dinarvand, R. (2014). "Optimization of tetrazolium salt assay for Pseudomonas aeruginosa biofilm using microtiter plate method", *Journal of Microbiological Methods*, Vol. 105: pp. 134-140.

Sabaeifard, P., Abdi-Ali, A., Soudi, M. R. and Dinarvand, R. (2014). "Optimization of tetrazolium salt assay for Pseudomonas aeruginosa biofilm using microtiter plate method", *Journal of Microbiology Methods*, Vol. 105: pp. 134-140.

Sahu, K., Bansal, H., Mukherjee, C., Sharma, M. and Gupta, P. K. (2009). "Atomic force microscopic study on morphological alterations induced by photodynamic action of Toluidine Blue O in *Staphylococcus aureus* and *Escherichia coli*", *Journal of Photochemistry and Photobiology B Biology*, Vol. 96, No. 1: pp. 9-16.

Salgadoa, J., Stephan, L. J., Leslie, H. K. and Robert S. H. (2001). "Membrane-bound structure and alignment of the antimicrobial β-sheet peptide gramicidin S derived from angular and distance constraints by solid state 19F-NMR", *Journal of Biomolecular NMR*, Vol. 21, No. 3: pp. 191-208.

Samanta, T., Roymahapatra, G., Porto, W. F., Seth, S., Ghorai, S., Saha, S., et al. (2013). "N, N′-Olefin Functionalized Bis-Imidazolium Gold(I) Salt Is an Efficient Candidate to Control Keratitis-Associated Eye Infection", *PLOS One*, Vol. 8, No. 3: e58346.

Samy, R. P., Thwin, M. M., Chow, V. T. K., Bow, H. and Gopalakrishnakone, P. (2011). "Evaluation of antibacterial activity of proteins and peptides using a specific animal model for

wound healing",*Methods in Molecular Biology*, Vol. 716: pp. 245-265.

Schmidtchen, A.; Pasupuleti, M.; Malmsten, M. Effect of hydrophobic modifications in antimicrobial peptides. Advances in colloid and interface science 2014, 205, 265-274. DOI:10.1016/j.cis.2013.06.009

Schneider, J. J., Unholzer, A., Schaller, M., Schäfer-Korting, M. and Korting, H. C. (2005). "Human defensins", *Journal of Molecular Medicine*, Vol. 83, No. 8: pp. 587-595.

Schweizer, F. Cationic amphiphilic peptides with cancer-selective toxicity. European journal of pharmacology 2009, 625, 190-194. DOI: 10.1016/j.ejphar.2009.08.043

Schweizer, F. Cationic amphiphilic peptides with cancer-selective toxicity. European journal of pharmacology 2009, 625, 190-194. DOI: 10.1016/j.ejphar.2009.08.043

Scocchi, M., Tossi, A. and Gennaro, R. (2011). "Proline-rich antimicrobial peptides: converging to a non-lytic mechanism of action", *Cellular and Molecular Life Sciences,* Vol. 68, No. 13: pp. 2317-2330.

Scott, M. G., Rosenberger, C. M., Gold, M. R., Finlay, B. B. and Hancock, R. E. (2000). "An alpha-helical cationic antimicrobial peptide selectively modulates macrophage responses to lipopolysaccharide and directly alters macrophage gene expression",*The Journal of Immunology*, Vol. 165: pp. 3358-65.

Seefeldt, A. C., Nguyen, F., Antunes, S., Pérébaskine, N., Graf. M., Arenz, S., Inampudi, K. K., Douat, C., Guichard, G., Wilson, D. N. and Innis, C. A. (2015) "The proline-rich antimicrobial peptide onc112 inhibits translation by blocking and destabilizing the initiation complex", *Nature Structural & Molecular Biology*, Vol. 22, No. 6: pp. 470-475.

Shai, Y. (1999). "Mechanism of the binding, insertion and destabilization of phospholipid

bilayer membranes by alpha-helical antimicrobial and cell non-selective

Shen, W., Chen, Y., Yao, H., Du, C., Luan, N. and Yan, X. (2016). "A novel defensin-like antimicrobial peptide from the skin secretions of the tree frog, Theloderma kwangsiensis", *Gene*, Vol, 576, No. 1: pp.135-140.

Shin, S. Y., Kang, J. H. and Hahm, K. S. (2007). "Structure-antibacterial, antitumor and hemolytic activity relationships of cecropin A-magainin 2 and cecropin A-melittin hybrid peptides", *Chemical Biology & Drug Design*, Vol. 53: pp. 82-90.

Silva, L.P.; Leite, J.R.S.; Brand, G.D.; Regis, W.B.; Tedesco, A.C.; Azevedo, R.B.; Freitas, S.M.; Bloch Jr, C. Dermaseptins from Phyllomedusa oreades and Phyllomedusa distincta: liposomes fusion and/or lysis investigated by fluorescence and atomic force microscopy. Comparative Biochemistry and Physiology Part A: Molecular & Integrative Physiology 2008, 151, 329-335. DOI: 10.1016/j.cbpa.2007.02.031

Simmaco, M., Barra, D., Chiarini, F., Noviello, L., Melchiorri, P., Kreil, G. and Richter, K. (1991). "A family of bombinin-related peptides from the skin of Bombina variegate", *Journal of Biological Chemistry*, Vol. 199, No. 1: 217-222.

Sinha, S., Cheshenko, N., Lehrer, R. I. and Herold, B. C. (2003). "NP-1, a rabbit alpha-defensin, prevents the entry and intercellular spread of herpes simplex virus type 2", *Antimicrob Agents Chemother*, Vol. 47, No. 2: pp. 494-500.

Smith, V. J., Desbois, A. P. and Dyrynda, E. A. (2010). "Conventional and Unconventional Antimicrobials from Fish, Marine Invertebrates and Micro-algae", *Marine Drugs*, Vol. 8, No. 4: pp. 1213-1262.

Song, G., Zhou, M., Chen, W., Chen, T., Walker, B. and Shaw, C. (2008). "HV-BBI-A novel amphibian skin Bowman-Birk-like trypsin inhibitor", *Biochemical and Biophysical Research*

Communications, Vol. 372, No. 1: pp. 191-196.

Strahilevitz, J.; Mor, A.; Nicolas, P.; Shai, Y. Spectrum of antimicrobial activity and assembly of dermaseptin-b and its precursor form in phospholipid membranes. Biochemistry 1994, 33, 10951-10960. DOI: 10.1021/bi00202a014

Tam, J. P., Wang, S., Wong, K. H. and Tan, W. L. (2015). "Antimicrobial peptides from plants", *Pharmaceuticals*, Vol. 8, No. 4: pp. 711-757.

Tencza, S. B., Creighton, D. J. Yuan, T., Vogel, H. J., Montelaro, R. C. and Mietzner, T. A. (1999). "Lentivirus-derived antimicrobial peptides: Increased potency by sequence engineering and dimerization", *Journal of Antimicrobial Chemotherapy*, Vol. 44, No. 1: pp. 33-41.

Terry, A. S., Poulter, L., Williams, D. H., Nutkins, J. C., Giovannini, M. G., Moore, C. H. and Gibson, B. W. (1988). "The cDNA sequence coding for prepro-PGS (prepro-magainins) and aspects of the processing of this prepro-polypeptide", *Journey of Biological Chemistry*, Vol. 263 No. 12: pp. 5745-5751.

Timofeeva, L; Kleshcheva, N. Antimicrobial polymers: mechanism of action, factors of activity, and applications. Applied microbiology and biotechnology 2011, 89(3), 475-492. DOI: 10.1007/s00253-010-2920-9

Toledo, R. C. and Jared C. (1995). "Cutaneous granular glands and amphibian venoms", *Comparative Biochemistry & Physiology Part A Physiology*, Vol. 111, No. 1: pp. 1-29.

Tompson, A. H. (2006). "A genomic/proteomic approach to isolating and identifying bioactive peptides from the skin secretions of *Phyllomedusa* hypochondrialis azurea", *University of Ulster*.

Travkova, O. G., Moehwald, H. and Brezesinski, G. (2017). "The interaction of antimicrobial peptides with membranes", *Advances in Colloid & Interface Science*, Vol. 247: pp. 521-532.

Trott, O. and Olson, A. J. (2010). "AutoDock Vina: Improving the Speed and Accuracy of Docking with a New Scoring Function, EfficientOptimization, and Multithreading",*Journal of Computational Chemistry*, Vol. 31, No. 2: pp. 455-61.

Tyler, M. J., Stone, D. J. M. and Bowie, J. H. (1992). "A novel method for the release and collection of dermal, glandular secretions from the skin of frogs", *Journal of Pharmacological & Toxicological Methods*, Vol.28, No. 4: pp. 199-200.

Tyler, M.J.; Stone, D.J.; Bowie, J.H. A novel method for the release and collection of dermal, glandular secretions from the skin of frogs. Journal of Pharmacological and Toxicological Methods 1992, 28, 199-200. DOI: 10.1016/1056-8719(92)90004-K

van der Weide, H., Brunetti, J., Pini, A., Bracci L2, Ambrosini C2, Lupetti P3, Paccagnini E3, Gentile M3, Bernini A4, Niccolai N4, Jongh DV1, Bakker-Woudenberg IAJM1, Goessens WHF1, Hays JP1, Falciani C5. (2017). "Investigations into the killing activity of an antimicrobial peptide active against extensively antibiotic-resistant K. pneumon iae and *P. aeruginosa*", B*iochimica et Biophysica Acta*, Vol. 1859, No. 10: pp. 1796-1804.

van Zoggel, H.; Carpentier, G.; Dos Santos, C.; Hamma-Kourbali, Y.; Courty, J.; Amiche, M.; Delbé, J. Antitumor and angiostatic activities of the antimicrobial peptide dermaseptin B2. PloS one 2012, 7, e44351. 10.1371/journal.pone.0044351

Van, H. W., Veerman, E. C., Helmerhorst, E. J. and Amerongen, A. V. (2001). "Antimicrobial peptides: propertics and applicability", *The Journal of Biological Chemistry*, Vol. 382, No. 4: pp.597-619.

Wang, G. S., Li, J. and Wang, Z. (2016). "APD3: the antimicrobial peptide database as a tool

for research and education", *Nucleic Acids Research*, Vol. 44, No. D1: pp. D1087-D1093.

Wang, J. and Pang, G. C. (2005). "Review on the Current Status and Development Trend of Mechanism of Antimicrobial peptides", *Food Science*, Vol. 26, No. 8: pp. 526-529.

Wang, J., Mura, M., Zhou, Y., Pinna, M., Zvelindovsky, A. V., Dennison, S. R. and Phoenix, D. A. (2014). "The cooperative behaviour of antimicrobial peptides in model membranes", *Biochimica et Biophysica Acta*, Vol. 1838, No. 11: pp. 2870-2881.

Wang, R., Chen, T., Zhou, M., Wang, L. and Shaw, C. (2013). "PsT-1: a new tryptophyllin peptide from the skin secretion of Waxy Monkey Leaf Frog, Phyllomedusa sauvagei", *Regulatory Peptides*, Vol. 184, pp. 14-21.

Wangkahart, E., Scott, C., Secombes, C. J. and Wang, T. (2016). " Re-examination of the rainbow trout (Oncorhynchus mykiss) immune response to flagellin: Yersinia ruckeri flagellin is a potent activator of acute phase proteins, anti-microbial peptides and pro-inflammatory cytokines in vitro", *Developmental and Comparative Immunology*, Vol. 57: pp. 75-87.

Webb, D. R. (2016). "Soluble Immune Response Suppressor (SIRS): Reassessing the immunosuppressant potential of an elusive peptide", *Biochemical Pharmacology*, Vol. 117: pp. 1-9.

Wechselberger, C. (1998). "Cloning of cDNAs encoding new peptides of the dermaseptin-family", *Biochimica et Biophysica Acta (BBA) - Protein Structure and Molecular Enzymology*, Vol. 1338, No. 1: pp. 279-283.

Wechselberger, C., Severini, C., Kreil, G. and Negri, L. (1998). "A new opioid peptide predicted from cloned cDNAs from skin of *Pachymedusa dacnicolor* and *Agalychnis annae*",*Febs Letters*, Vol. 429, No. 1: pp. 41-43.

Wiederstein, M., and Sippl, M. J. (2007). "ProSA-web: Interactive web service for the recognition of errors in three-dimensional structures of proteins", *Nucleic Acids Research*, Vol. 35, pp. 407–410.

Won, H. S., Kang, S. J. and Lee, B. J. (2009). "Action mechanism and structural requirements of the antimicrobial peptides, gaegurins", *Biochimica et Biophysica Acta (BBA) - Biomembranes*, Vol. 1788, No. 8: pp. 1620-1629.

Wu, D., Gao, Y., Wang, L., Xi, X., Wu, Y., Zhou, M., et al. (2016). "A Combined Molecular Cloning and Mass Spectrometric Method to Identify, Characterize, and Design Frenatin Peptides from the Skin Secretion of *Litoria infrafrenata*", *Molecules*, Vol. 21, No. 11: p. 1429.

Wu, D1, Gao, Y., Wang, L., Xi, X., Wu, Y., Zhou, M., Zhang Y, Ma, C., Chen T. and Shaw, C. (2016). " A Combined Molecular Cloning and Mass Spectrometric Method to Identify, Characterize, and Design Frenatin Peptides from the Skin Secretion of *Litoriainfrafrenata*", *Molecules*, Vol. 21, No. 11: pp. 1-12.

Xu, X. and Lai, R. (2015). "The chemistry and biological activities of peptides from amphibian skin secretions", *Chemical Reviews*, Vol. 115, No. 4: pp. 1760-1846.

Yamaguchi, Y. and Ouchi, Y. (2012). "Antimicrobial peptide defensin: Identification of novel isoforms and the characterization of their physiological roles and their significance in the pathogenesis of diseases", *Proceedings of the Japan Academy, Series B Physical and Biological Science*, Vol. 88, No. 4: pp. 152-166.

Yang, H., Kozicky, L., Saferali, A., Fung, S. Y., Afacan, N., Cai, B., Falsafi, R., Gill, E., Liu, M., Kollmann, T, R,, Hancock, R. E., Sly, L. M. and Turvey, S. E. (2016). "Endosomal pH modulation by peptide-gold nanoparticle hybrids enables potent anti-inflammatory activity in phagocytic immune cells", *Biomaterials*, Vol. 111, pp. 90-102.

Yang, J., Yan, R., Roy, A., Xu, D., J, P. and Zhang, Y. (2015). "The I-TASSER Suite: Protein structure and function prediction",*Nature Methods*,Vol. 12, No. 1: pp. 7-8.

Yashpal, M. and Mittal, A. K. (2014). "Serous goblet cells: the protein secreting cells in the oral cavity of a catfish, Rita rita (Hamilton, 1822) (Bagridae, Siluriformes)", *Tissue and Cell*, Vol. 46, No. 1: pp. 9-14.

Yeaman, M. R. and Yount, N. Y. (2003). "Mechanisms of antimicrobial peptide action and resistance", *Pharmacologic Reveal*, Vol. 55, No. 1: pp. 27-55.

Yi, L. L. and Zhao, S. F. (2006). "Research progress of natural immune molecular antimicrobial peptides", *Foreign Medical Sciences (Section of Pharmacy)*, Vol. 33, No. 1: pp. 14-17.

Zasloff, M. (1987). "Magainins, a class of antimicrobial peptides from Xenopus skin: isolation, characterization of two active forms, and partial cDNA sequence of precursor", *Proceeding of the Natlional Academy Science of the USA*, Vol. 84, No. 15: pp. 5449-5453.

Zhang, L., Yu, W., He, T., Yu, J., Caffrey, R. E., Dalmasso, E. A., Fu, S., Pham, T., Mei, J., Ho, J. J., Zhang W., Lopez, P. and Ho, D. D. (2002). "Contribution of human alpha-defensin 1, 2, and 3 to the anti-HIV-1 activity of CD8 antiviral factor", *Science*, Vol. 298, No. 5595: pp. 995-1000.

Zhang, L.; Chen, X.; Zhang, Ying.; Ma, C.; Xi, X.; Wang, L.; Zhou,M; F. Burrows, J.; Chen, T. Identification of novel Amurin-2 variants from the skin secretion of Rana amurensis, and the design of cationicity-enhanced analogues, Biochemical and Biophysical Research Communications 2018, 497, 943-949. DOI: 10.1016/j.bbrc.2018.01.124

Zhang, S.K., Song, J., Gong, F., Li, S.B., Chang, H.Y., Xie, H.M., et al. (2016). "Design of an α-helical antimicrobial peptide with improved cell-selective and potent anti-biofilm activity", *Scientific Reports*, Vol. 6, p. 27394.

Zhang, Y., Algburi, A., Wang, N., Kholodovych, V., Oh, D. O., Chikindas, M. and Uhrich, K. E. (2017). "Self-assembled cationic amphiphiles as antimicrobial peptides mimics: Role of hydrophobicity, linkage type, and assembly state", *Nanomedicine*, Vol. 13, No. 2: pp. 343-352.

Zhu, W. L., Song, Y. M., Park, Y., Park, K. Y., Yang, S. T., Kim, J., Park, S., Hahm, K. S. and Shin, S. Y. (2007). "Substitution of the leucine zipper sequencein melittin with peptide residues affects self association, cell selectivity, and mode of action". *Biochimica et Biophysica Acta (BBA) - Biomembranes*, Vol. 1768, No. 6: pp. 1506-1517.

Zug, G. R., Vitt, L. J. and Caldwell, J. P. (2001). "Herpetology (second edition)", *New York: Academic Press*.